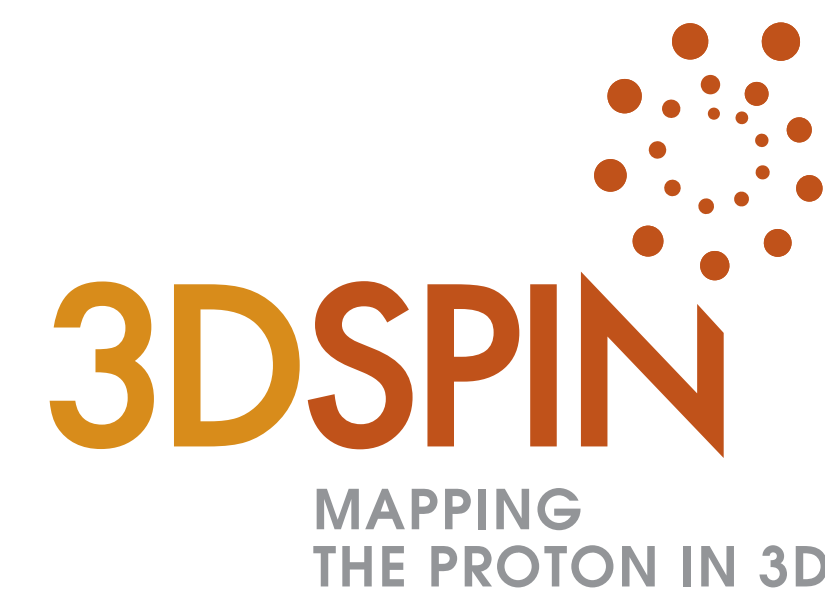


First attempts at a global fit of unpolarized Transverse Momentum Distributions

Alessandro Bacchetta

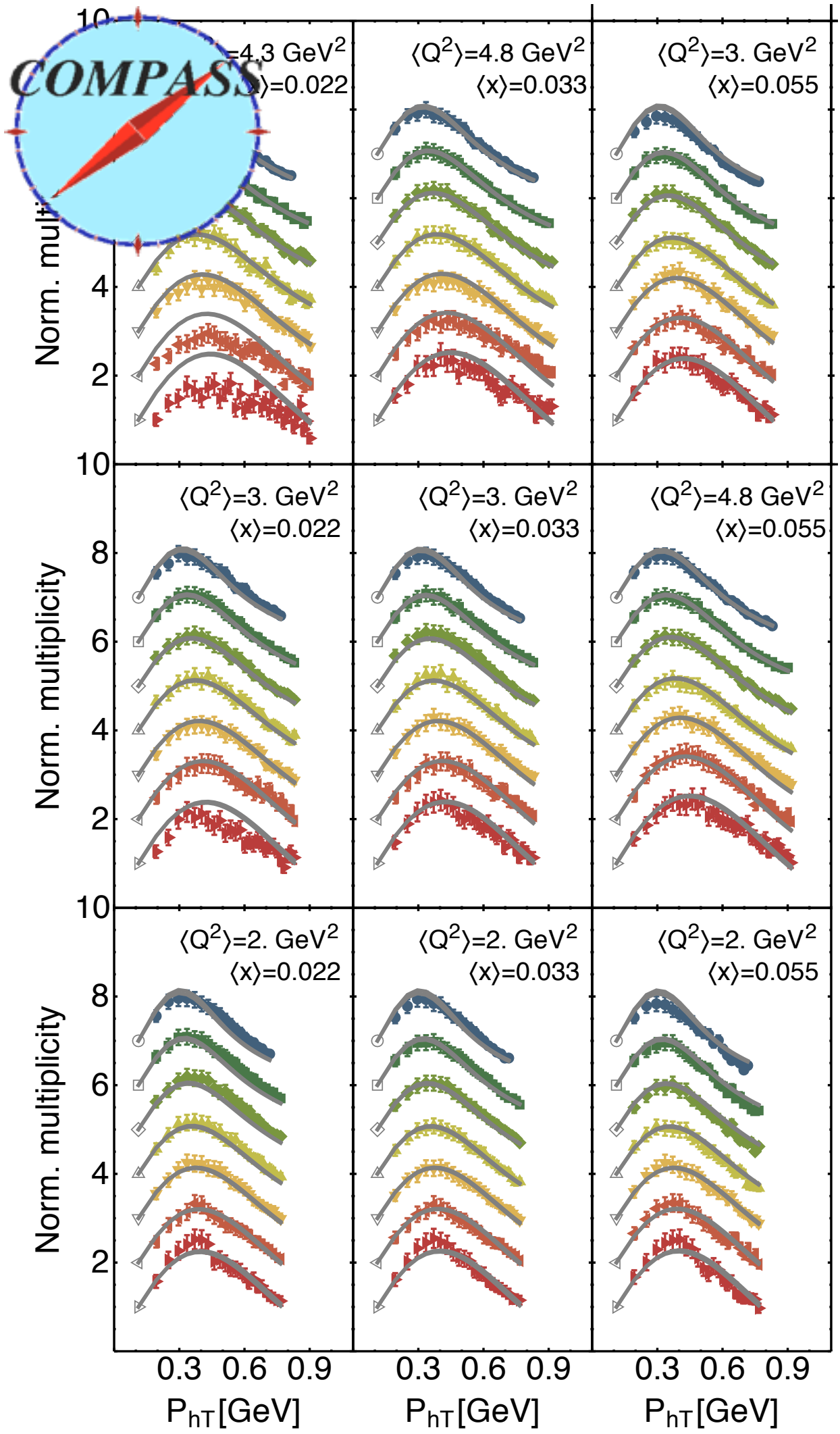
Funded by



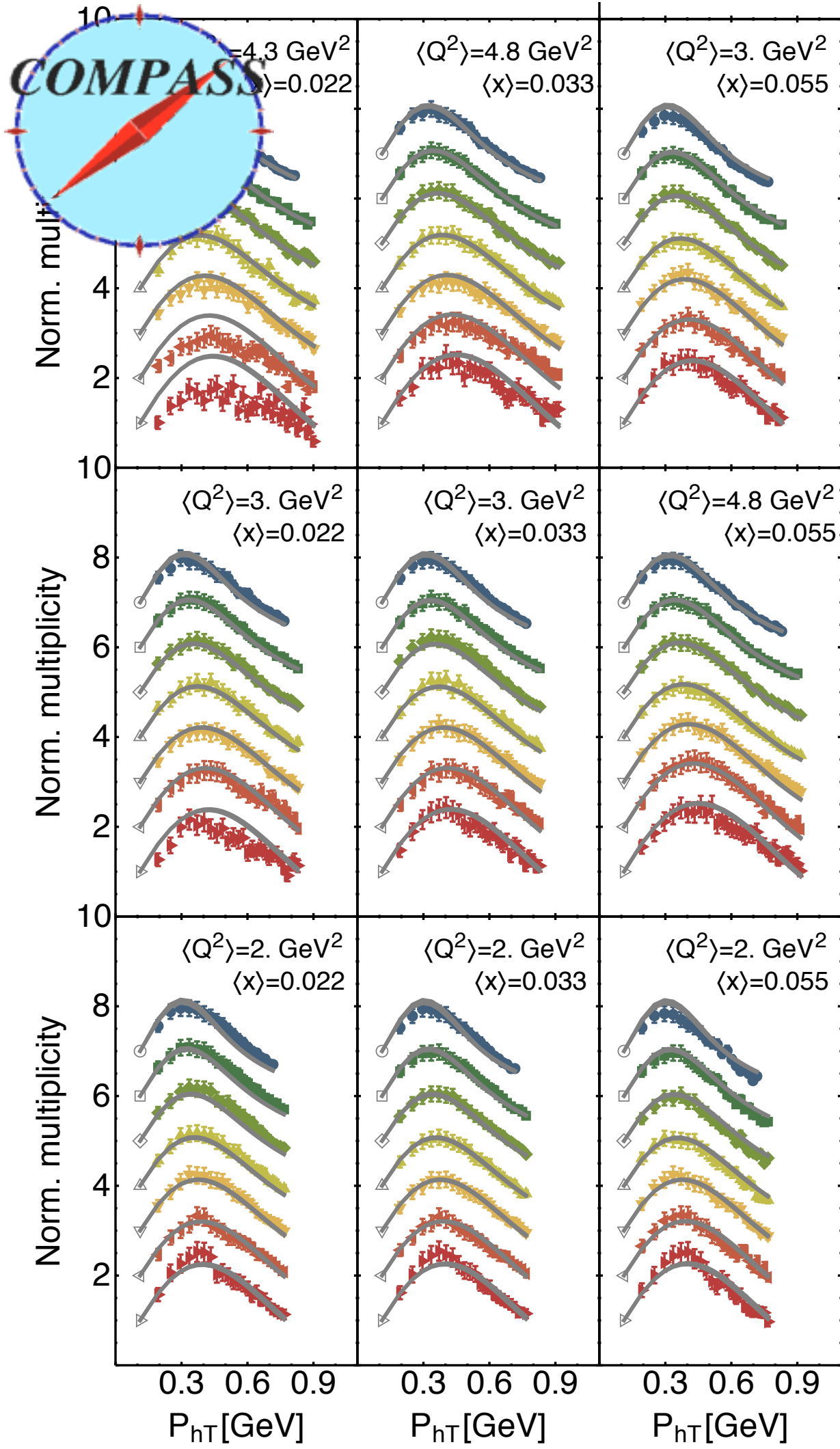
In collaboration with

- Filippo Delcarro (PhD student, University of Pavia and INFN Pavia)
- Cristian Pisano (University of Pavia and INFN Pavia)
- Marco Radici (INFN Pavia)
- Andrea Signori (Vrije Universiteit Amsterdam and NIKHEF)

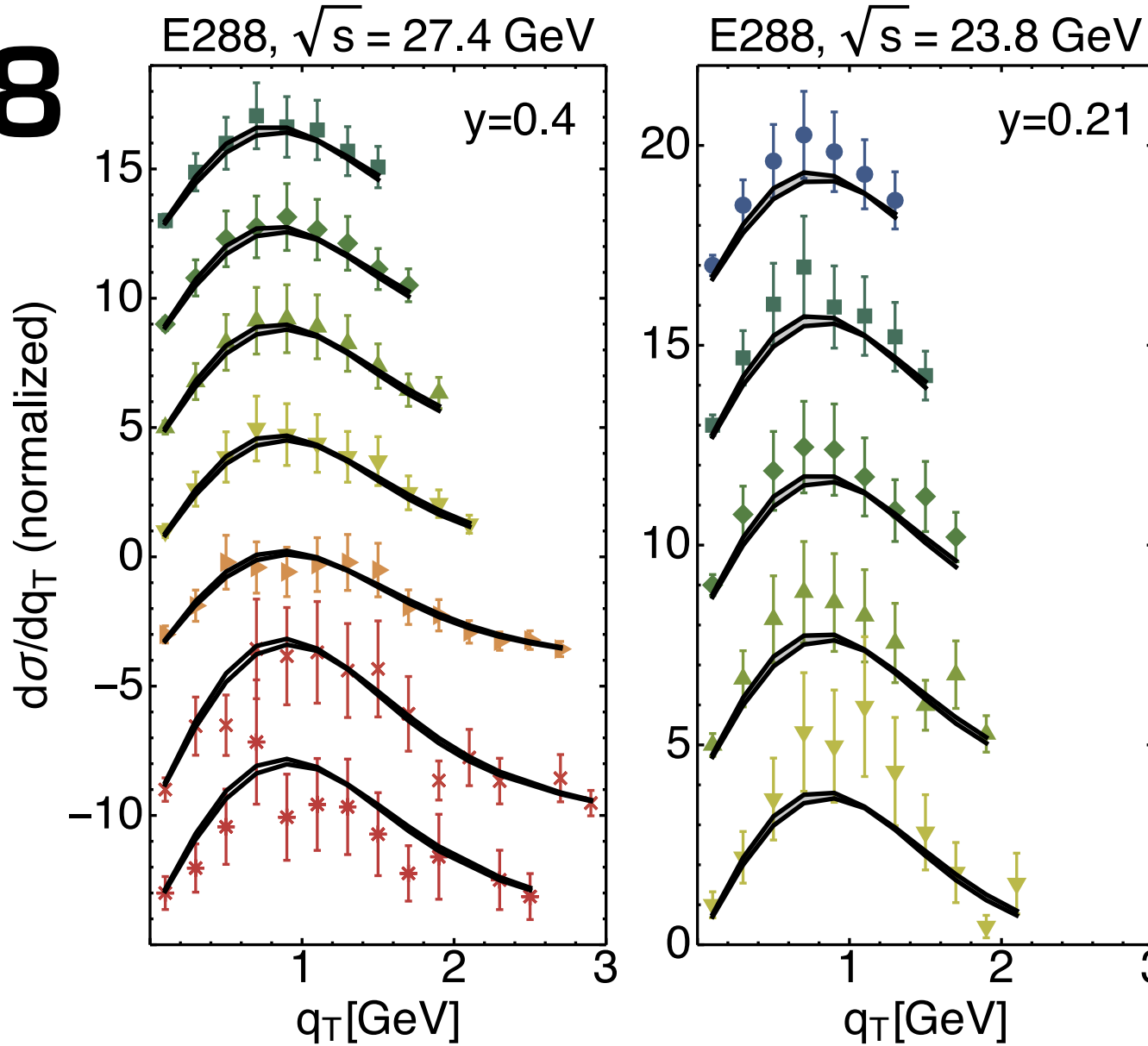
In a nutshell



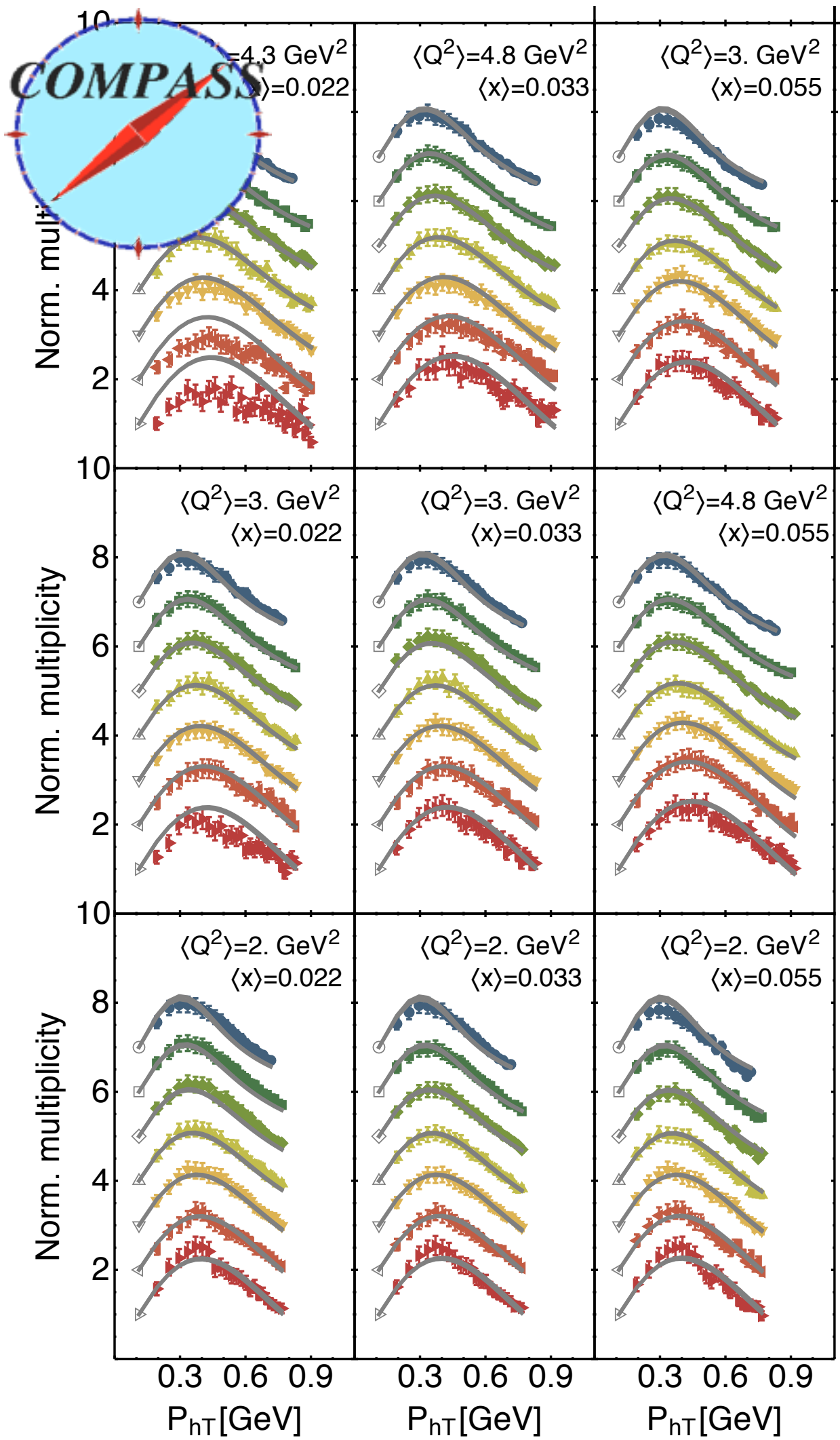
In a nutshell



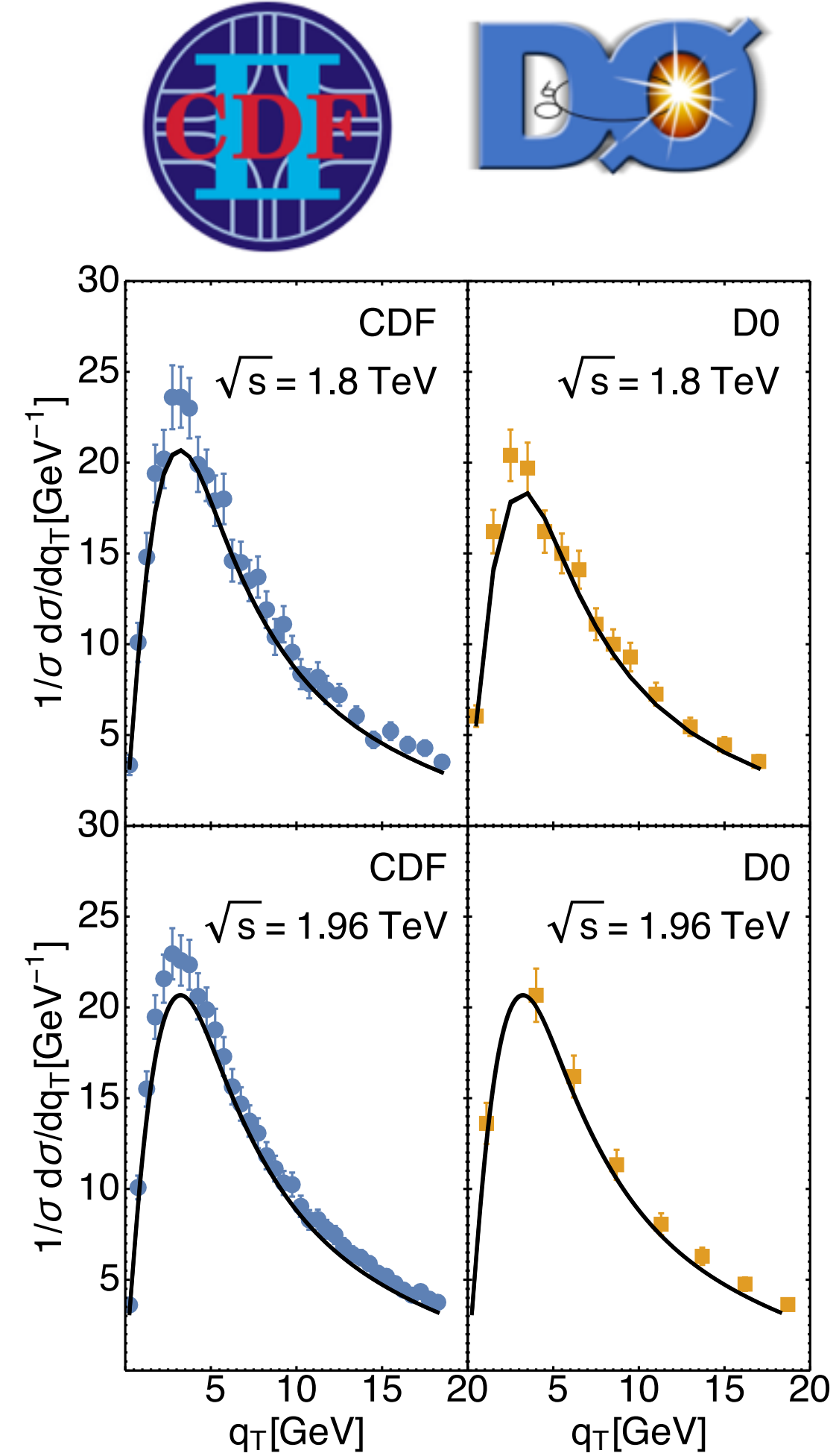
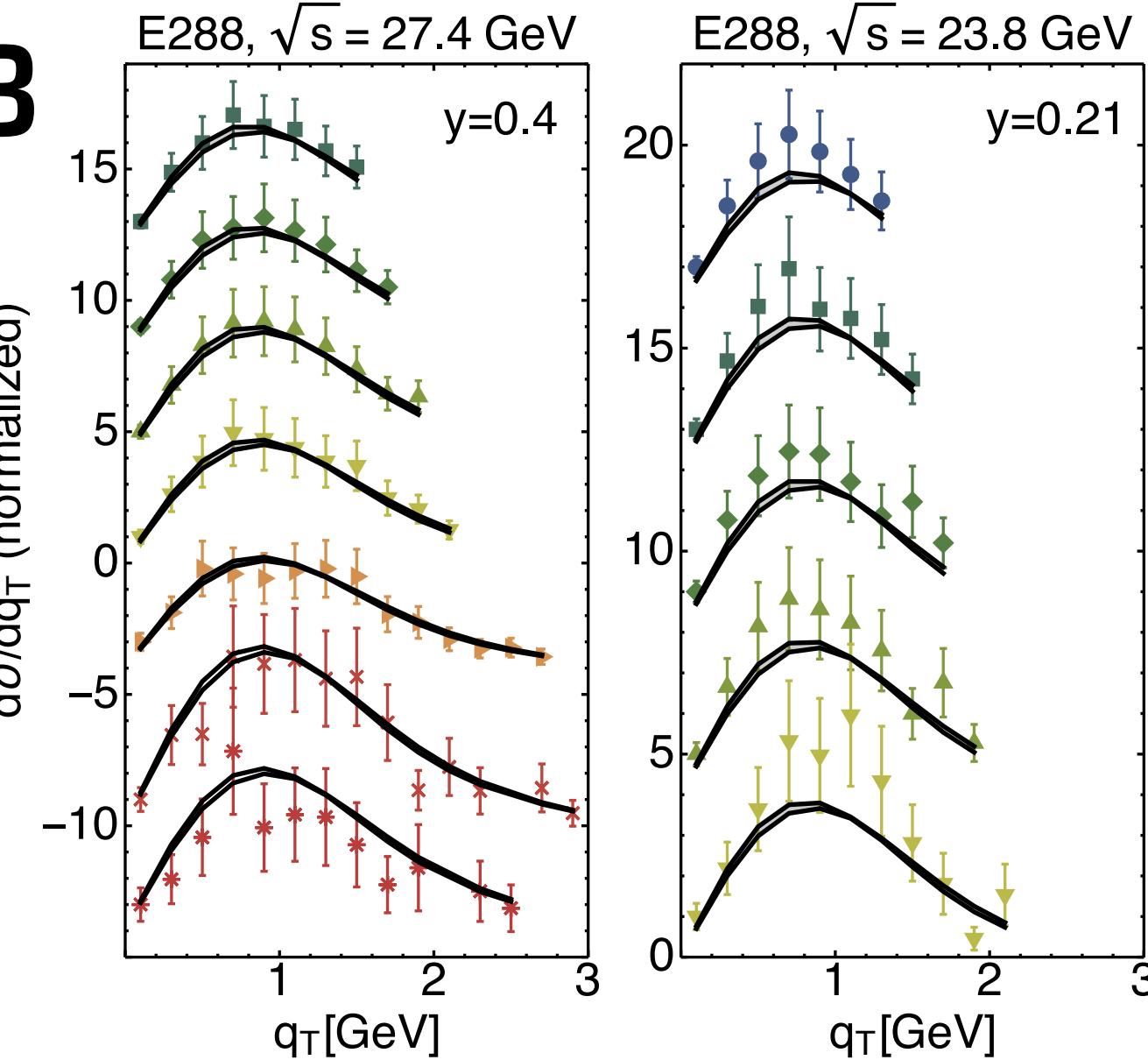
E288



In a nutshell

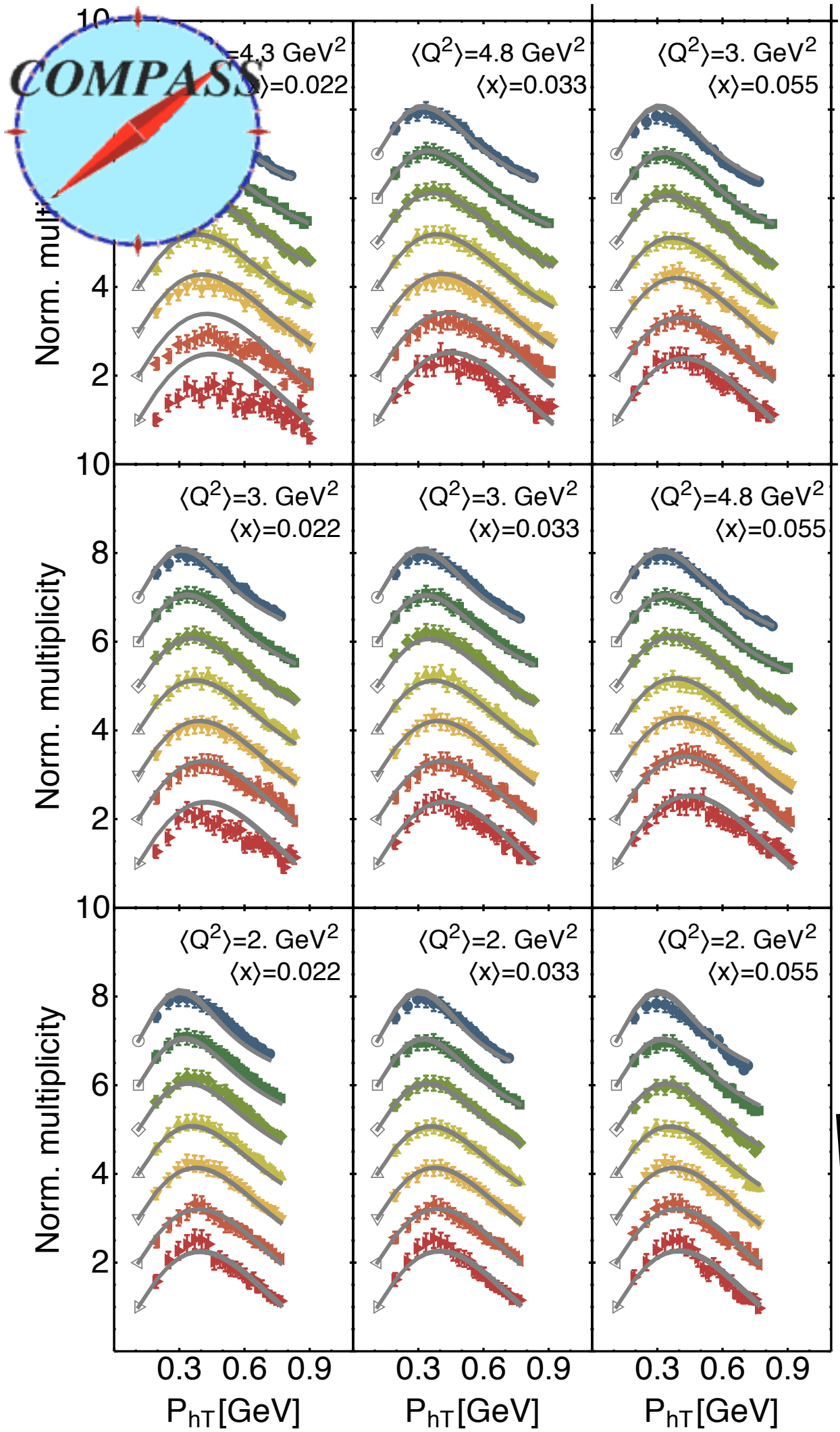


E288

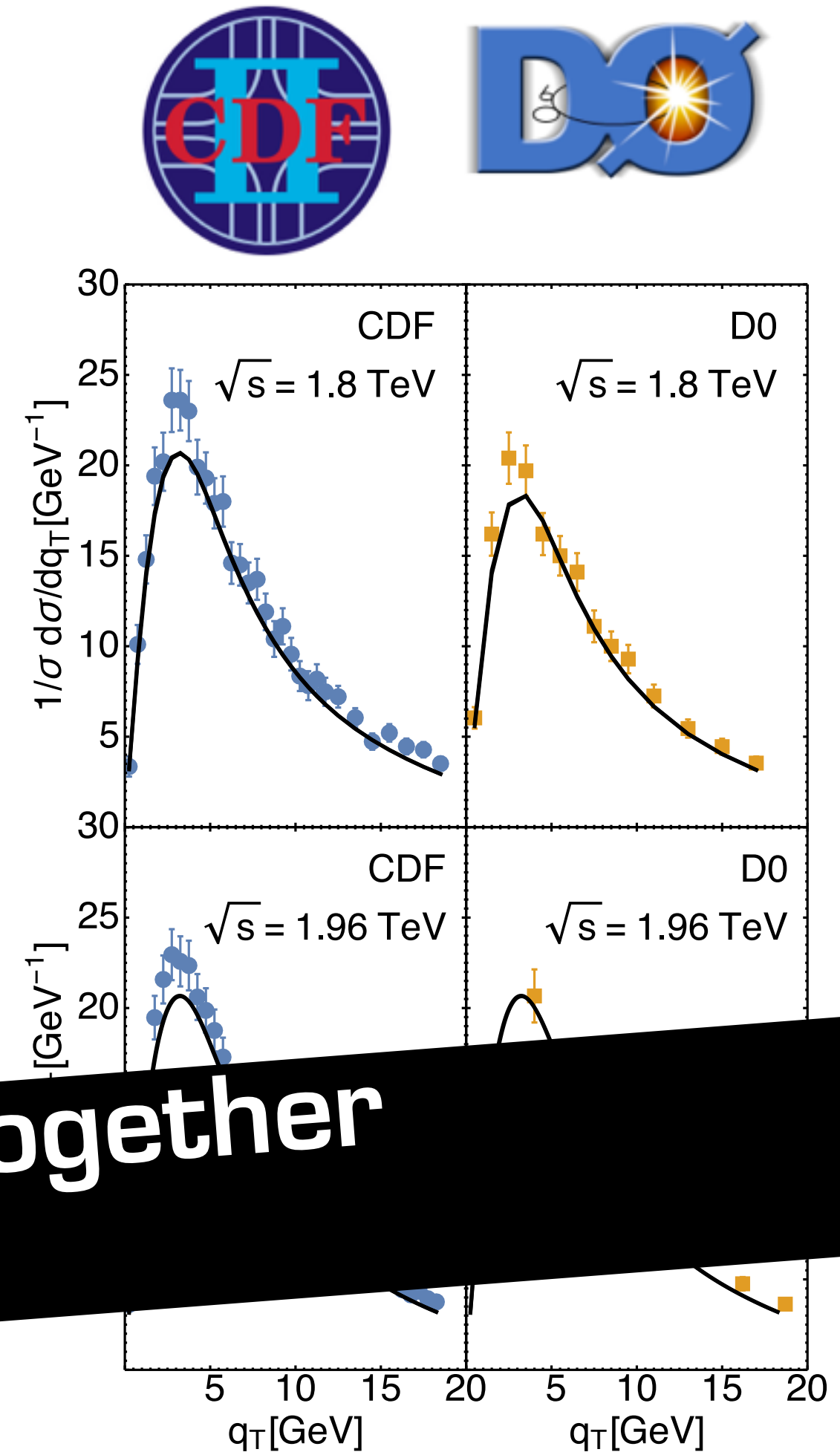
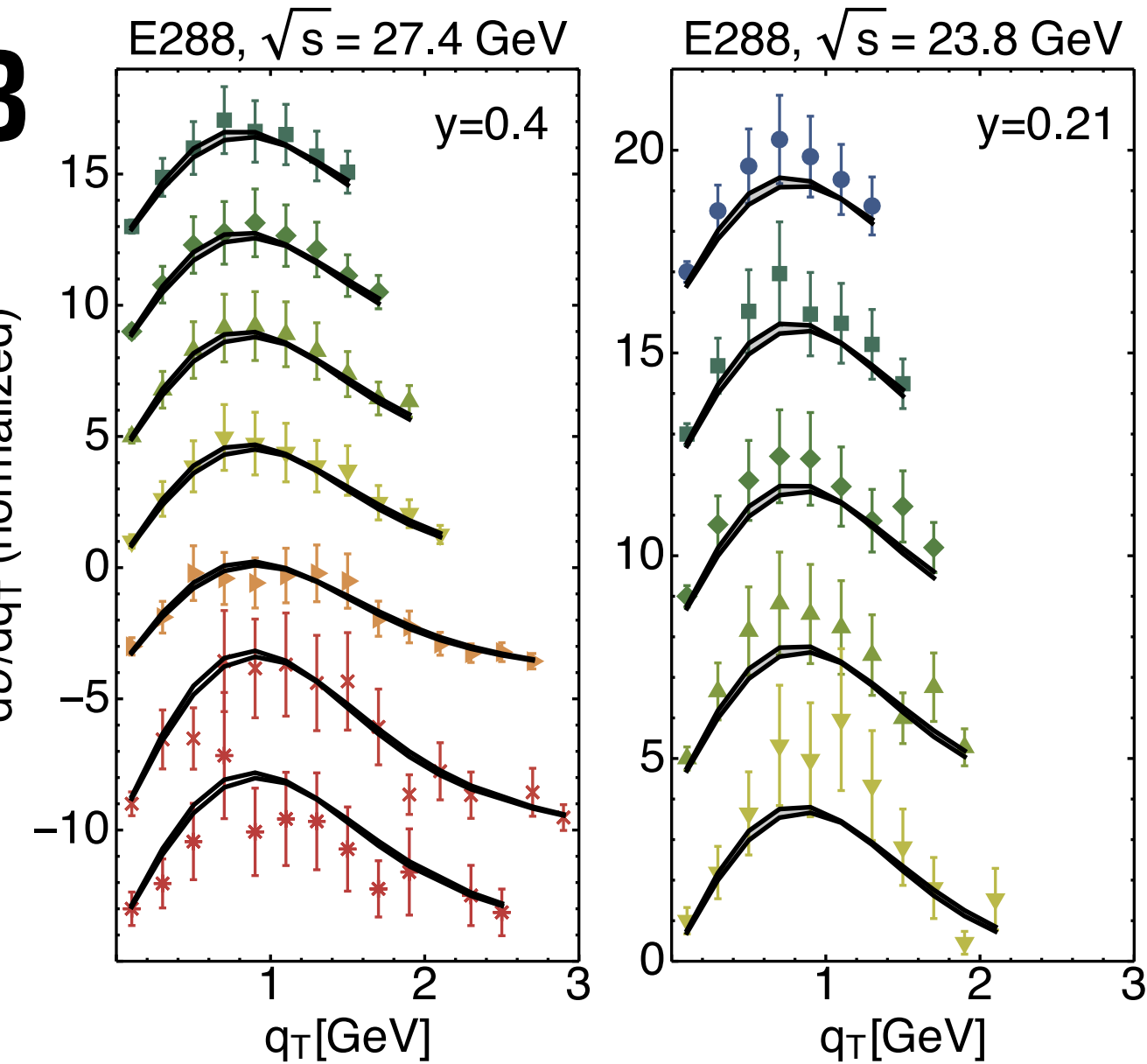


Bacchetta, Delcarro, Pisano, Radici, Signori, in preparation

In a nutshell



E288



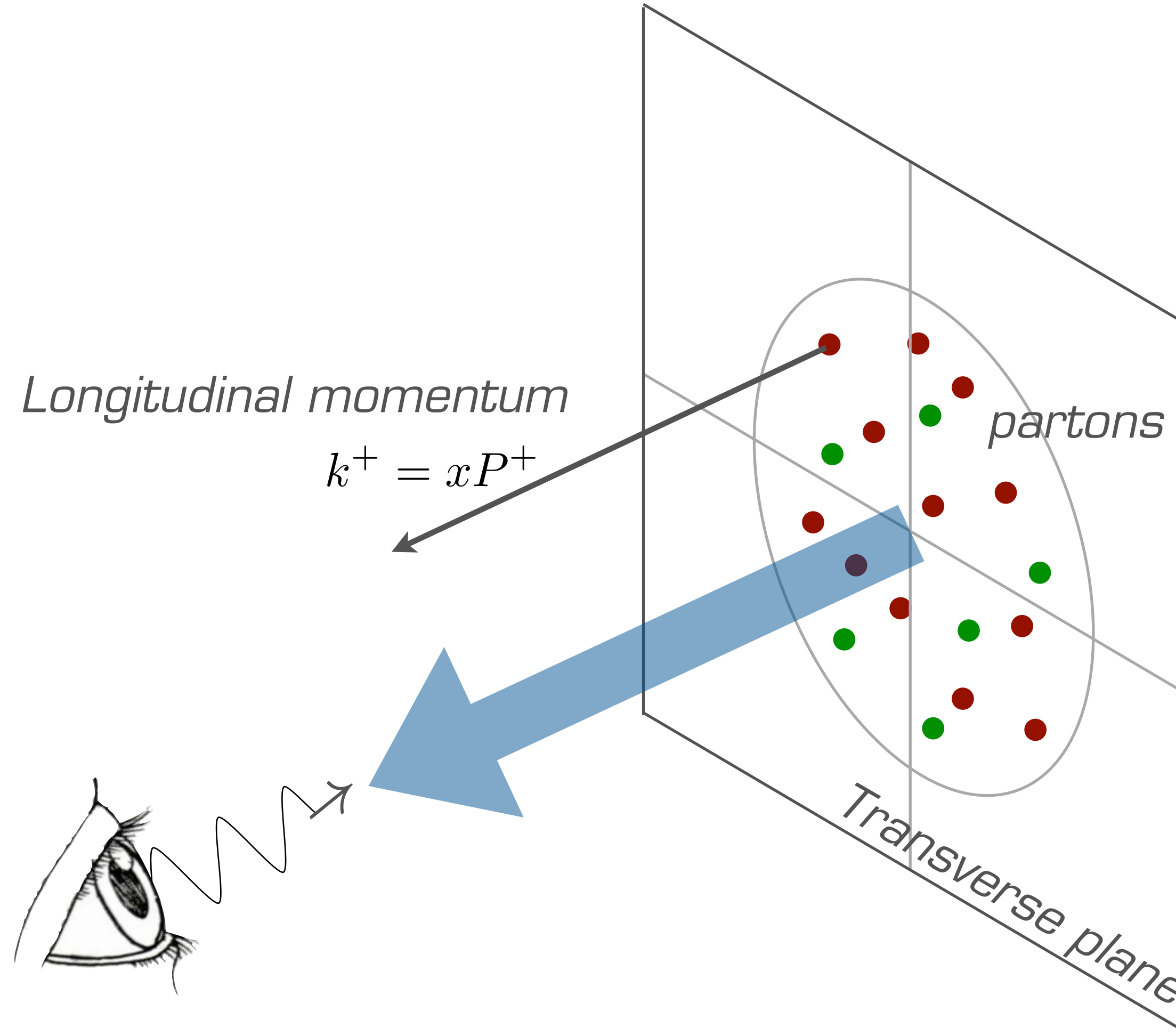
Pavia 2016: first TMD fit putting together
SIDIS + Drell-Yan + Z production

Bacchetta, Delcarro, Pisano, Radici, Signori, in preparation

Some introduction

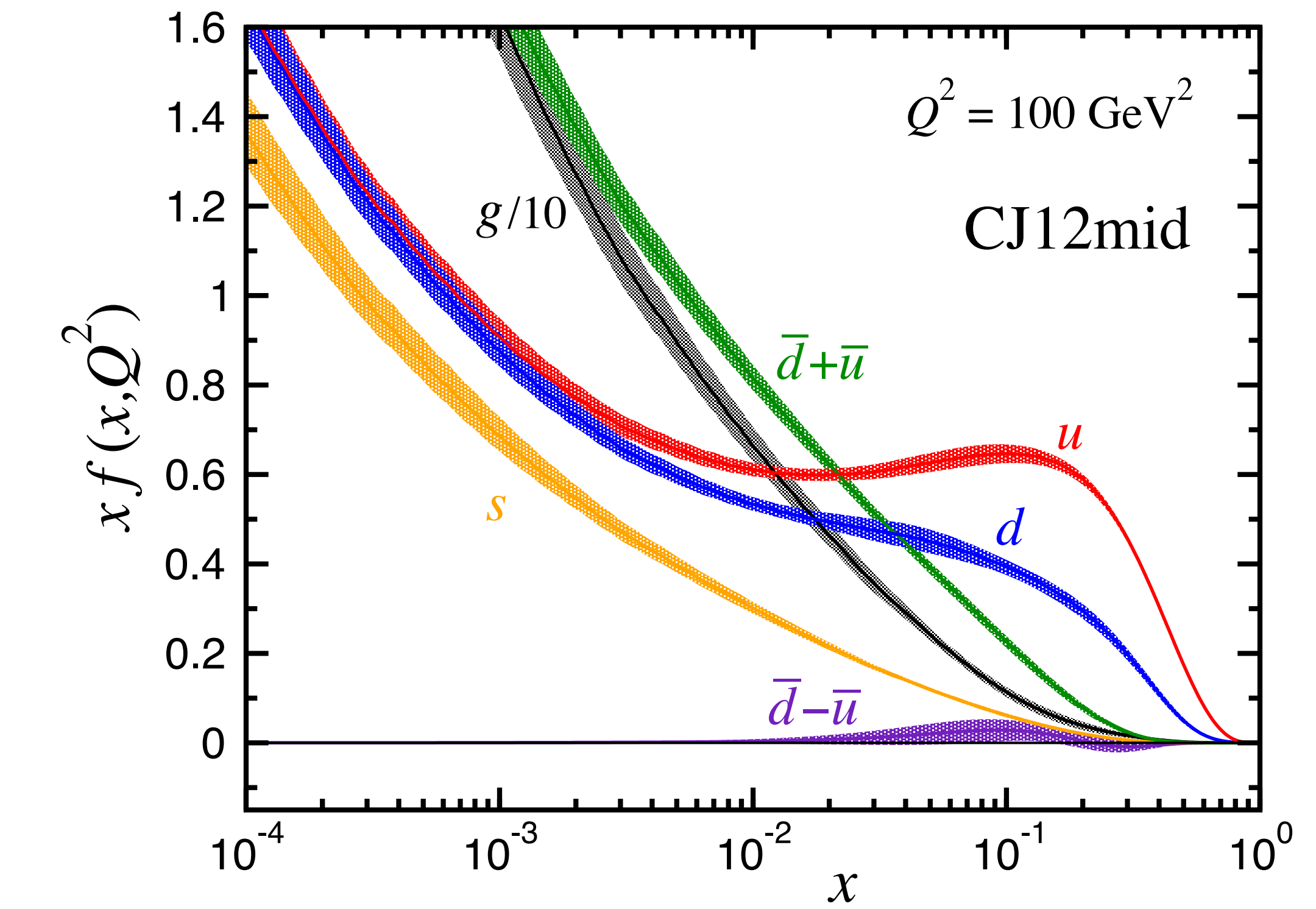
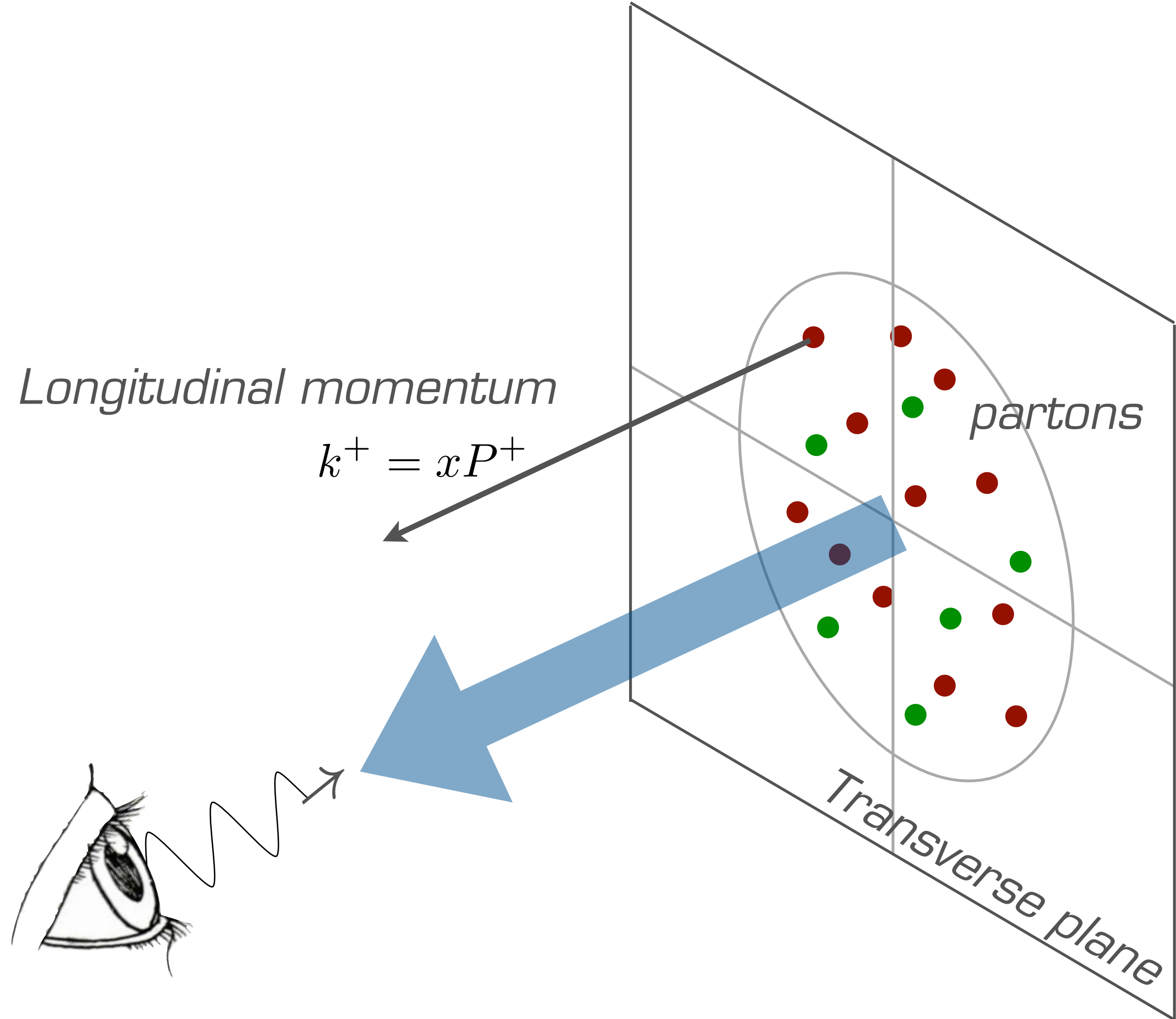
Standard parton distribution functions

Standard collinear PDFs describe the distribution of partons in one dimension in momentum space



Standard parton distribution functions

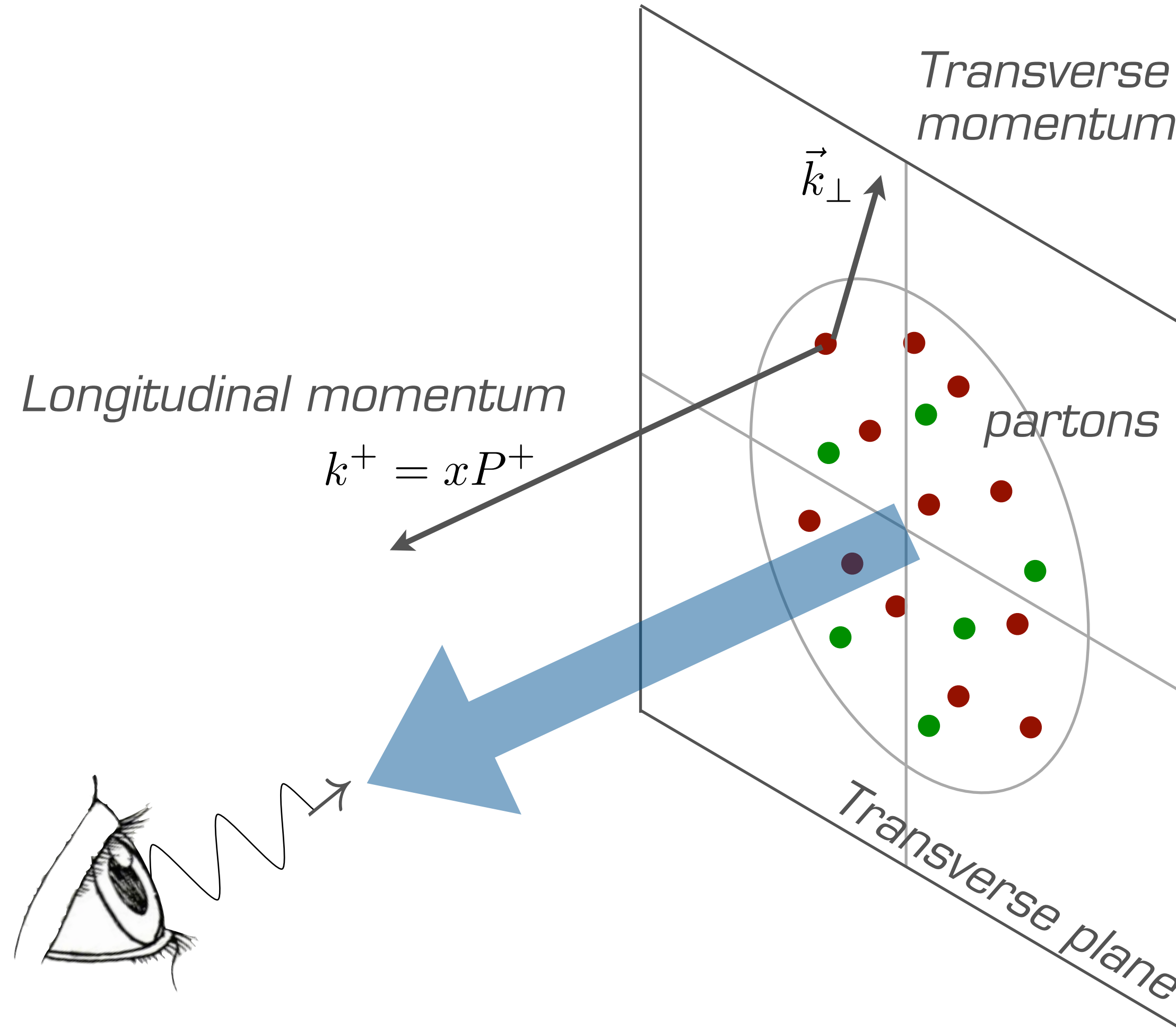
Standard collinear PDFs describe the distribution of partons in one dimension in momentum space



CTEQ-JLAB 12 set, Owens, Accardi, Melnitchouk, PRD87 (13)

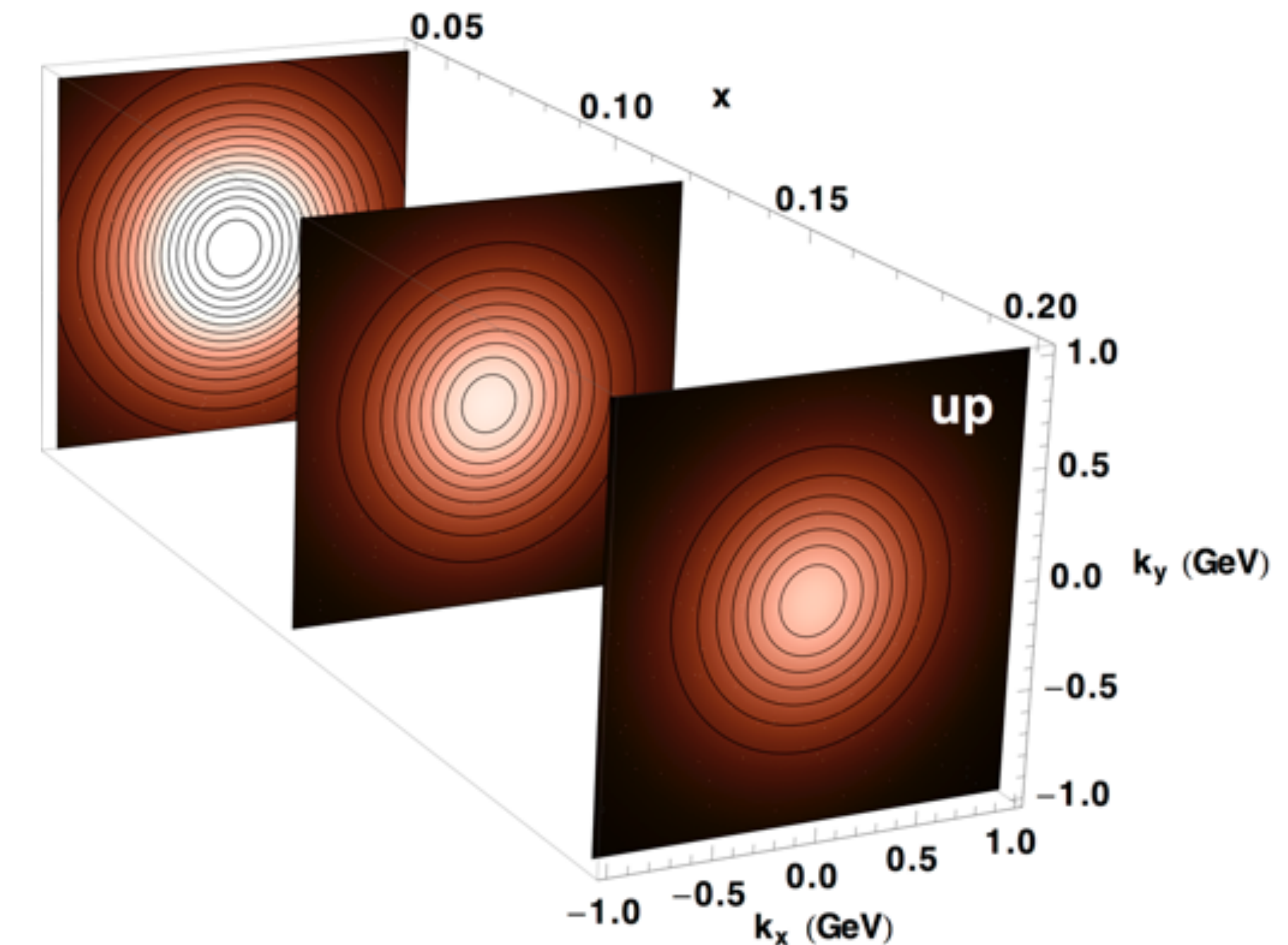
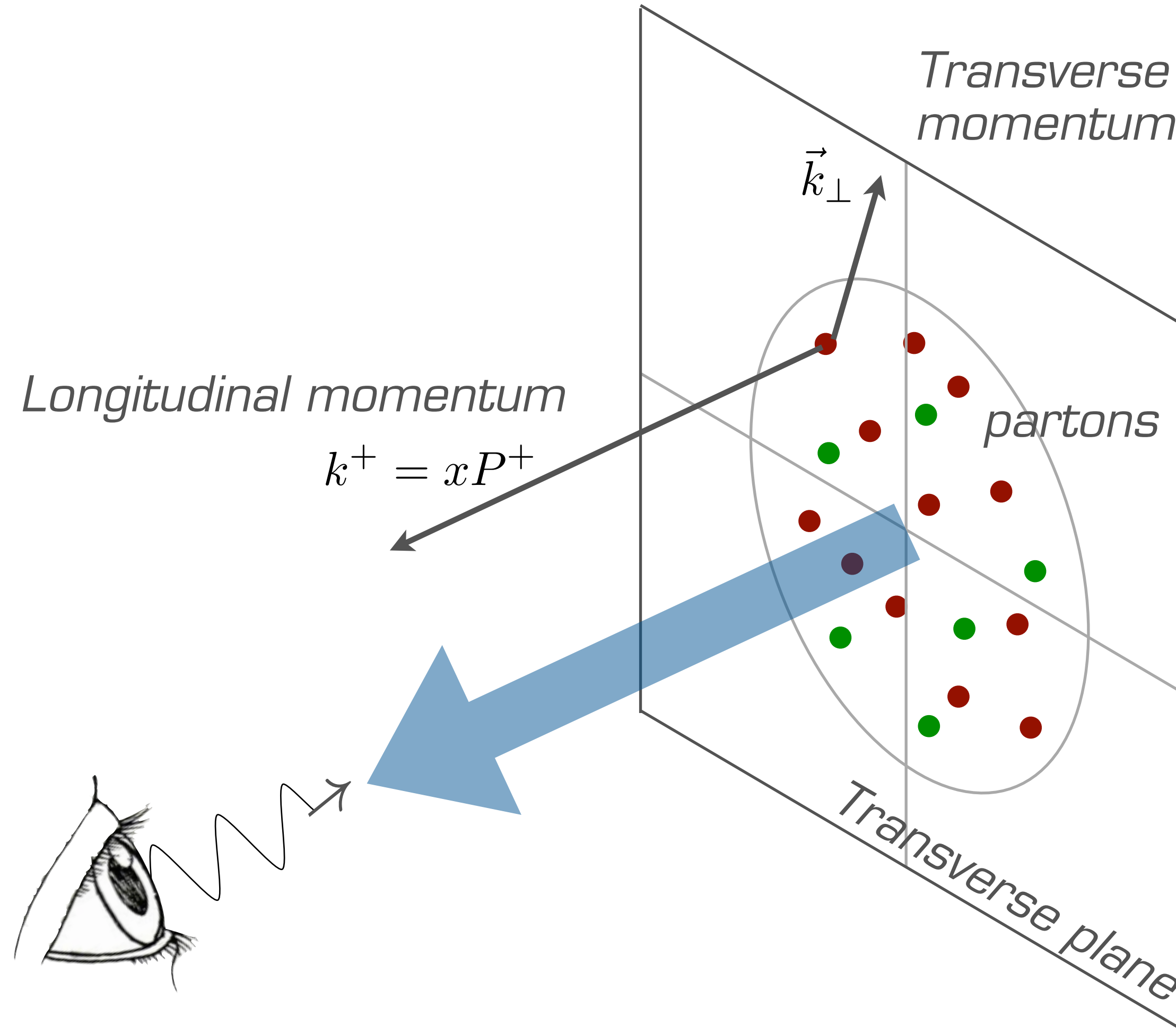
Transverse Momentum Distributions

TMDs describe the distribution of partons in three dimensions in momentum space

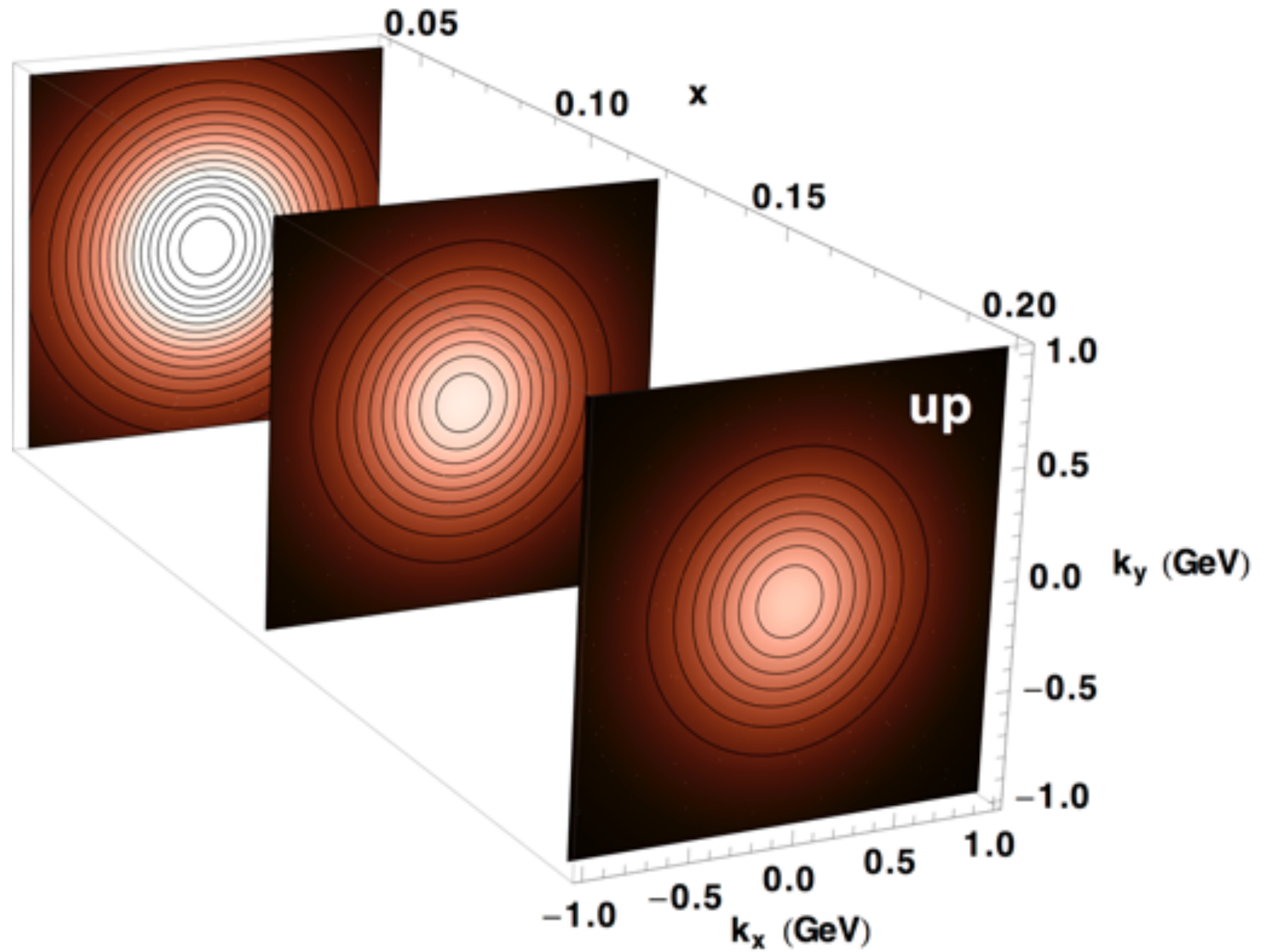


Transverse Momentum Distributions

TMDs describe the distribution of partons in three dimensions in momentum space

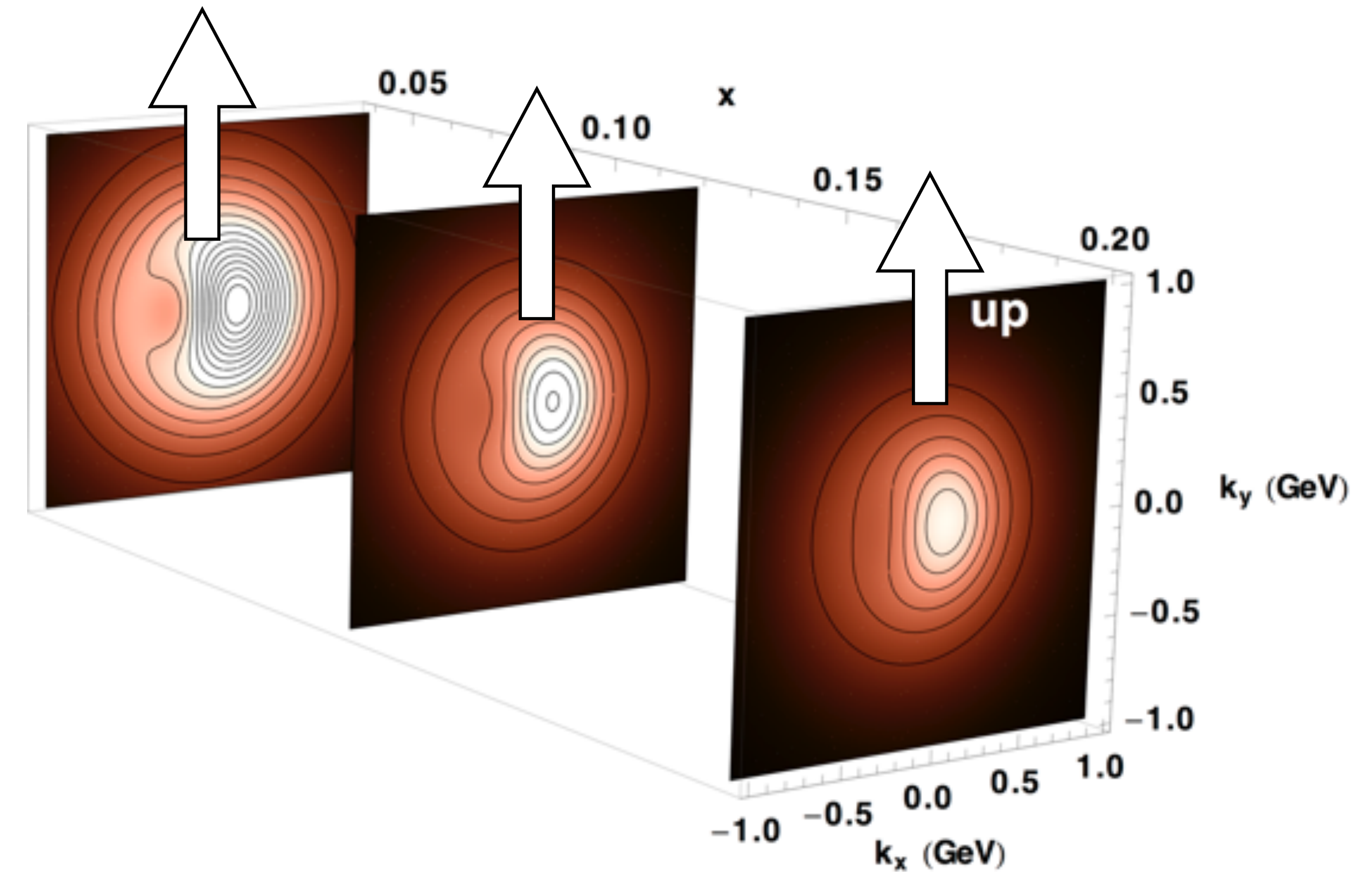
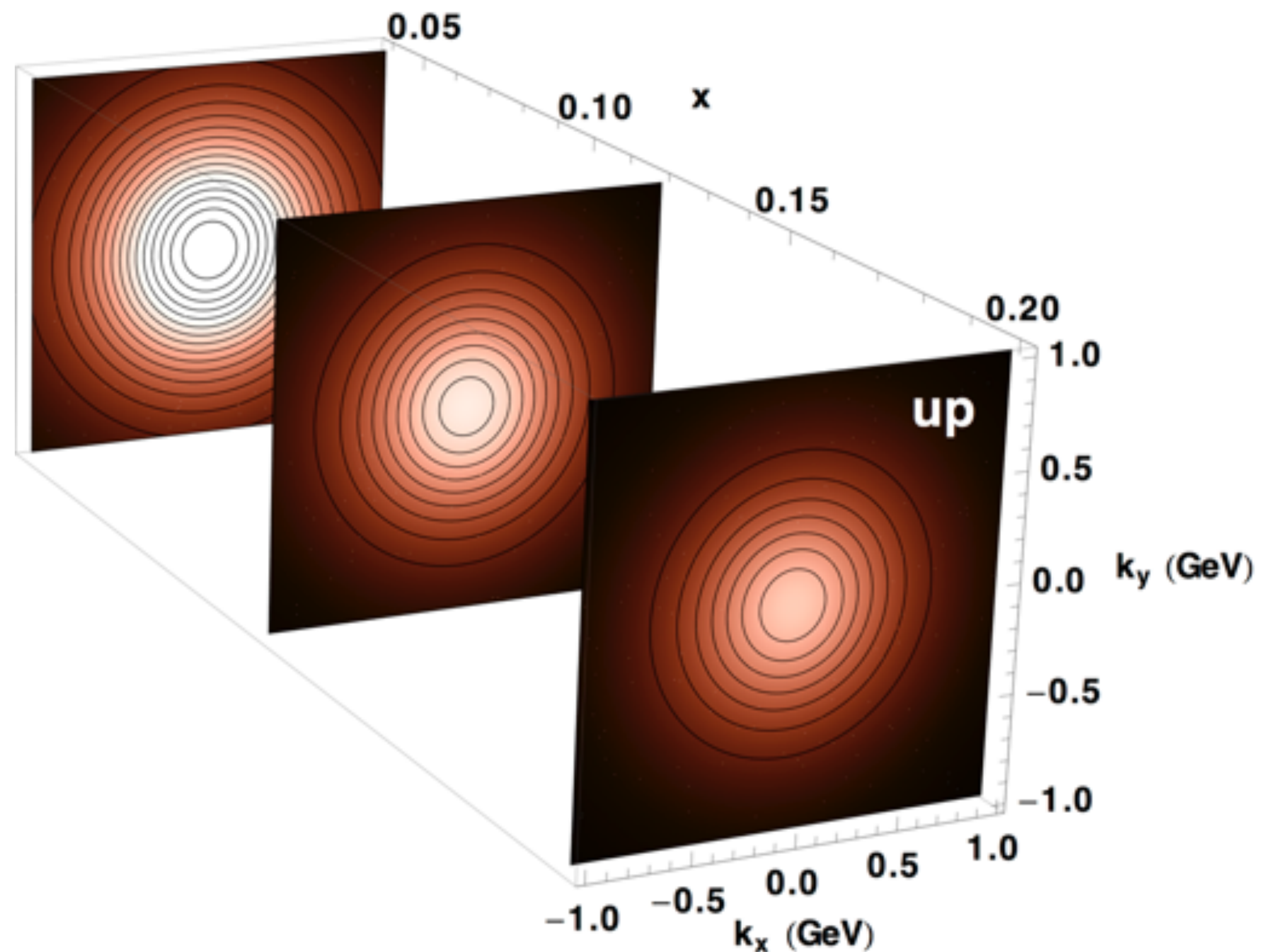


3D structure in momentum space



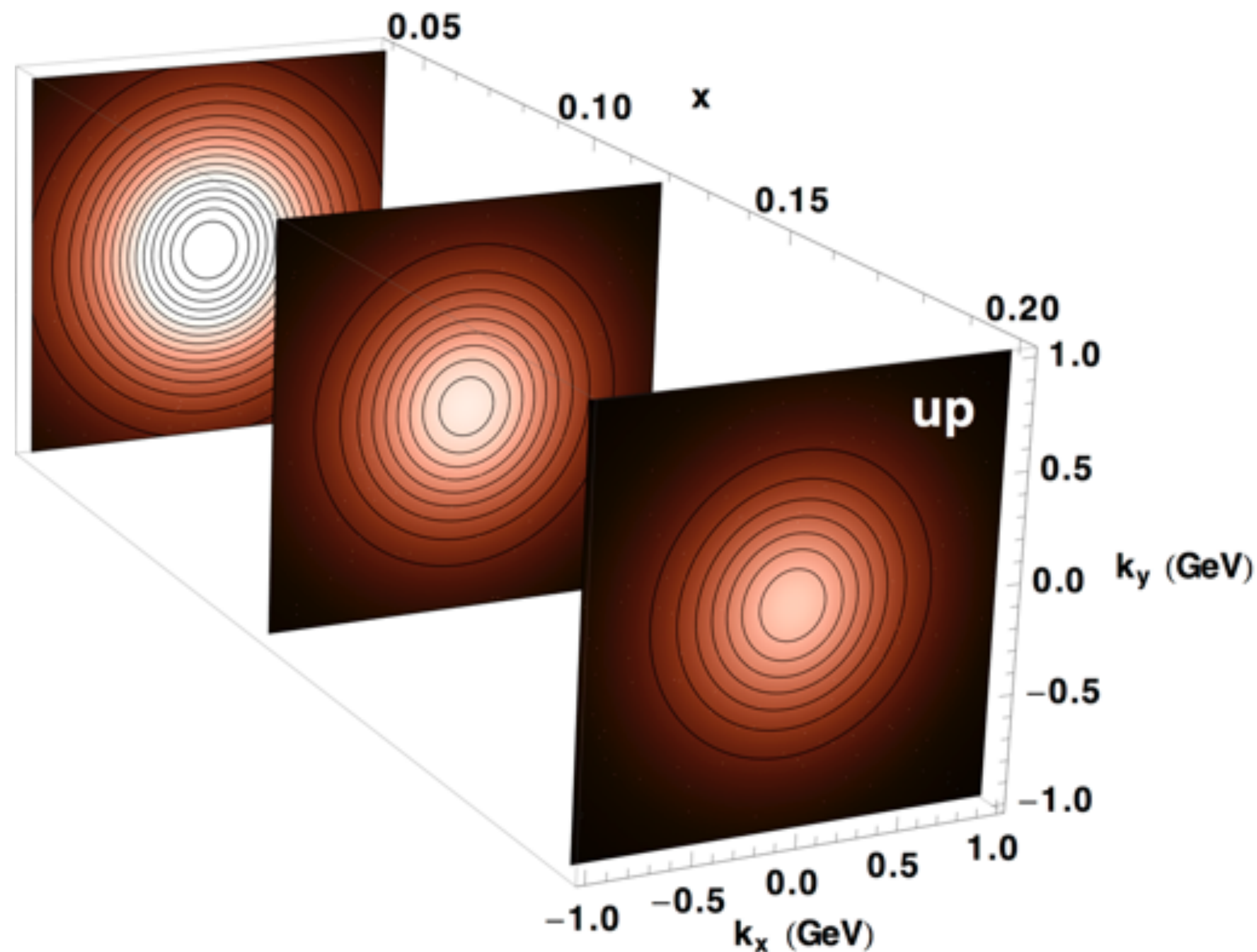
Unpolarized TMD: cylindrically symmetric

3D structure in momentum space

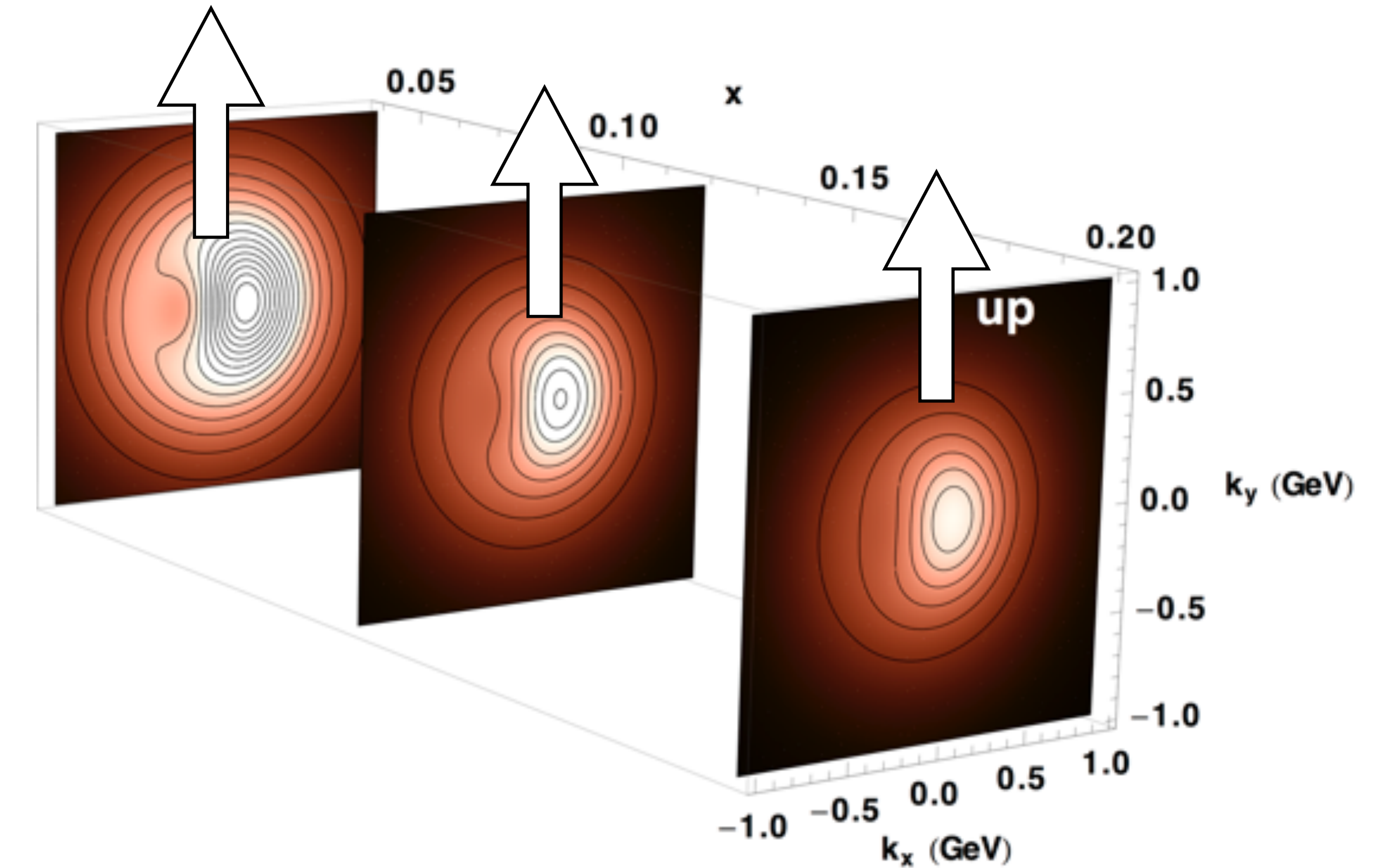


Unpolarized TMD: cylindrically symmetric

3D structure in momentum space



Unpolarized TMD: cylindrically symmetric



With transverse spin: distortions can occur,
encoded in Sivers TMD
Requires presence of orbital angular momentum

PDFs

Parton distribution
functions (x)

Transverse-momentum
distributions (x, \vec{k}_\perp)

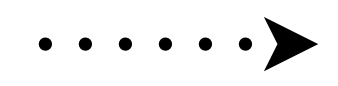
TMDs

Impact-parameter
distributions (x, \vec{b}_\perp)

Wigner distributions
($x, \vec{k}_\perp, \vec{b}_\perp$)



\vec{b}_\perp dependence



\vec{k}_\perp dependence



these two variables are NOT Fourier conjugate

see, e.g., C. Lorcé, B. Pasquini, M. Vanderhaeghen, JHEP 1105 (11)

PDFs

Parton distribution
functions (x)

Transverse-momentum
distributions (x, \vec{k}_\perp)

TMDs

Wigner distributions
($x, \vec{k}_\perp, \vec{b}_\perp$)

Impact-parameter
distributions (x, \vec{b}_\perp)

2D Fourier
transform (\vec{b}_\perp)

Generalized parton
distributions
($x, \xi = 0, \vec{\Delta}_T$)

GPDs



\vec{b}_\perp dependence



these two variables are NOT Fourier conjugate



\vec{k}_\perp dependence

see, e.g., C. Lorcé, B. Pasquini, M. Vanderhaeghen, JHEP 1105 (11)

PDFs

Parton distribution
functions (x)

Transverse-momentum
distributions (x, \vec{k}_\perp)

TMDs

Wigner distributions
($x, \vec{k}_\perp, \vec{b}_\perp$)

Impact-parameter
distributions (x, \vec{b}_\perp)

GPDs

Form factors
($\vec{\Delta}_T^2$)

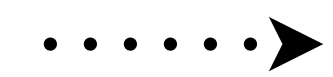
Integral
over x

2D Fourier
transform (\vec{b}_\perp)

Generalized parton
distributions
($x, \xi = 0, \vec{\Delta}_T$)



\vec{b}_\perp dependence



\vec{k}_\perp dependence



these two variables are NOT Fourier conjugate

see, e.g., C. Lorcé, B. Pasquini, M. Vanderhaeghen, JHEP 1105 (11)

PDFs

Parton distribution
functions (x)

Transverse-momentum
distributions (x, \vec{k}_\perp)

TMDs

Wigner distributions
($x, \vec{k}_\perp, \vec{b}_\perp$)

→ \vec{b}_\perp dependence
..... → \vec{k}_\perp dependence



these two variables are NOT Fourier conjugate

see, e.g., C. Lorcé, B. Pasquini, M. Vanderhaeghen, JHEP 1105 (11)

Form factors
($\vec{\Delta}_T^2$)

Integral
over x

Impact-parameter
distributions (x, \vec{b}_\perp)

2D Fourier
transform (\vec{b}_\perp)

Generalized parton
distributions
($x, \xi = 0, \vec{\Delta}_T$)

GPDs

GTMDs

PDFs

Parton distribution
functions (x)

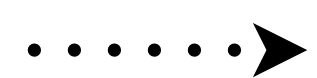
Transverse-momentum
distributions (x, \vec{k}_\perp)

TMDs

Wigner distributions
($x, \vec{k}_\perp, \vec{b}_\perp$)



\vec{b}_\perp dependence



\vec{k}_\perp dependence



these two variables are NOT Fourier conjugate

Impact-parameter
distributions (x, \vec{b}_\perp)

2D Fourier
transform (\vec{b}_\perp)

Generalized TMDs
($x, \xi = 0, k_\perp, \vec{\Delta}_T$)

Form factors
($\vec{\Delta}_T^2$)

Integral
over x

Generalized parton
distributions
($x, \xi = 0, \vec{\Delta}_T$)

GPDs

GTMDs

see talk by A. Metz

see, e.g., C. Lorcé, B. Pasquini, M. Vanderhaeghen, JHEP 1105 (11)

Recent review

EPJ A (2016) 52

The European Physical Journal A
All Volumes & Issues

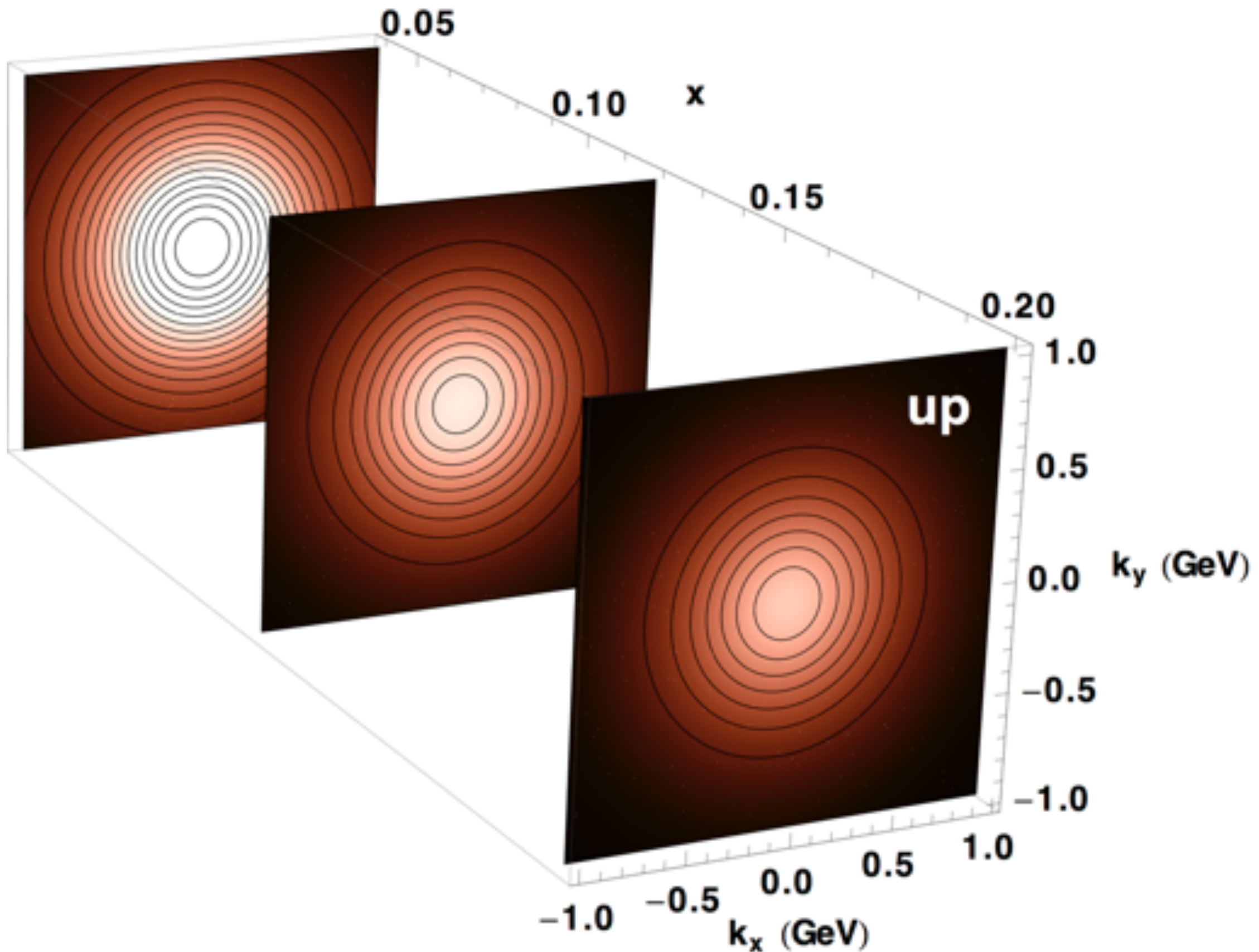
The 3-D Structure of the Nucleon

ISSN: 1434-6001 (Print) 1434-601X (Online)

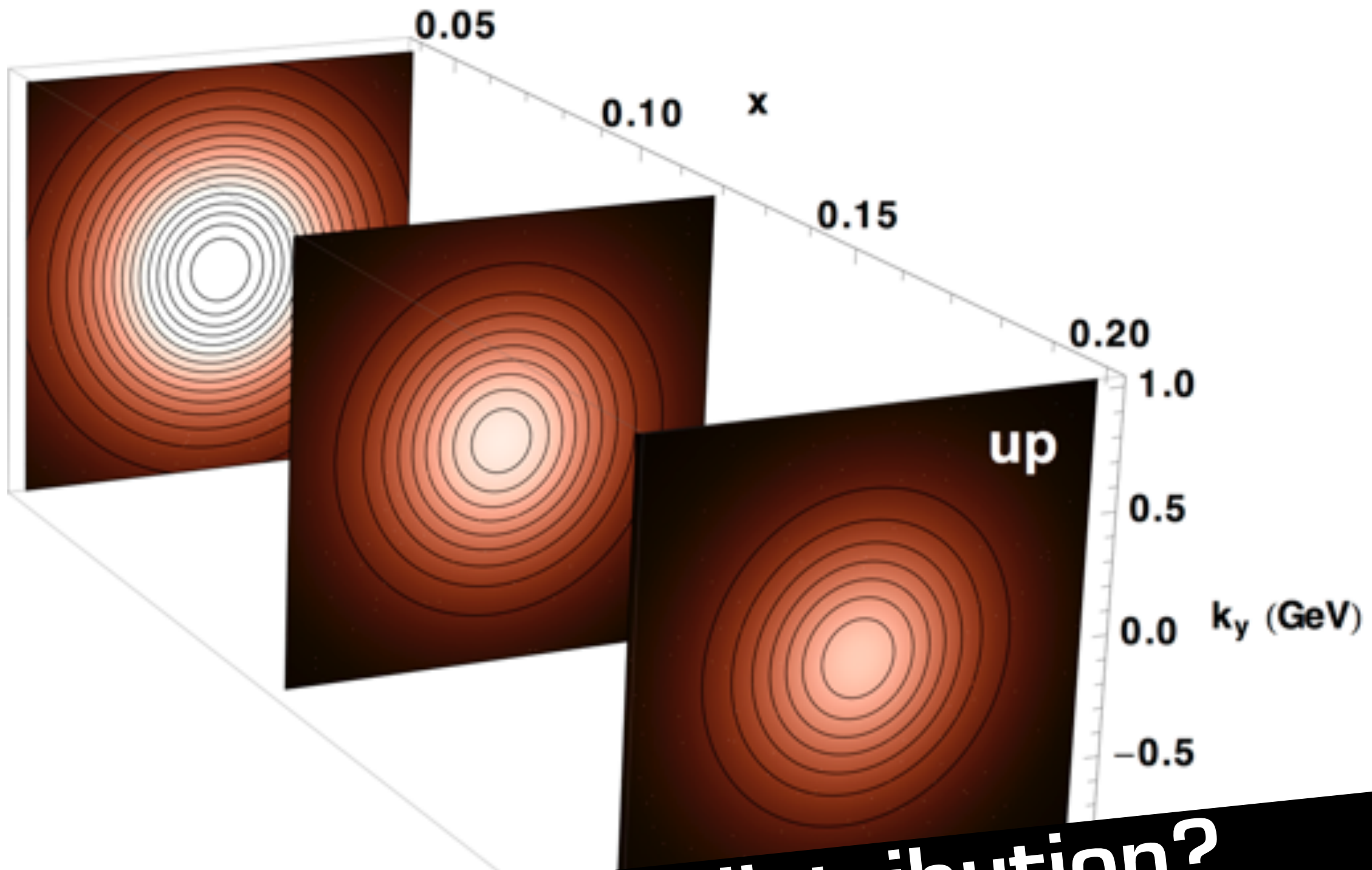
In this topical collection (17 articles)



The unpolarized TMD



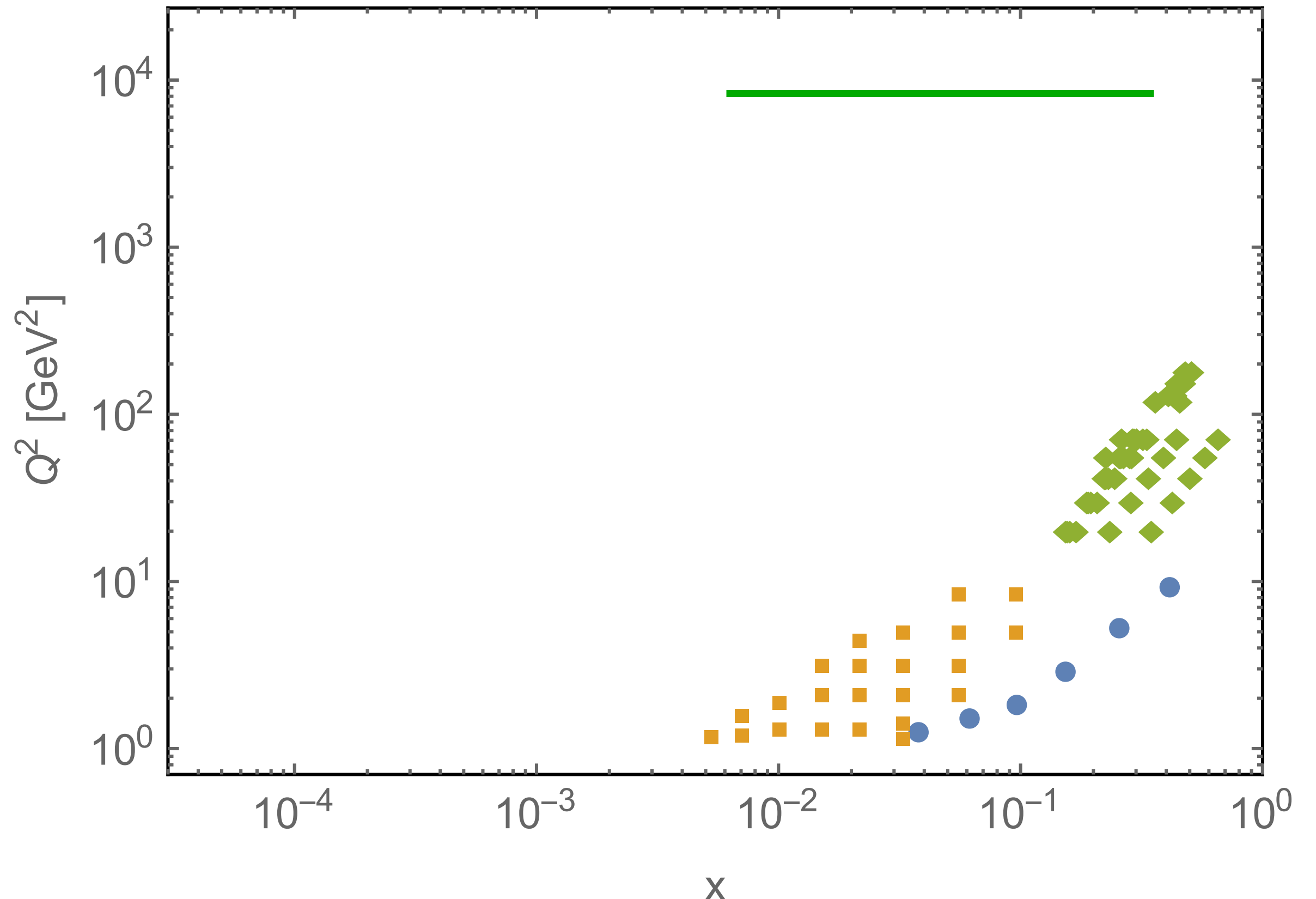
The unpolarized TMD



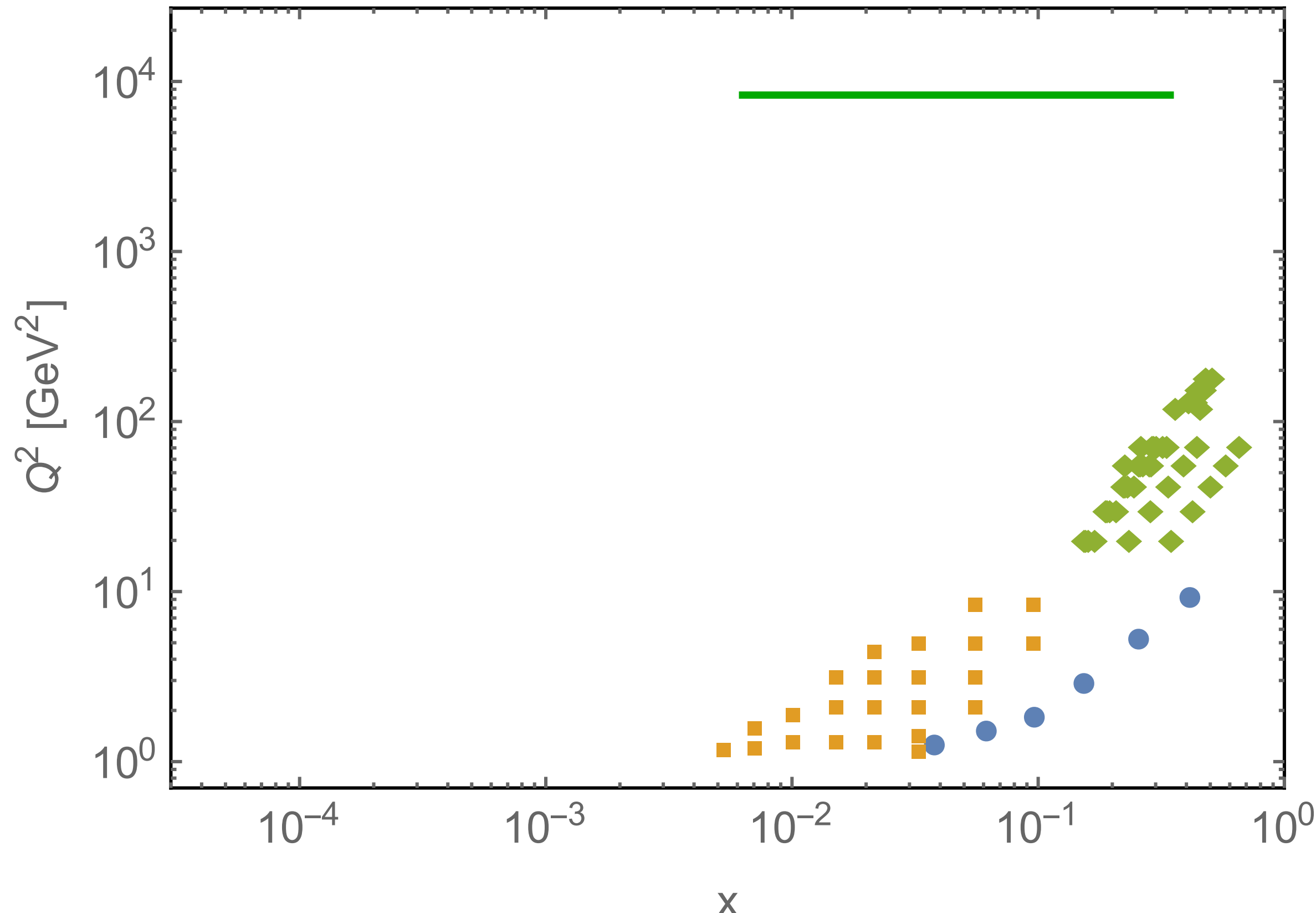
How “wide” is the distribution?
Is there a difference between flavors?
Does it get wider at low x ?

Extracting TMDs

Experiments



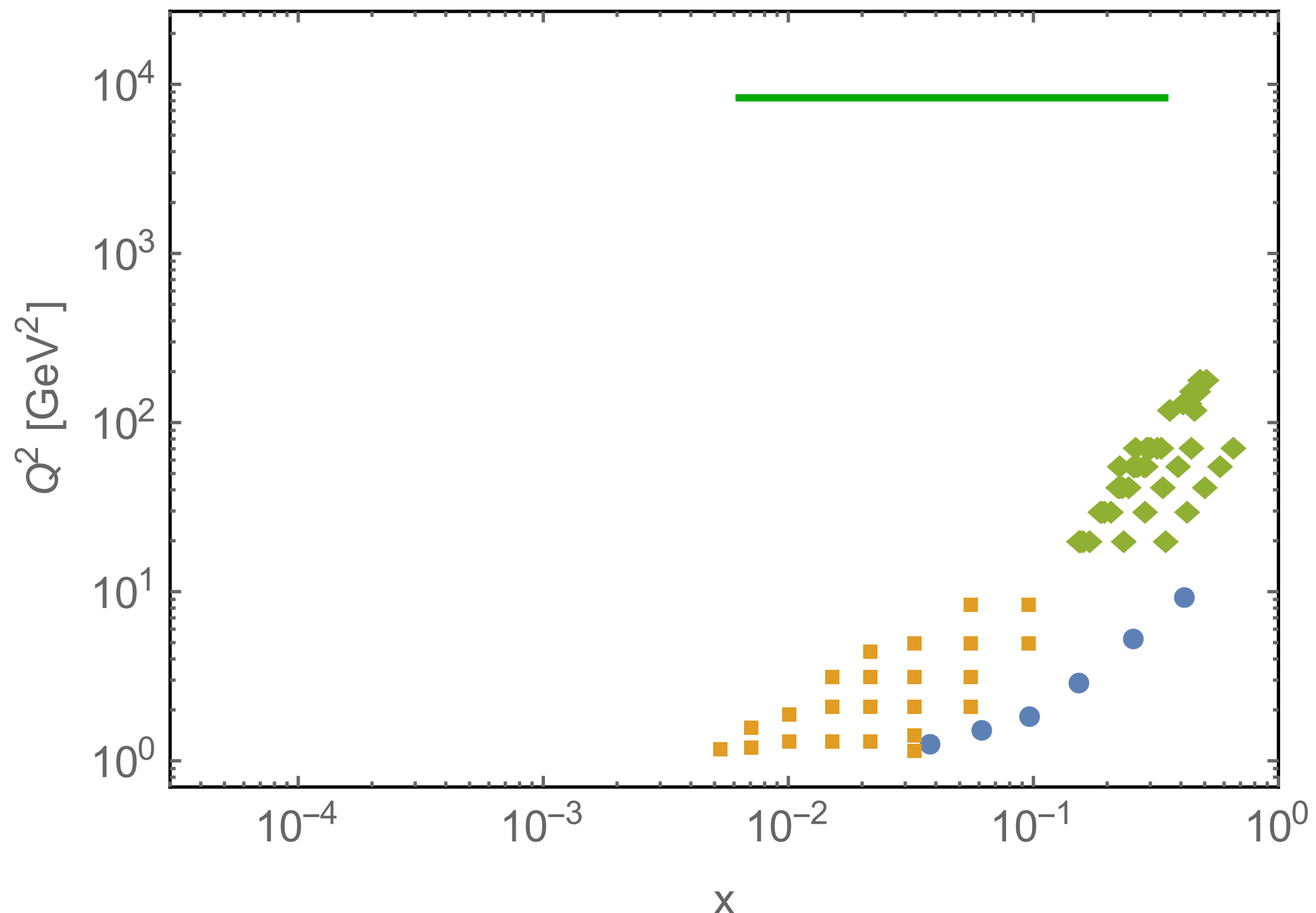
Experiments



Drell-Yan@
Fermilab

Ito et al., PRD93 (81)
Moreno et al. PRD 43 (91)
Antreyan et al. PRL47 (81)

Experiments



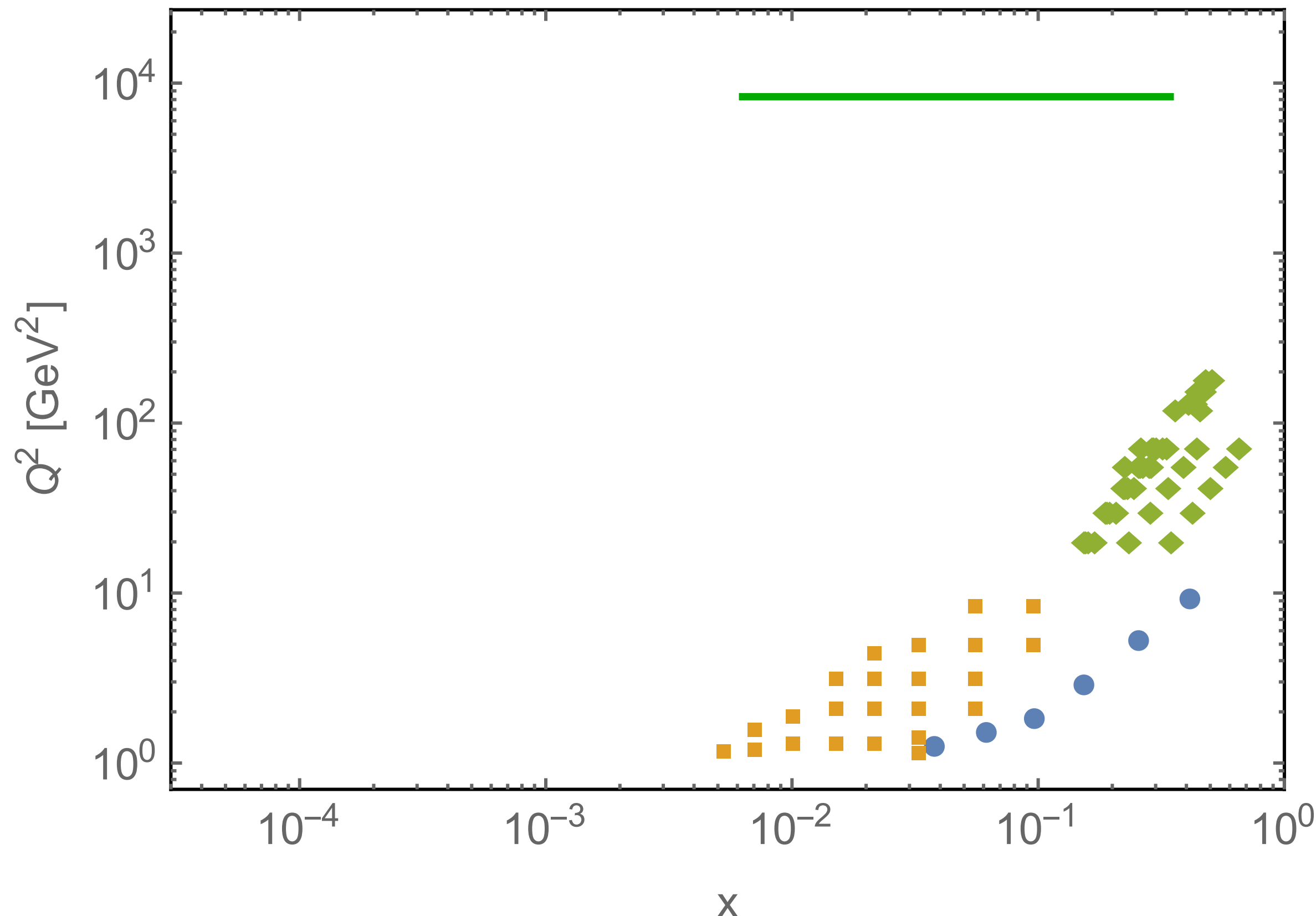
Z production@
Fermilab

Abbot et al. hep-ex/9909020
Affolder et al. hep-ex/0001021
Abazov et al. arXiv:0712.0803
Aaltonen et al. arXiv:1207.7138

Drell-Yan@
Fermilab

Ito et al., PRD93 (81)
Moreno et al. PRD 43 (91)
Antreyan et al. PRL47 (81)

Experiments



Z production@
Fermilab

Abbot et al. hep-ex/9909020
Affolder et al. hep-ex/0001021
Abazov et al. arXiv:0712.0803
Aaltonen et al. arXiv:1207.7138

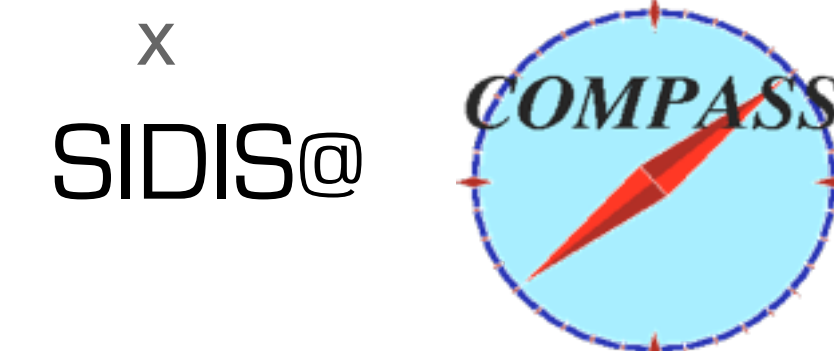
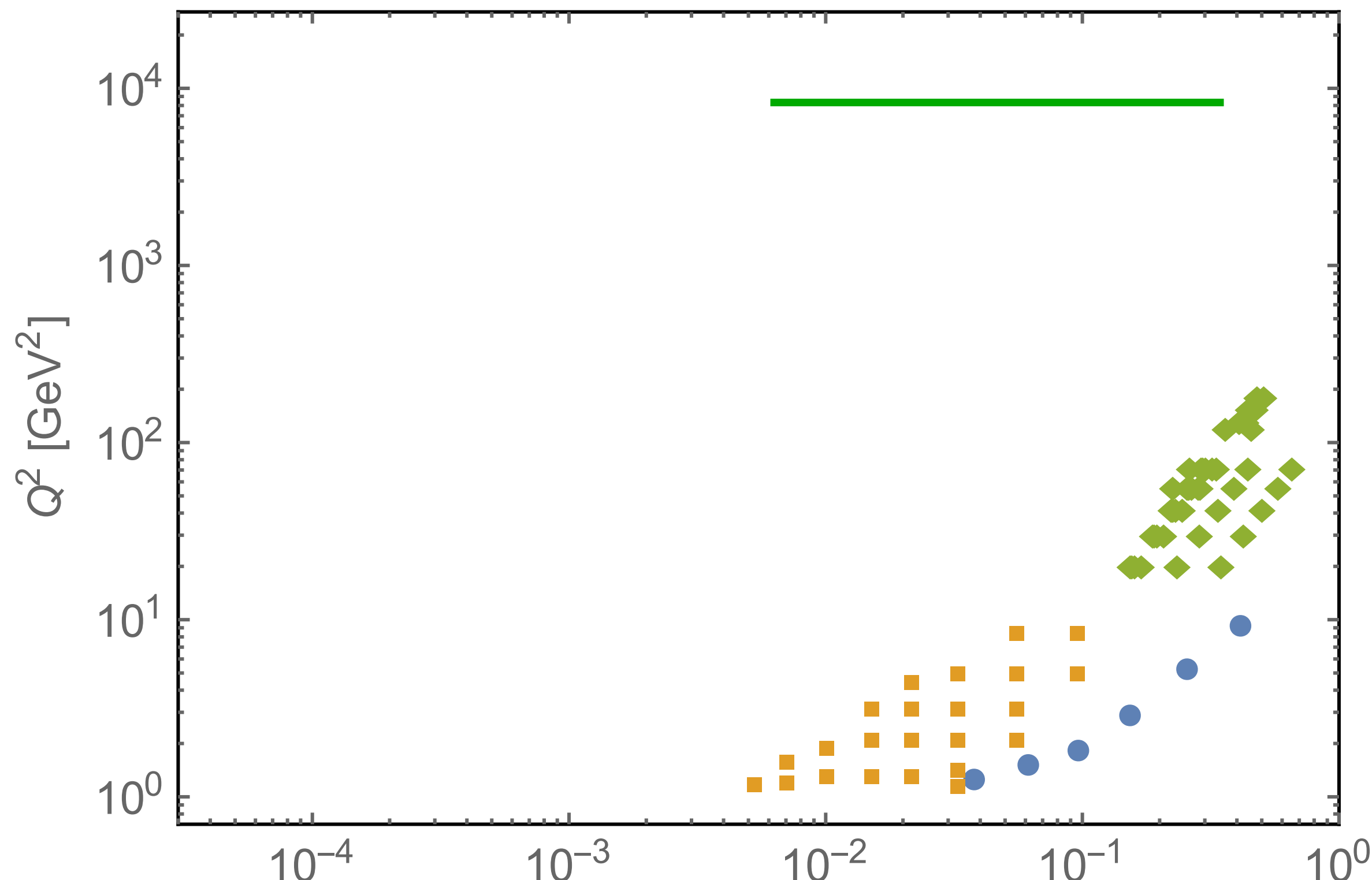
Drell-Yan@
Fermilab

Ito et al., PRD93 (81)
Moreno et al. PRD 43 (91)
Antreyan et al. PRL47 (81)

SIDIS@
hermes

Airapetian et al., PRD87 (2013)

Experiments



SIDIS@

X

Adolph et al., EPJ C73 (13)

Z production@
Fermilab

Abbot et al. hep-ex/9909020
Affolder et al. hep-ex/0001021
Abazov et al. arXiv:0712.0803
Aaltonen et al. arXiv:1207.7138

Drell-Yan@
Fermilab

Ito et al., PRD93 (81)
Moreno et al. PRD 43 (91)
Antreyan et al. PRL47 (81)

SIDIS@
hermes

Airapetian et al., PRD87 (2013)

Presently or soon available fits

	Framework	HERMES	COMPASS	DY	Z production	N of points
KN 2006 <i>hep-ph/0506225</i>	NLL	✗	✗	✓	✓	98
Pavia 2013 (+Amsterdam,Bilbao) <i>arXiv:1309.3507</i>	No evo	✓	✗	✗	✗	1538
Torino 2014 (+JLab) <i>arXiv:1312.6261</i>	No evo	✓ (separately)	✓ (separately)	✗	✗	576 (H) 6284 (C)
DEMS 2014 <i>arXiv:1407.3311</i>	NNLL	✗	✗	✓	✓	223
EIKV 2014 <i>arXiv:1401.5078</i>	NLL	1 [x,Q ²] bin	1 [x,Q ²] bin	✓	✓	500 (?)
Pavia 2016	NLL	✓	✓	✓	✓	8059

The TMD “eight-thousander” fit



Broad Peak, Karakorum, 8051 m

The TMD “eight-thousander” fit

Pavia 2016

8000 data points

Broad Peak, Karakorum, 8051 m

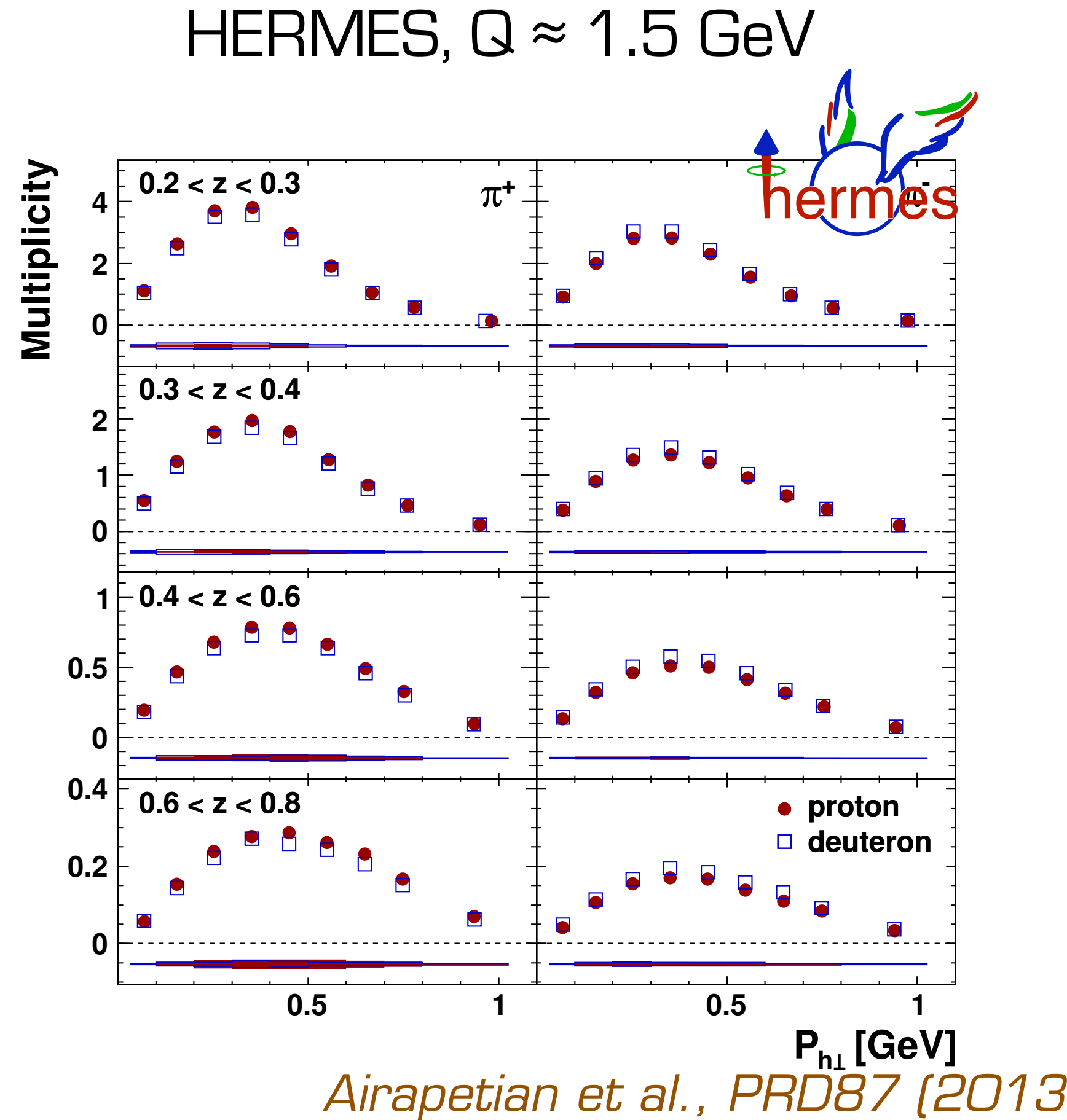
Executive summary of Pavia 2016 results 1/3

Total number of data points: 8059

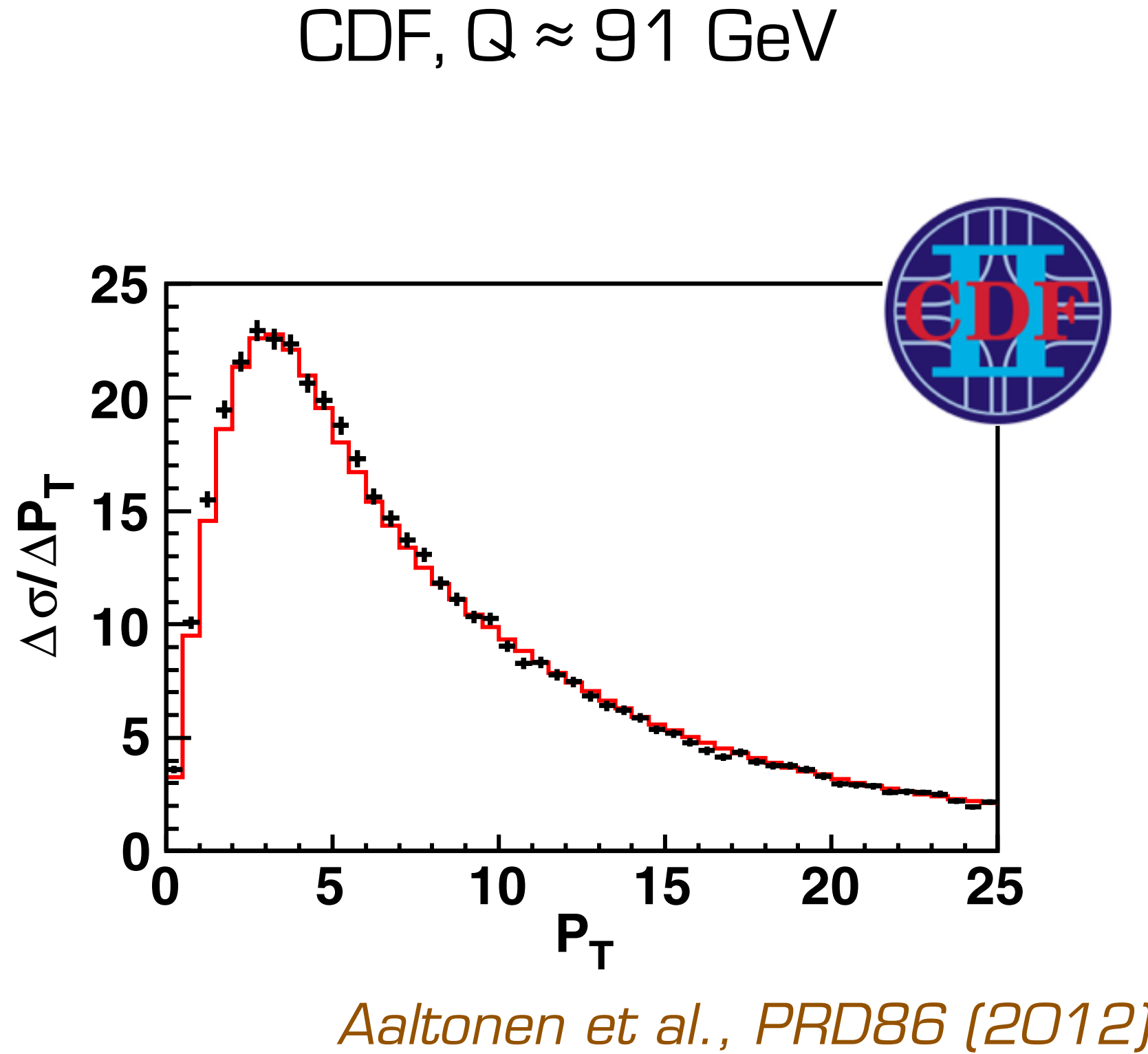
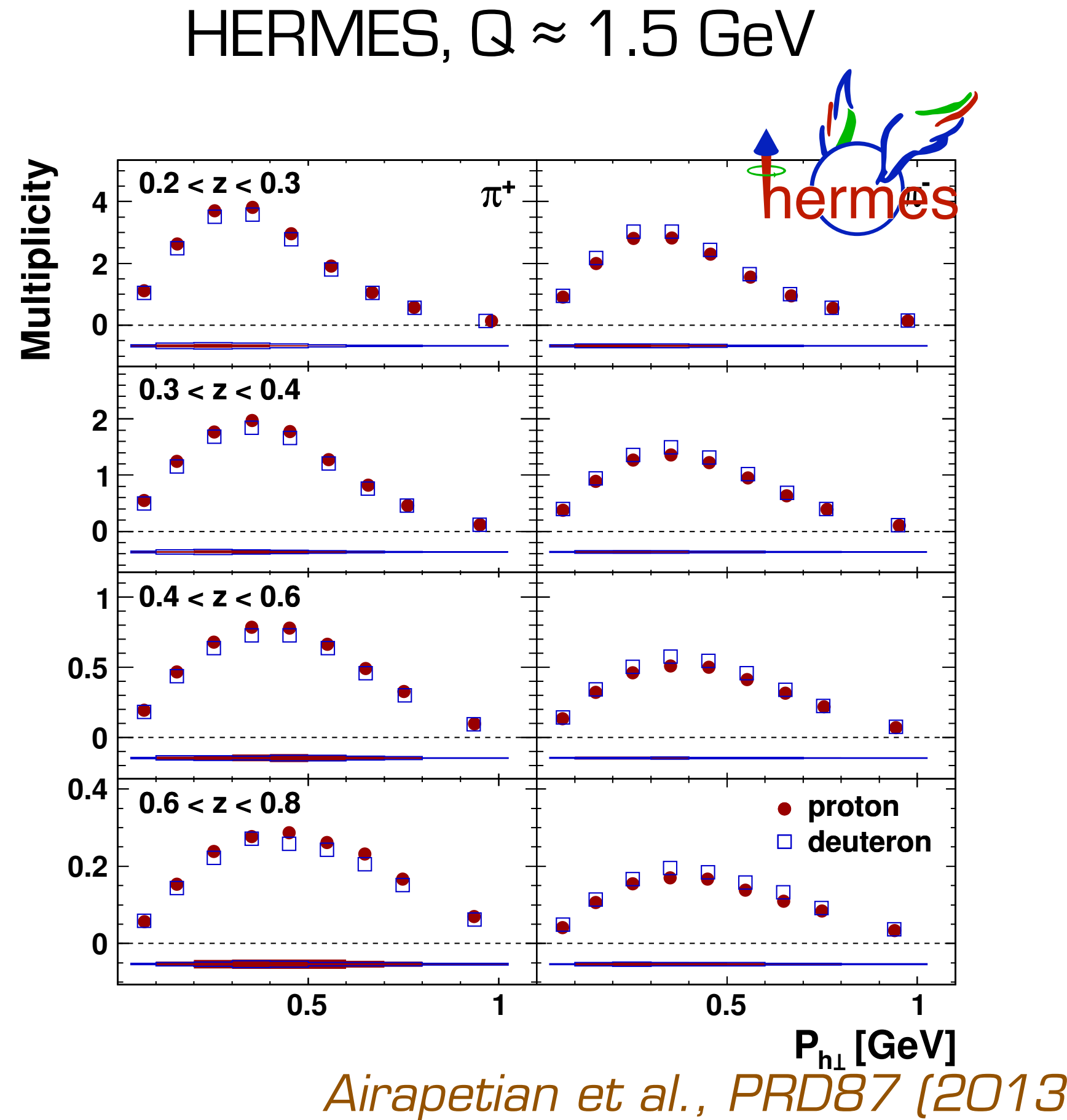
Total number of free parameters: 11
(4 for TMD PDFs, 6 for TMD FFs, 1 for TMD evolution)

Total $\chi^2/\text{dof} = 1.52 \pm 0.03$

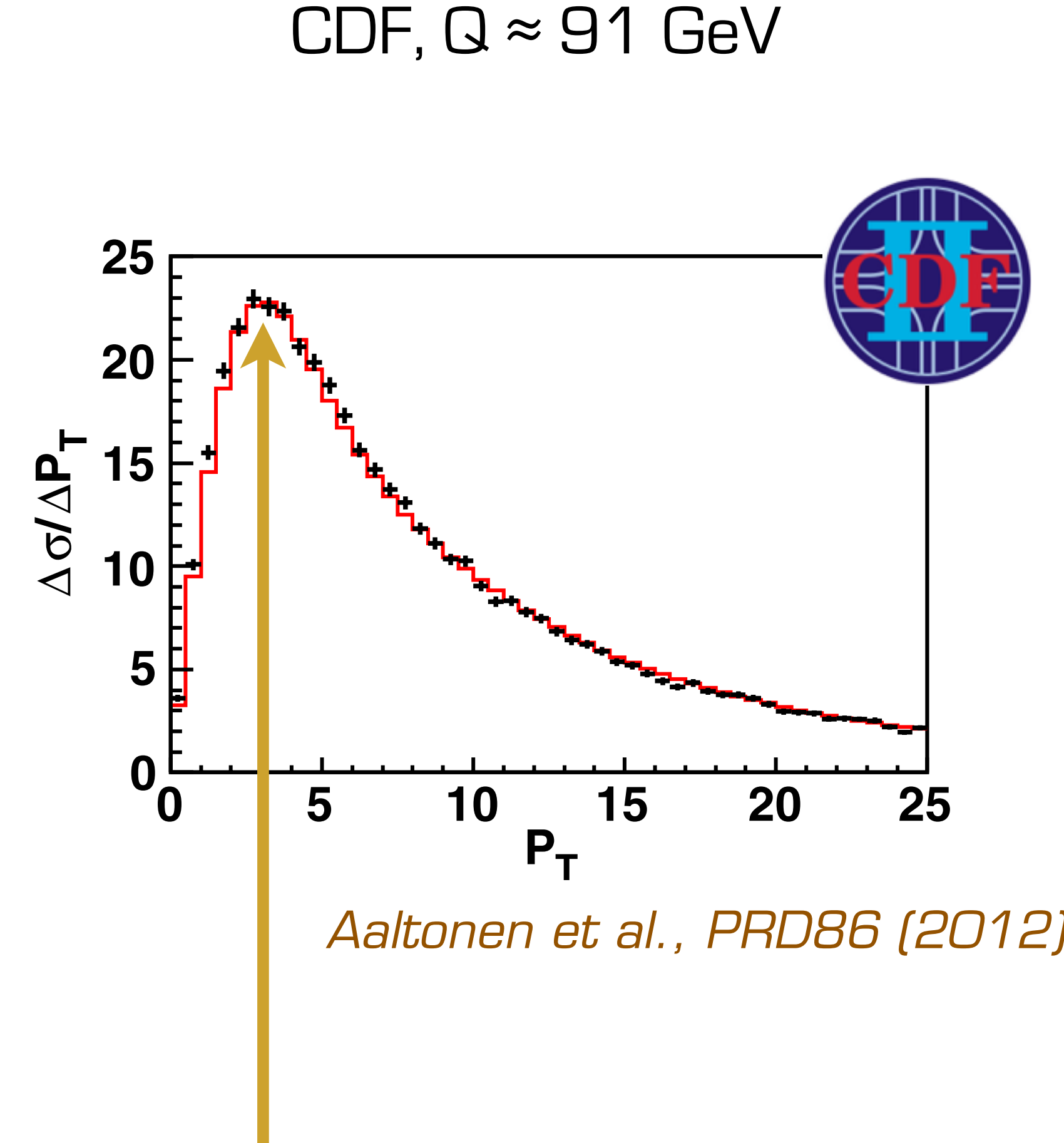
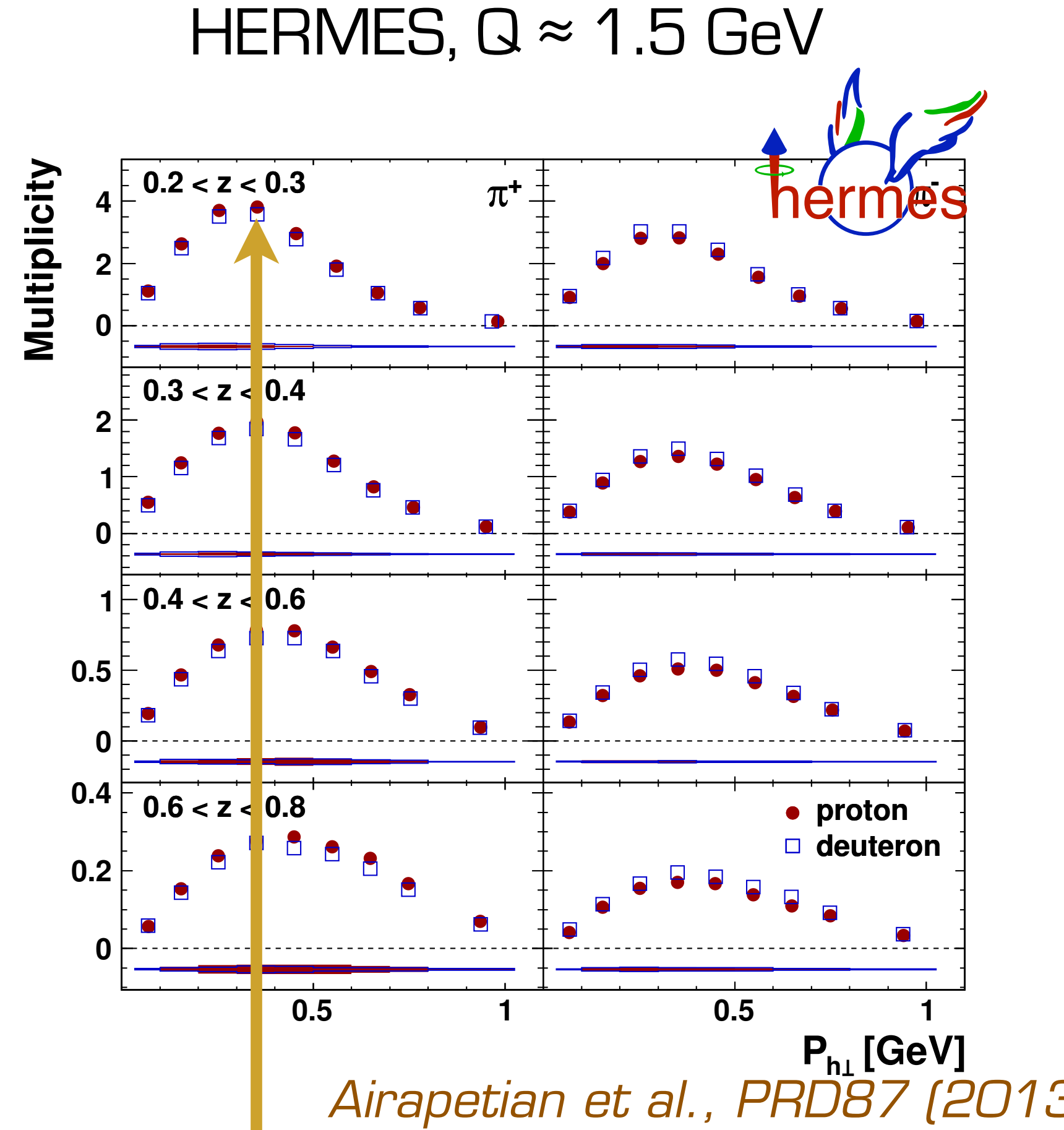
Executive summary of results 2/3



Executive summary of results 2/3

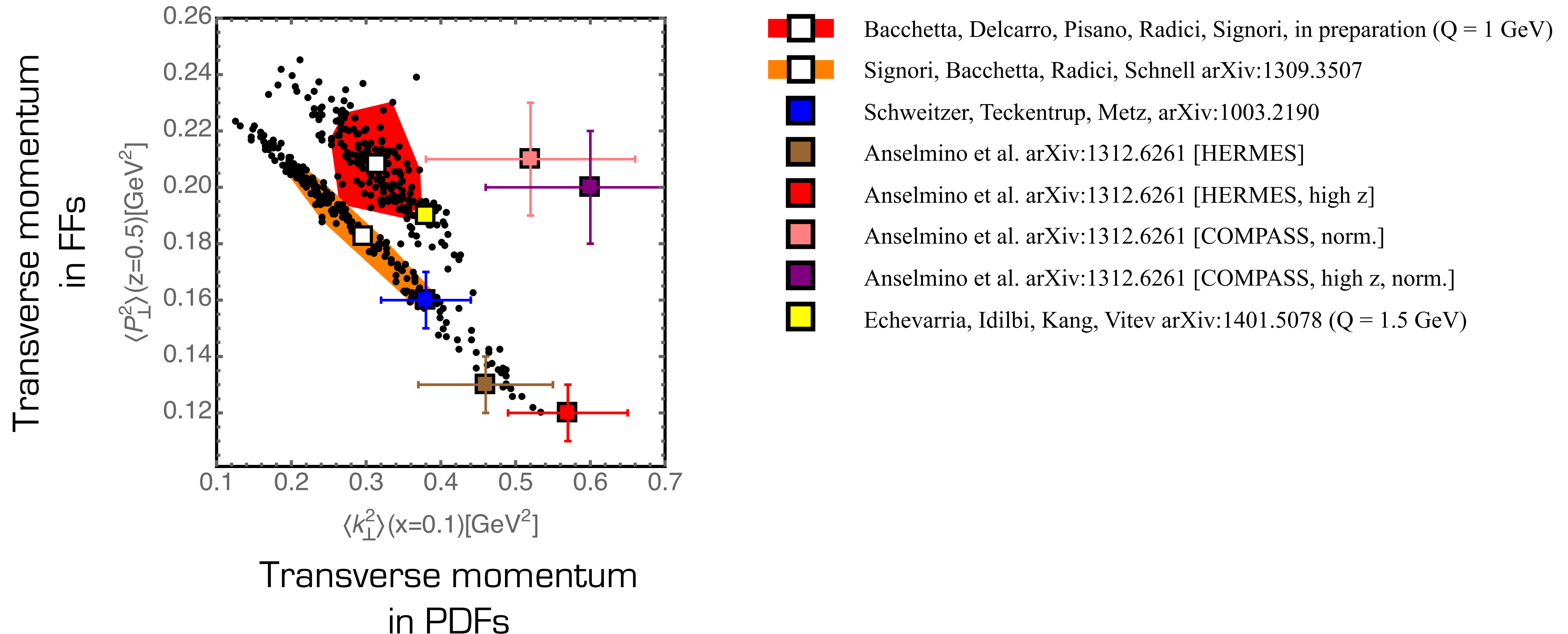


Executive summary of results 2/3

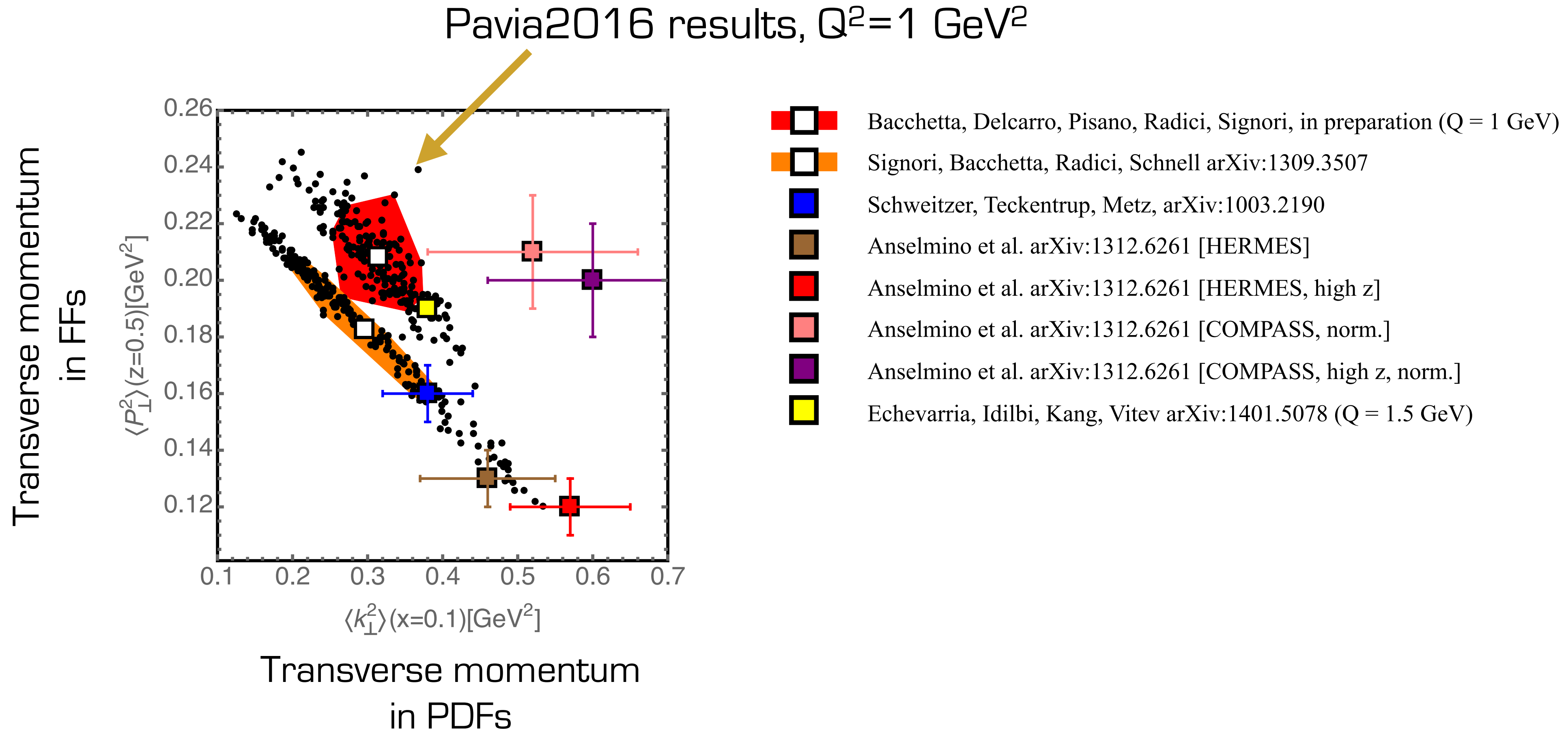


Width of TMDs changes of one order of magnitude: we can explain this with TMD evolution

Executive summary of results 3/3

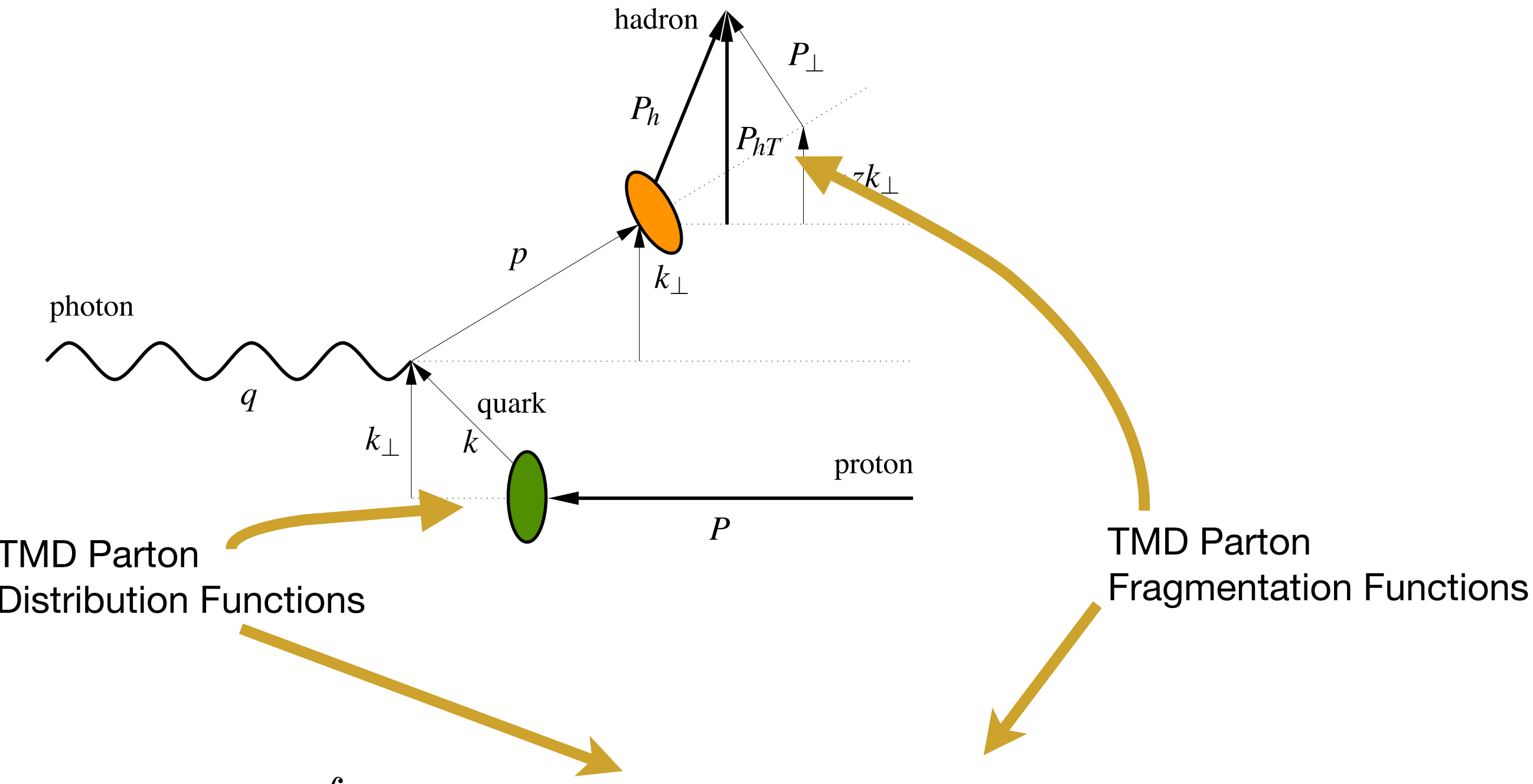


Executive summary of results 3/3



Some details

Structure functions and TMDs



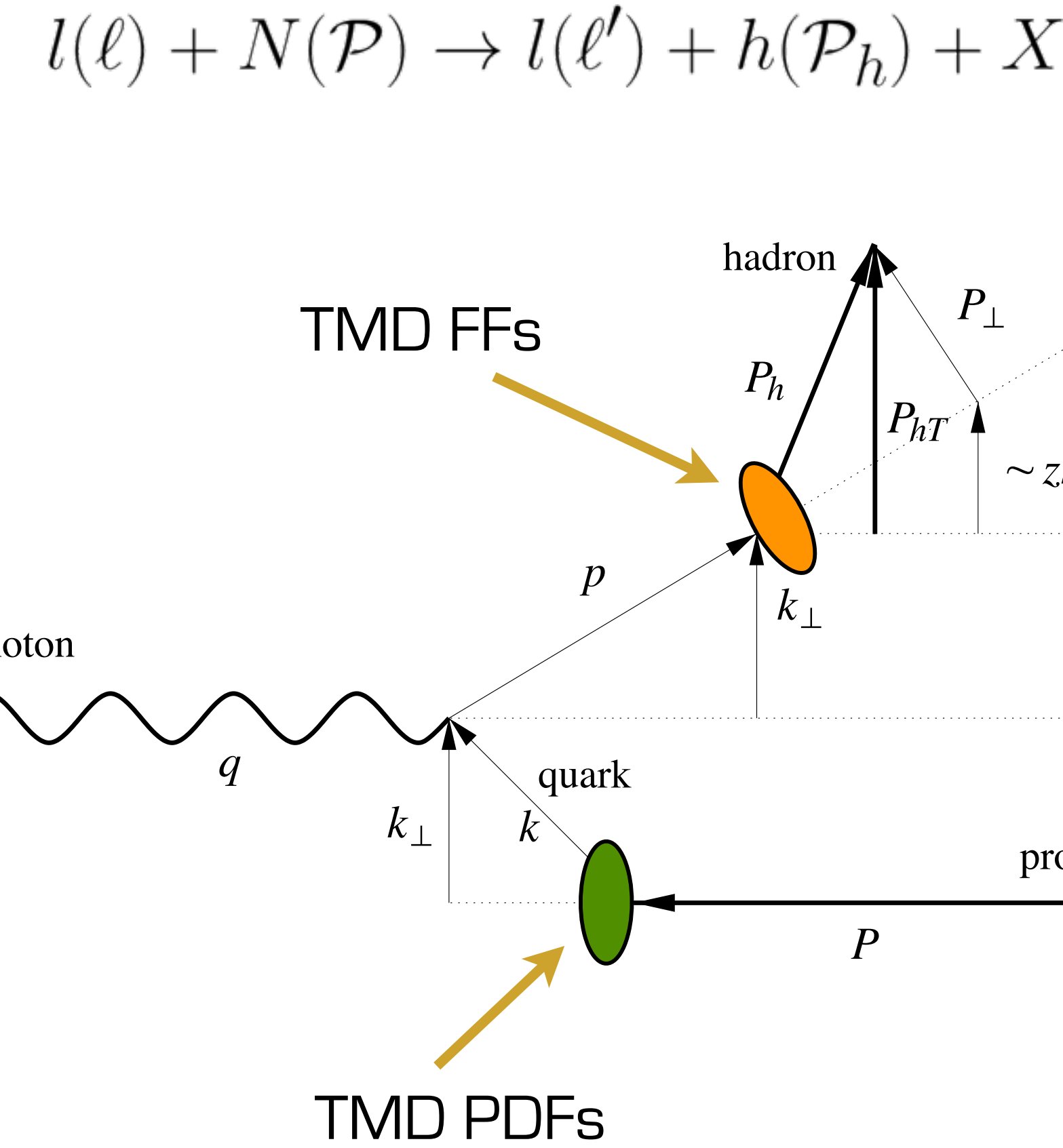
$$F_{UU,T}(x, z, \mathbf{P}_{hT}^2, Q^2) = \sum_a \mathcal{H}_{UU,T}^a(Q^2; \mu^2) \int d\mathbf{k}_\perp d\mathbf{P}_\perp f_1^a(x, \mathbf{k}_\perp^2; \mu^2) D_1^{a \rightarrow h}(z, \mathbf{P}_\perp^2; \mu^2) \delta(z\mathbf{k}_\perp - \mathbf{P}_{hT} + \mathbf{P}_\perp)$$
$$+ \cancel{Y_{UU,T}(Q^2, \mathbf{P}_{hT}^2)} + \mathcal{O}(M^2/Q^2)$$

see talk by Bowen Wang

Semi-inclusive DIS

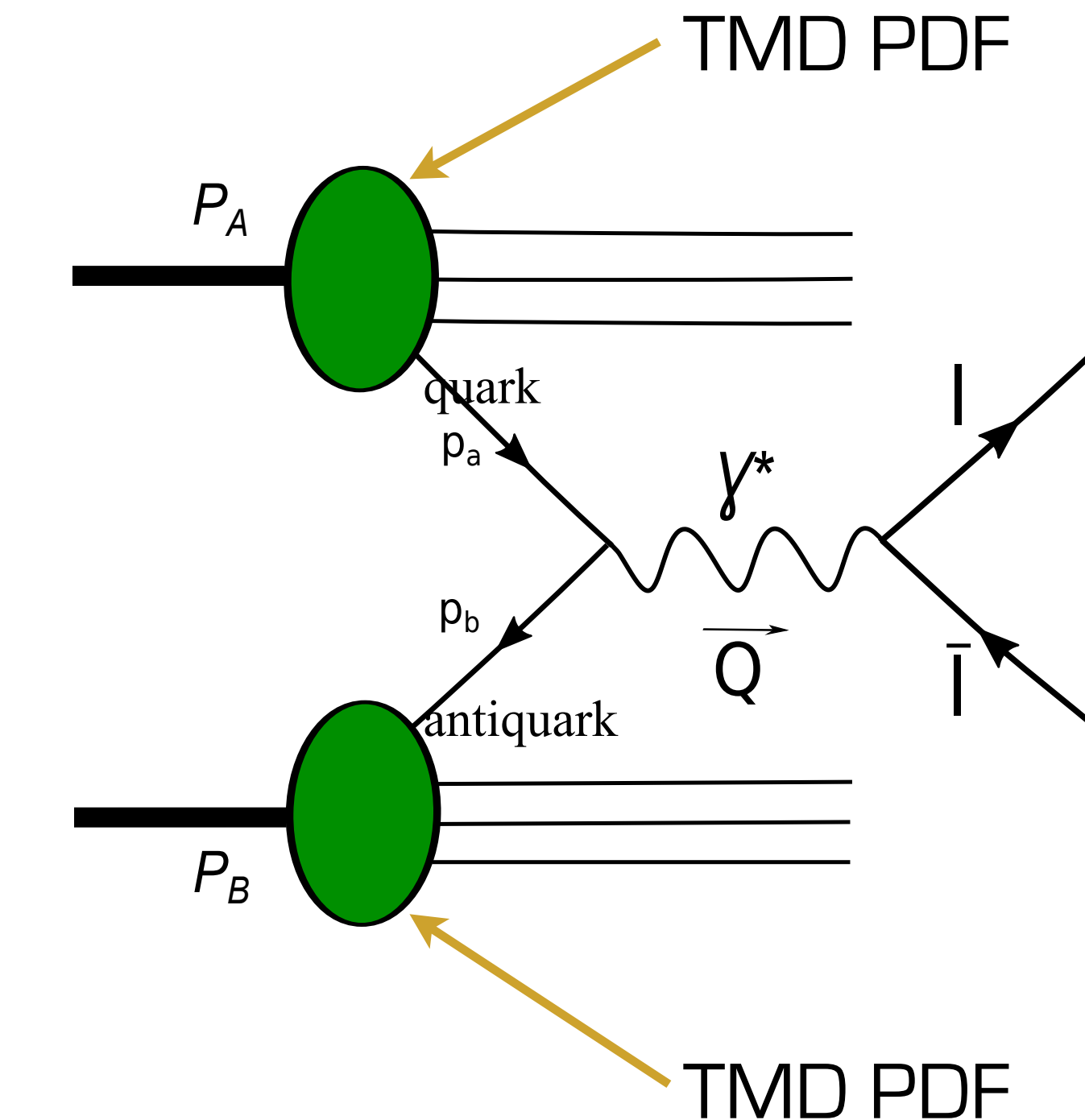
vs.

Drell-Yan/Z production



$$A + B \rightarrow \gamma^* \rightarrow l^+ l^-$$

$$A + B \rightarrow Z \rightarrow l^+ l^-$$



TMD evolution: Fourier transform

$$f_1^a(x, k_\perp; \mu^2) = \frac{1}{2\pi} \int d^2 b_T e^{-ib_T \cdot k_\perp} \tilde{f}_1^a(x, b_T; \mu^2)$$

*Rogers, Aybat, PRD 83 (11)
Collins, "Foundations of Perturbative QCD" (11)*

*possible schemes, e.g.,
Collins, Soper, Sterman, NPB250 (85)
Laenen, Sterman, Vogelsang, PRL 84 (00)
Echevarria, Idilbi, Schaefer, Scimemi, EPJ C73 (13)*

TMD evolution: Fourier transform

$$f_1^a(x, k_\perp; \mu^2) = \frac{1}{2\pi} \int d^2 b_T e^{-ib_T \cdot k_\perp} \tilde{f}_1^a(x, b_T; \mu^2)$$

$$\tilde{f}_1^a(x, b_T; \mu^2) = \sum_i (\tilde{C}_{a/i} \otimes f_1^i)(x, b_*; \mu_b) e^{\tilde{S}(b_*; \mu_b, \mu)} e^{g_K(b_T) \ln \frac{\mu}{\mu_0}} \hat{f}_{\text{NP}}^a(x, b_T)$$

*Rogers, Aybat, PRD 83 (11)
Collins, "Foundations of Perturbative QCD" (11)*

*possible schemes, e.g.,
Collins, Soper, Sterman, NPB250 (85)
Laenen, Sterman, Vogelsang, PRL 84 (00)
Echevarria, Idilbi, Schaefer, Scimemi, EPJ C73 (13)*

TMD evolution: Fourier transform

$$f_1^a(x, k_\perp; \mu^2) = \frac{1}{2\pi} \int d^2 b_T e^{-ib_T \cdot k_\perp} \tilde{f}_1^a(x, b_T; \mu^2)$$

$$\tilde{f}_1^a(x, b_T; \mu^2) = \sum_i (\tilde{C}_{a/i} \otimes f_1^i)(x, b_*; \mu_b) e^{\tilde{S}(b_*; \mu_b, \mu)} e^{g_K(b_T) \ln \frac{\mu}{\mu_0}} \hat{f}_{\text{NP}}^a(x, b_T)$$

collinear PDF

i

pQCD

nonperturbative part of evolution

nonperturbative part of TMD

Rogers, Aybat, PRD 83 (11)
Collins, "Foundations of Perturbative QCD" (11)

possible schemes, e.g.,
Collins, Soper, Sterman, NPB250 (85)
Laenen, Sterman, Vogelsang, PRL 84 (00)
Echevarria, Idilbi, Schaefer, Scimemi, EPJ C73 (13)

Perturbative ingredients

$$\tilde{f}_1^a(x, b_T; \mu^2) = \sum_i (\tilde{C}_{a/i} \otimes f_1^i)(x, b_*; \mu_b) e^{\tilde{S}(b_*; \mu_b, \mu)} e^{g_K(b_T) \ln \frac{\mu}{\mu_0}} \hat{f}_{\text{NP}}^a(x, b_T)$$

Perturbative ingredients

$$\tilde{f}_1^a(x, b_T; \mu^2) = \sum_i (\tilde{C}_{a/i} \otimes f_1^i)(x, b_*; \mu_b) e^{\tilde{S}(b_*; \mu_b, \mu)} e^{g_K(b_T) \ln \frac{\mu}{\mu_0}} \hat{f}_{\text{NP}}^a(x, b_T)$$

A diagram illustrating the perturbative expansion of the function \tilde{f}_1^a . A red curved arrow originates from the term $\tilde{C}_{a/i}$ in the sum and points to two sets of terms: $A_i(\mathcal{O}(\alpha_S^1))$ and $B_i(\mathcal{O}(\alpha_S^1))$. Below these, another set of terms $A_{i+1}(\mathcal{O}(\alpha_S^2))$ and $B_{i+1}(\mathcal{O}(\alpha_S^2))$ are shown, followed by ellipses.

$$A_1(\mathcal{O}(\alpha_S^1)) \quad A_2(\mathcal{O}(\alpha_S^2)) \quad A_3(\mathcal{O}(\alpha_S^3)) \quad \dots$$
$$B_1(\mathcal{O}(\alpha_S^1)) \quad B_2(\mathcal{O}(\alpha_S^2)) \quad \dots$$

Perturbative ingredients

$$\tilde{f}_1^a(x, b_T; \mu^2) = \sum_i (\tilde{C}_{a/i} \otimes f_1^i)(x, b_*; \mu_b) e^{\tilde{S}(b_*; \mu_b, \mu)} e^{g_K(b_T) \ln \frac{\mu}{\mu_0}} \hat{f}_{\text{NP}}^a(x, b_T)$$

The diagram illustrates the perturbative expansion of the function \tilde{f}_1^a . A red curved arrow originates from the term $\tilde{C}_{a/i} \otimes f_1^i$ in the sum and points to three parallel rows of terms. The first row contains $A_1(\mathcal{O}(\alpha_S^1))$, $A_2(\mathcal{O}(\alpha_S^2))$, $A_3(\mathcal{O}(\alpha_S^3))$, and three ellipses. The second row contains $B_1(\mathcal{O}(\alpha_S^1))$, $B_2(\mathcal{O}(\alpha_S^2))$, and two ellipses. The third row contains $C_0(\mathcal{O}(\alpha_S^0))$, $C_1(\mathcal{O}(\alpha_S^1))$, $C_2(\mathcal{O}(\alpha_S^2))$, and three ellipses.

$$A_1(\mathcal{O}(\alpha_S^1)) \quad A_2(\mathcal{O}(\alpha_S^2)) \quad A_3(\mathcal{O}(\alpha_S^3)) \quad \dots$$
$$B_1(\mathcal{O}(\alpha_S^1)) \quad B_2(\mathcal{O}(\alpha_S^2)) \quad \dots$$
$$C_0(\mathcal{O}(\alpha_S^0)) \quad C_1(\mathcal{O}(\alpha_S^1)) \quad C_2(\mathcal{O}(\alpha_S^2)) \quad \dots$$

Perturbative ingredients

$$\tilde{f}_1^a(x, b_T; \mu^2) = \sum_i (\tilde{C}_{a/i} \otimes f_1^i)(x, b_*; \mu_b) e^{\tilde{S}(b_*; \mu_b, \mu)} e^{g_K(b_T) \ln \frac{\mu}{\mu_0}} \hat{f}_{\text{NP}}^a(x, b_T)$$

$A_1(\mathcal{O}(\alpha_S^1))$	$A_2(\mathcal{O}(\alpha_S^2))$	$A_3(\mathcal{O}(\alpha_S^3))$	\dots
$B_1(\mathcal{O}(\alpha_S^1))$	$B_2(\mathcal{O}(\alpha_S^2))$	\dots	
$C_0(\mathcal{O}(\alpha_S^0))$	$C_1(\mathcal{O}(\alpha_S^1))$	$C_2(\mathcal{O}(\alpha_S^2))$	\dots
<hr/>			
$H_0(\mathcal{O}(\alpha_S^0))$	$H_1(\mathcal{O}(\alpha_S^1))$	$H_2(\mathcal{O}(\alpha_S^2))$	\dots
	$Y_1(\mathcal{O}(\alpha_S^1))$	$Y_2(\mathcal{O}(\alpha_S^2))$	\dots

Pavia 2016 perturbative ingredients

$$\tilde{f}_1^a(x, b_T; \mu^2) = \sum_i (\tilde{C}_{a/i} \otimes f_1^i)(x, b_*; \mu_b) e^{\tilde{S}(b_*; \mu_b, \mu)} e^{g_K(b_T) \ln \frac{\mu}{\mu_0}} \hat{f}_{\text{NP}}^a(x, b_T)$$

$A_1(\mathcal{O}(\alpha_S^1))$	$A_2(\mathcal{O}(\alpha_S^2))$	$A_3(\mathcal{O}(\alpha_S^3))$	\dots
$B_1(\mathcal{O}(\alpha_S^1))$	$B_2(\mathcal{O}(\alpha_S^2))$	\dots	
$C_0(\mathcal{O}(\alpha_S^0))$	$C_1(\mathcal{O}(\alpha_S^1))$	$C_2(\mathcal{O}(\alpha_S^2))$	\dots
<hr/>			
$H_0(\mathcal{O}(\alpha_S^0))$	$H_1(\mathcal{O}(\alpha_S^1))$	$H_2(\mathcal{O}(\alpha_S^2))$	\dots
	$Y_1(\mathcal{O}(\alpha_S^1))$	$Y_2(\mathcal{O}(\alpha_S^2))$	\dots

μ and b_* prescriptions

$$\tilde{f}_1^a(x, b_T; \mu^2) = \sum_i (\tilde{C}_{a/i} \otimes f_1^i)(x, b_*; \mu_b) e^{\tilde{S}(b_*; \mu_b, \mu)} e^{g_K(b_T) \ln \frac{\mu}{\mu_0}} \hat{f}_{\text{NP}}^a(x, b_T)$$

μ and b_* prescriptions

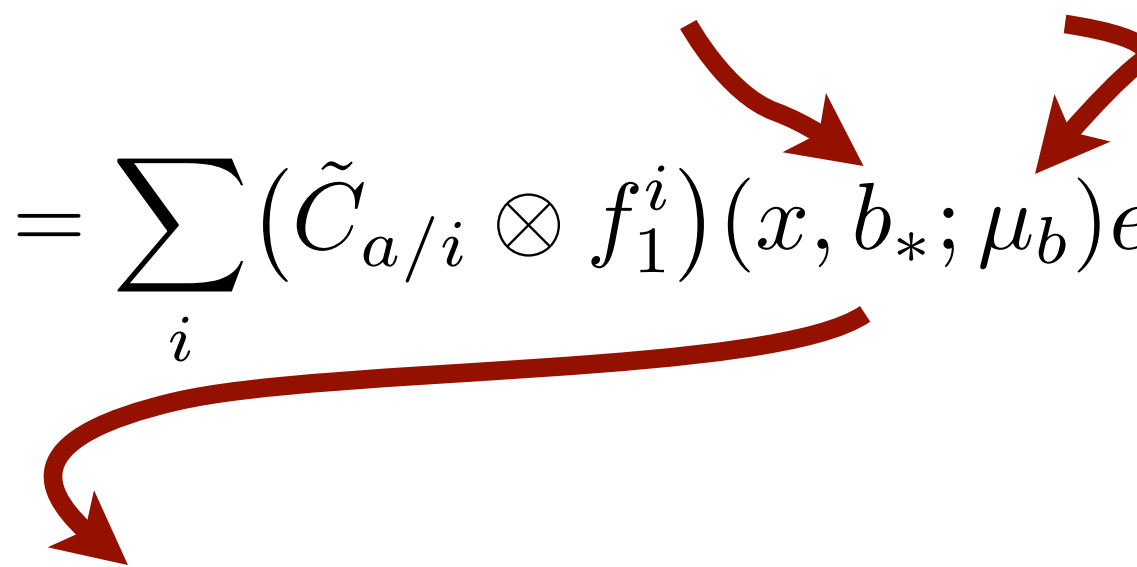
Choice Choice

$$\tilde{f}_1^a(x, b_T; \mu^2) = \sum_i (\tilde{C}_{a/i} \otimes f_1^i)(x, b_*; \mu_b) e^{\tilde{S}(b_*; \mu_b, \mu)} e^{g_K(b_T) \ln \frac{\mu}{\mu_0}} \hat{f}_{\text{NP}}^a(x, b_T)$$

μ and b_* prescriptions

Choice Choice

$$\tilde{f}_1^a(x, b_T; \mu^2) = \sum_i (\tilde{C}_{a/i} \otimes f_1^i)(x, b_*; \mu_b) e^{\tilde{S}(b_*; \mu_b, \mu)} e^{g_K(b_T) \ln \frac{\mu}{\mu_0}} \hat{f}_{\text{NP}}^a(x, b_T)$$



$$\mu_b = 2e^{-\gamma_E}/b_* \quad b_* \equiv \frac{b_T}{\sqrt{1 + b_T^2/b_{\max}^2}}$$

Collins, Soper, Sterman, NPB250 (85)

$$\mu_b = 2e^{-\gamma_E}/b_* \quad b_* \equiv b_{\max} \left(1 - e^{-\frac{b_T^4}{b_{\max}^4}}\right)^{1/4}$$

Bacchetta, Echevarria, Mulders, Radici, Signori
[arXiv:1508.00402](https://arxiv.org/abs/1508.00402)

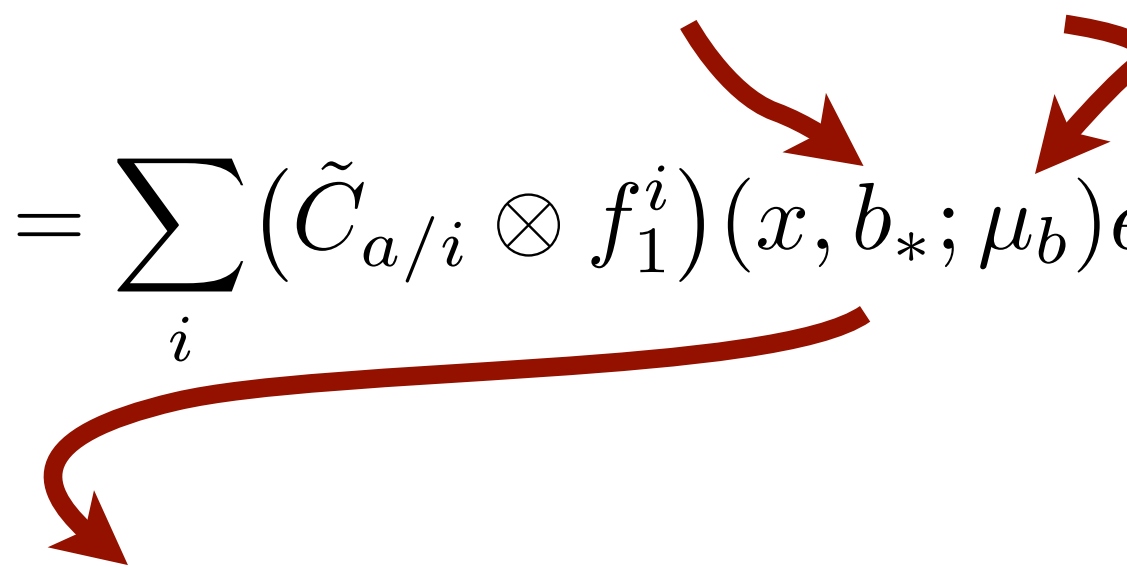
$$\mu_b = Q_0 + q_T \quad b_* = b_T$$

DEMS 2014

μ and b_* prescriptions

Choice Choice

$$\tilde{f}_1^a(x, b_T; \mu^2) = \sum_i (\tilde{C}_{a/i} \otimes f_1^i)(x, b_*; \mu_b) e^{\tilde{S}(b_*; \mu_b, \mu)} e^{g_K(b_T) \ln \frac{\mu}{\mu_0}} \hat{f}_{\text{NP}}^a(x, b_T)$$



$$\mu_b = 2e^{-\gamma_E}/b_* \quad b_* \equiv \frac{b_T}{\sqrt{1 + b_T^2/b_{\max}^2}}$$

Collins, Soper, Sterman, NPB250 (85)

$$\mu_b = 2e^{-\gamma_E}/b_* \quad b_* \equiv b_{\max} \left(1 - e^{-\frac{b_T^4}{b_{\max}^4}} \right)^{1/4}$$

Bacchetta, Echevarria, Mulders, Radici, Signori
[arXiv:1508.00402](https://arxiv.org/abs/1508.00402)

$$\mu_b = Q_0 + q_T \quad b_* = b_T$$

DEMS 2014

Complex-b prescription

Laenen, Sterman, Vogelsang, PRL 84 (00)

Nonperturbative ingredients 1

$$\tilde{f}_1^a(x, b_T; \mu^2) = \sum_i (\tilde{C}_{a/i} \otimes f_1^i)(x, b_*; \mu_b) e^{\tilde{S}(b_*; \mu_b, \mu)} e^{g_K(b_T) \ln \frac{\mu}{\mu_0}} \hat{f}_{\text{NP}}^a(x, b_T)$$

Nonperturbative ingredients 1

$$\tilde{f}_1^a(x, b_T; \mu^2) = \sum_i (\tilde{C}_{a/i} \otimes f_1^i)(x, b_*; \mu_b) e^{\tilde{S}(b_*; \mu_b, \mu)} e^{g_K(b_T) \ln \frac{\mu}{\mu_0}} \hat{f}_{\text{NP}}^a(x, b_T)$$

Choice
↗

Nonperturbative ingredients 1

$$\tilde{f}_1^a(x, b_T; \mu^2) = \sum_i (\tilde{C}_{a/i} \otimes f_1^i)(x, b_*; \mu_b) e^{\tilde{S}(b_*; \mu_b, \mu)} e^{g_K(b_T) \ln \frac{\mu}{\mu_0}} \hat{f}_{\text{NP}}^a(x, b_T)$$

$$e^{-\frac{b_T^2}{\langle b_T^2 \rangle}}$$

almost everybody

Choice

$$e^{-\frac{b_T^2}{\langle b_T^2(x) \rangle_a}}$$

Pavia 2013, KN 2006

$$e^{-\lambda_1 b_T} (1 + \lambda_2 b_T^2)$$

DEMS 2014

Nonperturbative ingredients 2

$$\tilde{f}_1^a(x, b_T; \mu^2) = \sum_i (\tilde{C}_{a/i} \otimes f_1^i)(x, b_*; \mu_b) e^{\tilde{S}(b_*; \mu_b, \mu)} e^{g_K(b_T) \ln \frac{\mu}{\mu_0}} \hat{f}_{\text{NP}}^a(x, b_T)$$

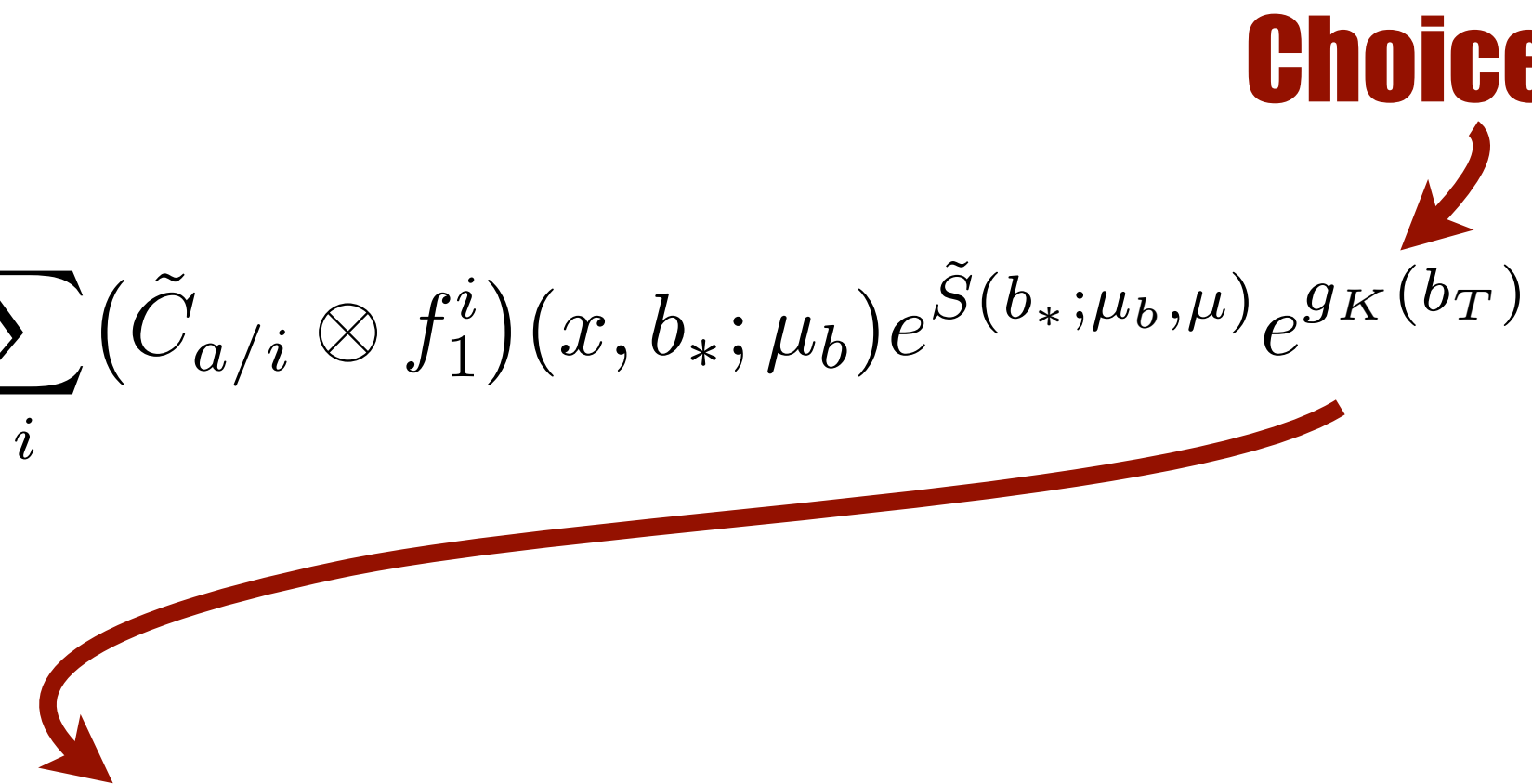
Nonperturbative ingredients 2

$$\tilde{f}_1^a(x, b_T; \mu^2) = \sum_i (\tilde{C}_{a/i} \otimes f_1^i)(x, b_*; \mu_b) e^{\tilde{S}(b_*; \mu_b, \mu)} e^{g_K(b_T) \ln \frac{\mu}{\mu_0}} \hat{f}_{\text{NP}}^a(x, b_T)$$

Choice
↓

Nonperturbative ingredients 2

$$\tilde{f}_1^a(x, b_T; \mu^2) = \sum_i (\tilde{C}_{a/i} \otimes f_1^i)(x, b_*; \mu_b) e^{\tilde{S}(b_*; \mu_b, \mu)} e^{g_K(b_T) \ln \frac{\mu}{\mu_0}} \hat{f}_{\text{NP}}^a(x, b_T)$$



Collins, Soper, Sterman, NPB250 (85)

$$-g_2 \frac{b_T^2}{2}$$

$$-2 g_2 \ln \left(1 + \frac{b_T^2}{4} \right)$$

Aidala, Field, Gumberg, Rogers, arXiv:1401.2654

$$-g_0(b_{\max}) \left(1 - \exp \left[- \frac{C_F \alpha_s(\mu_{b_*}) b_T^2}{\pi g_0(b_{\max}) b_{\max}^2} \right] \right)$$

Collins, Rogers, arXiv:1412.3820

Low- b_T modifications

$$\log(Q^2 b_T^2) \rightarrow \log(Q^2 b_T^2 + 1)$$

*see, e.g., Bozzi, Catani, De Florian, Grazzini
[hep-ph/0302104](#)*

Low- b_T modifications

$$\log(Q^2 b_T^2) \rightarrow \log(Q^2 b_T^2 + 1)$$

*see, e.g., Bozzi, Catani, De Florian, Grazzini
[hep-ph/0302104](#)*

$$b_*(b_c(b_T)) = \sqrt{\frac{b_T^2 + b_0^2/(C_5^2 Q^2)}{1 + b_T^2/b_{\max}^2 + b_0^2/(C_5^2 Q^2 b_{\max}^2)}}$$

$$b_{\min} \equiv b_*(b_c(0)) = \frac{b_0}{C_5 Q} \sqrt{\frac{1}{1 + b_0^2/(C_5^2 Q^2 b_{\max}^2)}}$$

Collins et al., [arXiv:1605.00671](#)

Low- b_T modifications

$$\log(Q^2 b_T^2) \rightarrow \log(Q^2 b_T^2 + 1)$$

*see, e.g., Bozzi, Catani, De Florian, Grazzini
[hep-ph/0302104](#)*

$$b_*(b_c(b_T)) = \sqrt{\frac{b_T^2 + b_0^2/(C_5^2 Q^2)}{1 + b_T^2/b_{\max}^2 + b_0^2/(C_5^2 Q^2 b_{\max}^2)}}$$

$$b_{\min} \equiv b_*(b_c(0)) = \frac{b_0}{C_5 Q} \sqrt{\frac{1}{1 + b_0^2/(C_5^2 Q^2 b_{\max}^2)}}$$

Collins et al., [arXiv:1605.00671](#)

Justification: the modification is allowed because it affects a region where the TMD formalism is anyway unreliable (high transverse momentum), and allows us to recover the integrated cross-section (unitarity constraint) instead of leading to infinite results.

Pavia 2016 “choices”

$$\tilde{f}_1^a(x, b_T; \mu^2) = \sum_i (\tilde{C}_{a/i} \otimes f_1^i)(x, \bar{b}_*; \mu_b) e^{\tilde{S}(\bar{b}_*; \mu_b, \mu)} e^{g_K(b_T) \ln \frac{\mu}{\mu_0}} \hat{f}_{\text{NP}}^a(x, b_T)$$

Pavia 2016 “choices”

$$\tilde{f}_1^a(x, b_T; \mu^2) = \sum_i (\tilde{C}_{a/i} \otimes f_1^i)(x, \bar{b}_*; \mu_b) e^{\tilde{S}(\bar{b}_*; \mu_b, \mu)} e^{g_K(b_T) \ln \frac{\mu}{\mu_0}} \hat{f}_{\text{NP}}^a(x, b_T)$$

$$g_K = -g_2 \frac{b_T^2}{2} \quad \mu_0 = 1 \text{ GeV}$$

Pavia 2016 “choices”

$$\tilde{f}_1^a(x, b_T; \mu^2) = \sum_i (\tilde{C}_{a/i} \otimes f_1^i)(x, \bar{b}_*; \mu_b) e^{\tilde{S}(\bar{b}_*; \mu_b, \mu)} e^{g_K(b_T) \ln \frac{\mu}{\mu_0}} \hat{f}_{\text{NP}}^a(x, b_T)$$

$$g_K = -g_2 \frac{b_T^2}{2} \quad \mu_0 = 1 \text{ GeV}$$

$$\mu_b = 2e^{-\gamma_E}/b_* \quad \bar{b}_* \equiv b_{\max} \left(\frac{1 - e^{-b_T^4/b_{\max}^4}}{1 - e^{-b_T^4/b_{\min}^4}} \right)^{1/4} \quad b_{\max} = 2e^{-\gamma_E}$$

$$b_{\min} = \frac{2e^{-\gamma_E}}{Q}$$

Pavia 2016 “choices”

$$\tilde{f}_1^a(x, b_T; \mu^2) = \sum_i (\tilde{C}_{a/i} \otimes f_1^i)(x, \bar{b}_*; \mu_b) e^{\tilde{S}(\bar{b}_*; \mu_b, \mu)} e^{g_K(b_T) \ln \frac{\mu}{\mu_0}} \hat{f}_{\text{NP}}^a(x, b_T)$$

$$g_K = -g_2 \frac{b_T^2}{2} \quad \mu_0 = 1 \text{ GeV}$$

$$\mu_b = 2e^{-\gamma_E}/b_* \quad \bar{b}_* \equiv b_{\max} \left(\frac{1 - e^{-b_T^4/b_{\max}^4}}{1 - e^{-b_T^4/b_{\min}^4}} \right)^{1/4} \quad b_{\max} = 2e^{-\gamma_E}$$

$$b_{\min} = \frac{2e^{-\gamma_E}}{Q}$$

Collinear PDF and FF sets: GJR08 NLO, DSS14 NLO for pions, DSS 07 for kaons

Pavia 2016 “choices”

$$\tilde{f}_1^a(x, b_T; \mu^2) = \sum_i (\tilde{C}_{a/i} \otimes f_1^i)(x, \bar{b}_*; \mu_b) e^{\tilde{S}(\bar{b}_*; \mu_b, \mu)} e^{g_K(b_T) \ln \frac{\mu}{\mu_0}} \hat{f}_{\text{NP}}^a(x, b_T)$$

$$g_K = -g_2 \frac{b_T^2}{2}$$

$$\mu_0 = 1 \text{ GeV}$$

$$\mu_b = 2e^{-\gamma_E}/b_*$$

$$\bar{b}_* \equiv b_{\max} \left(\frac{1 - e^{-b_T^4/b_{\max}^4}}{1 - e^{-b_T^4/b_{\min}^4}} \right)^{1/4} \quad b_{\max} = 2e^{-\gamma_E}$$

$$b_{\min} = \frac{2e^{-\gamma_E}}{Q}$$

These are all choices that should be
at some point checked/challenged

Collinear PDF and FF sets: GJR08 NLO, DSS14 NLO for pions, DSS 07 for kaons

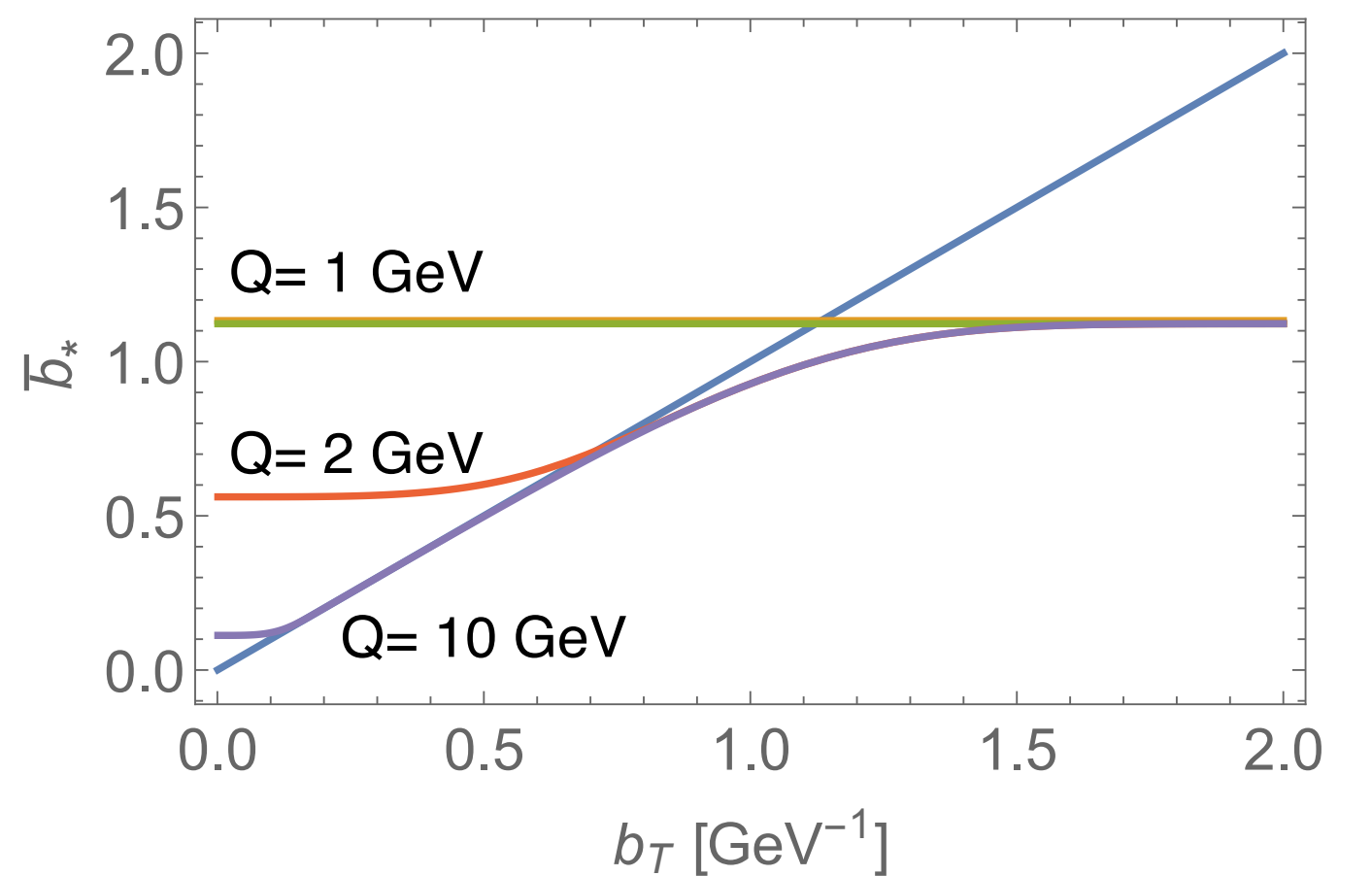
Effects of b_* prescription

$$\bar{b}_* \equiv b_{\max} \left(\frac{1 - e^{-b_T^4/b_{\max}^4}}{1 - e^{-b_T^4/b_{\min}^4}} \right)^{1/4}$$

$$b_{\max} = 2e^{-\gamma_E}$$

$$b_{\min} = \frac{2e^{-\gamma_E}}{Q}$$

$$\mu_b = 2e^{-\gamma_E}/b_*$$



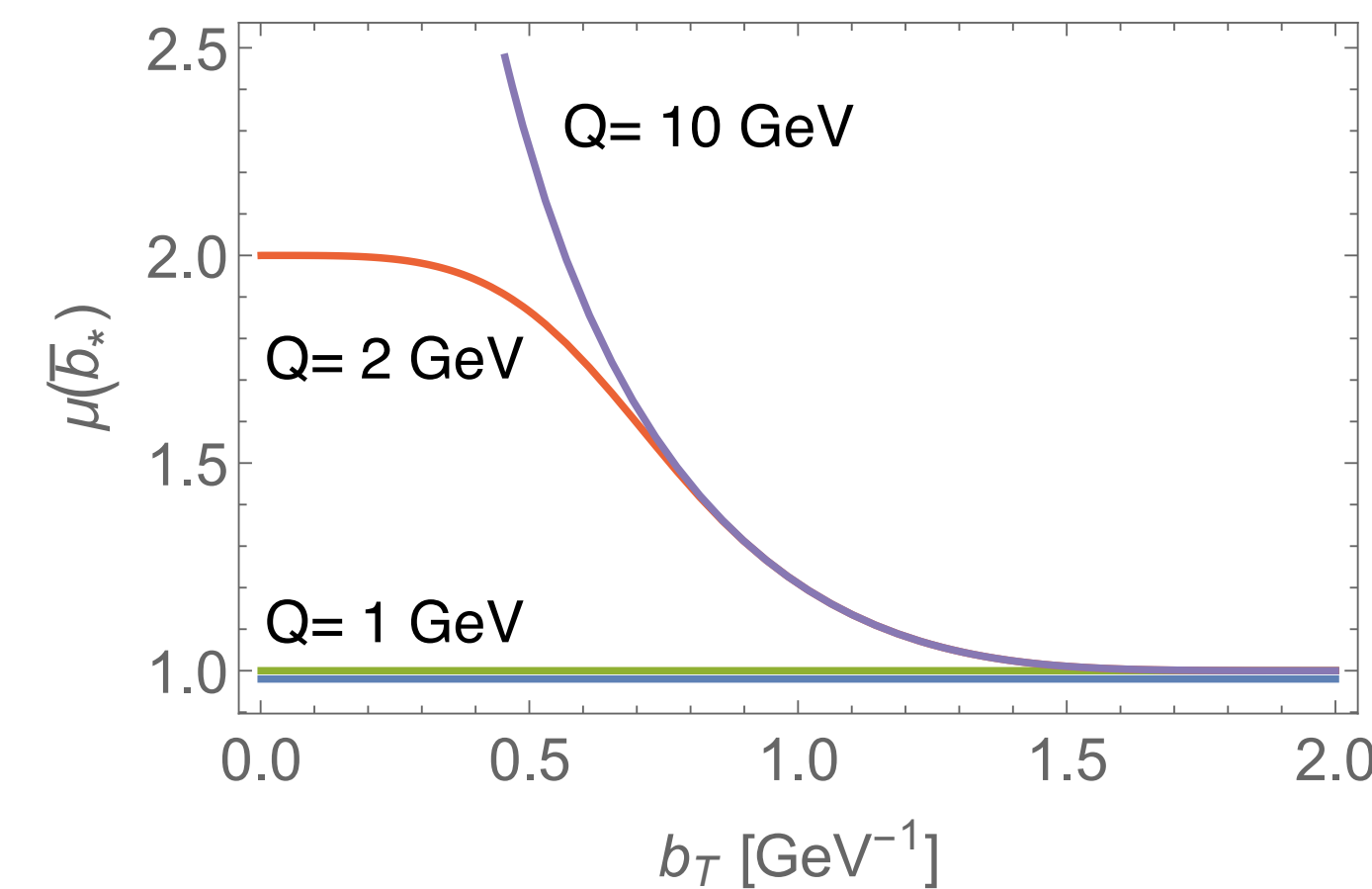
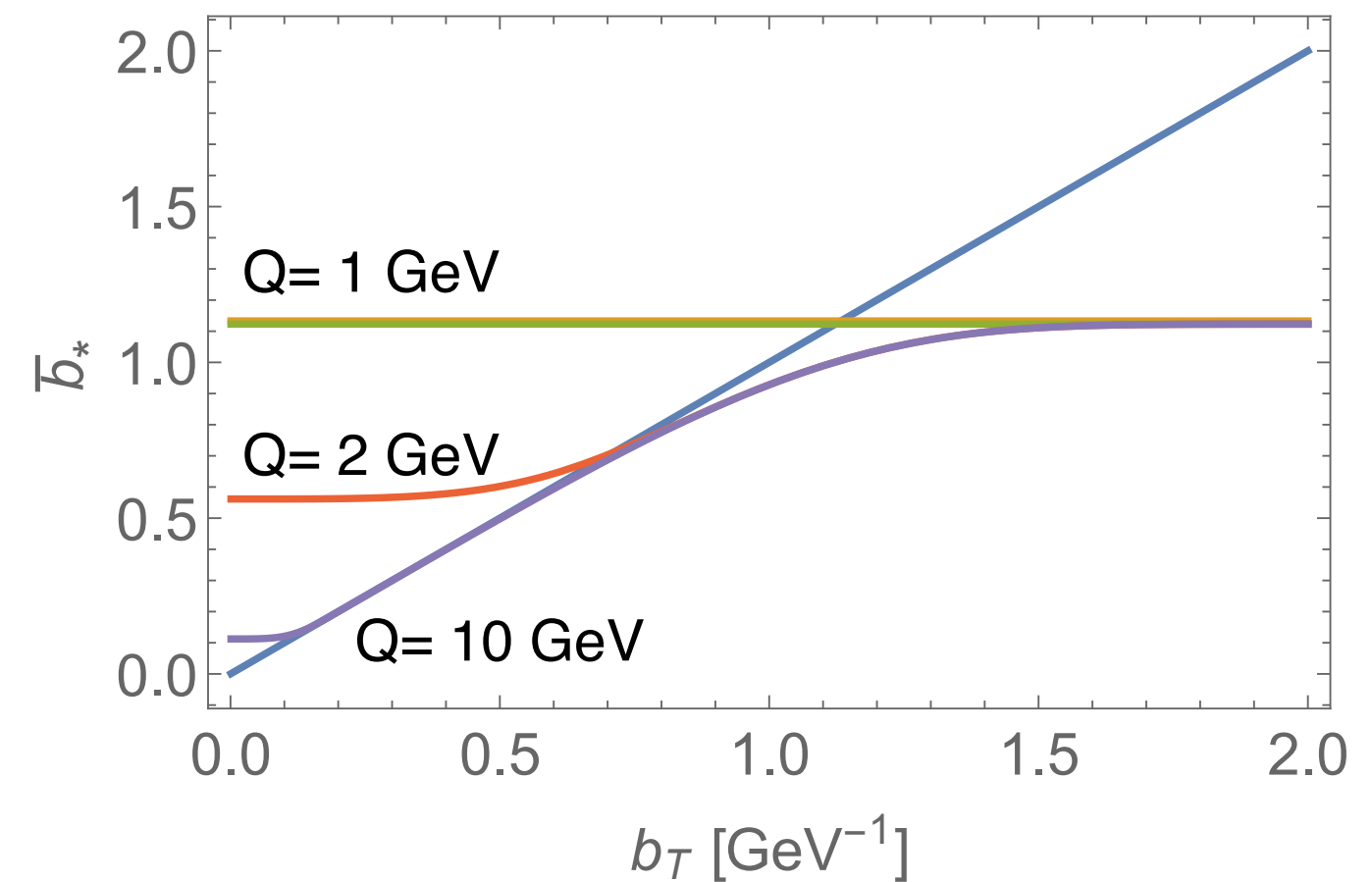
Effects of b_* prescription

$$\bar{b}_* \equiv b_{\max} \left(\frac{1 - e^{-b_T^4/b_{\max}^4}}{1 - e^{-b_T^4/b_{\min}^4}} \right)^{1/4}$$

$$b_{\max} = 2e^{-\gamma_E}$$

$$b_{\min} = \frac{2e^{-\gamma_E}}{Q}$$

$$\mu_b = 2e^{-\gamma_E}/b_*$$



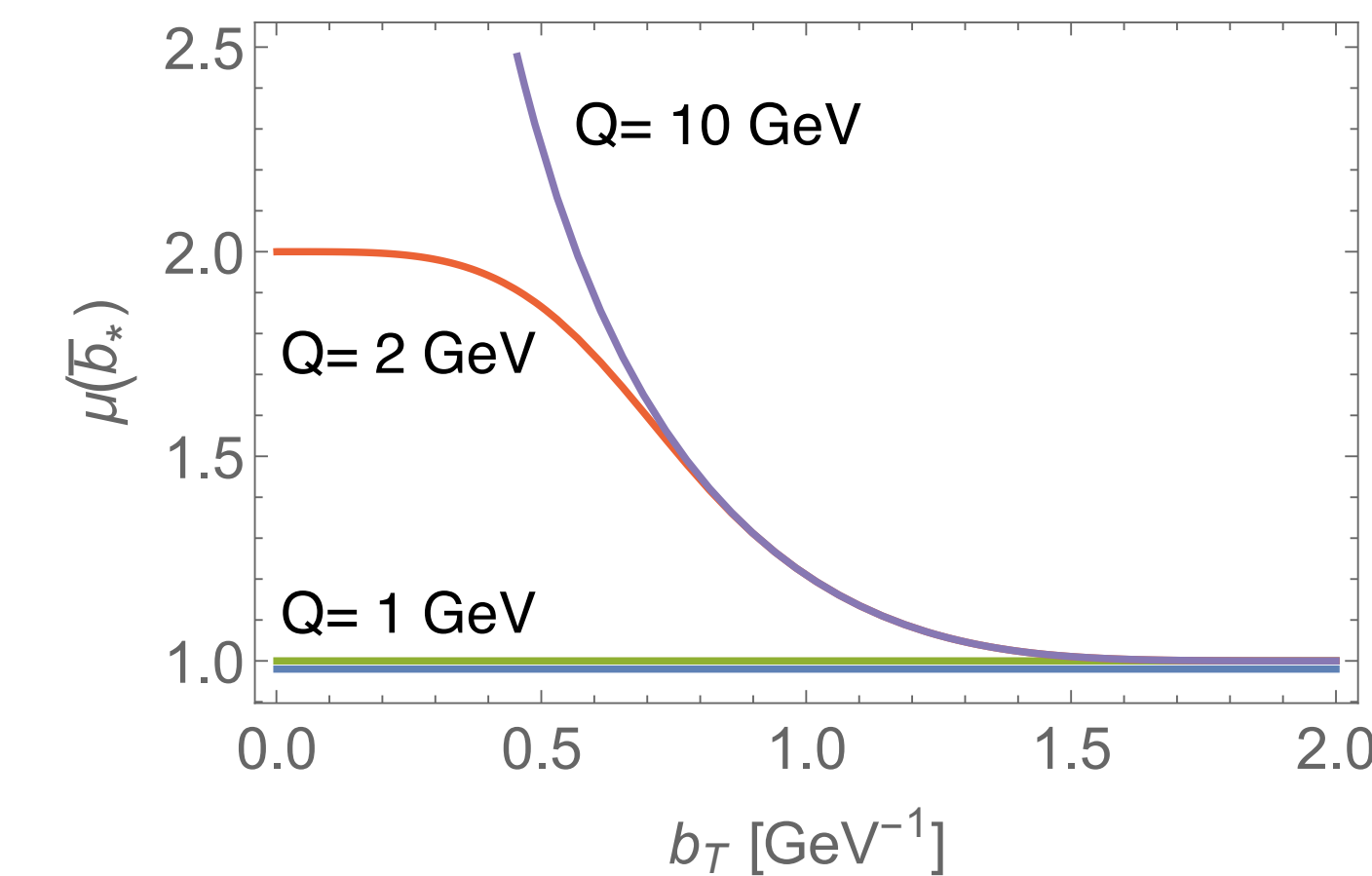
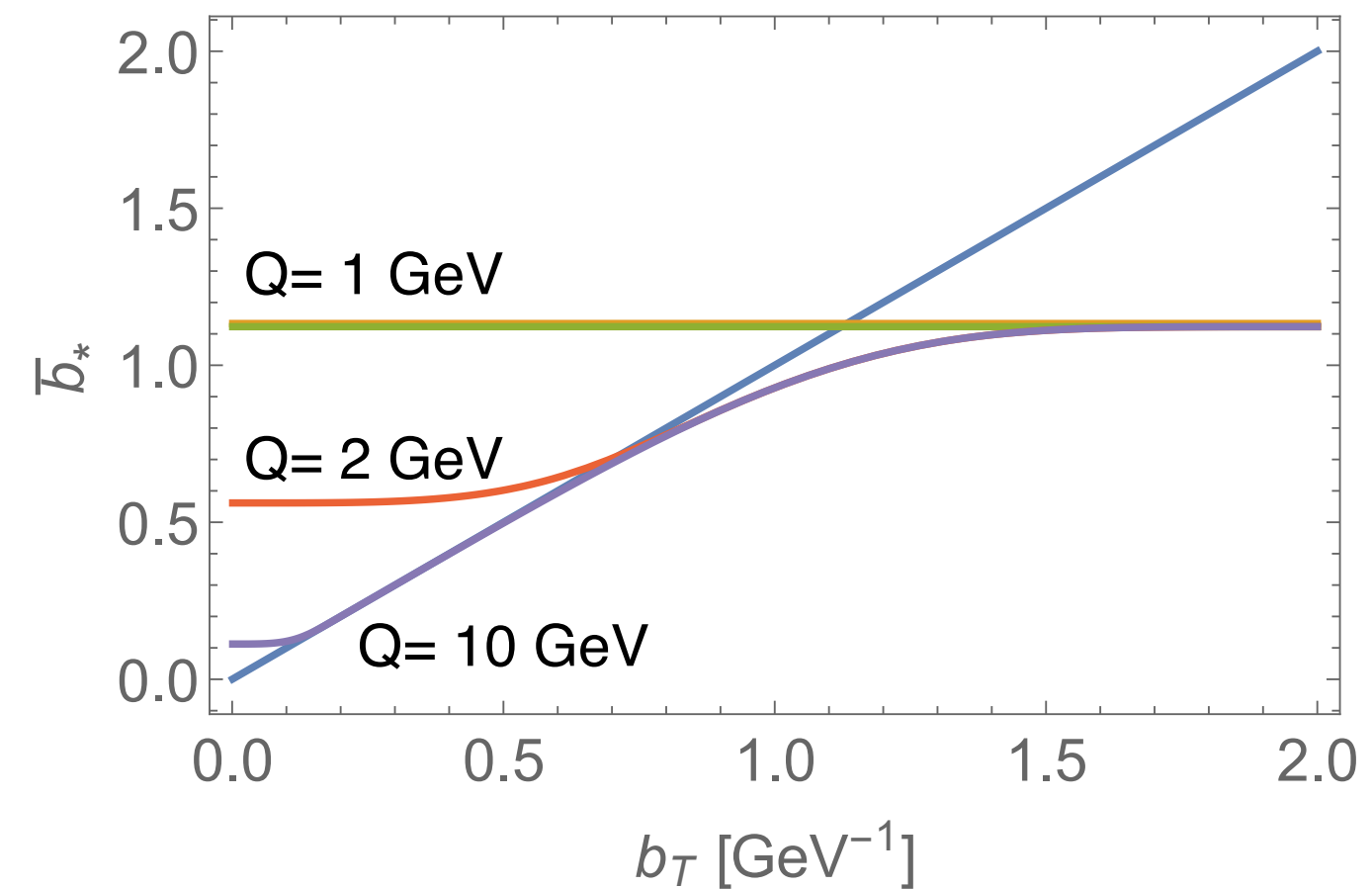
Effects of b_* prescription

$$\bar{b}_* \equiv b_{\max} \left(\frac{1 - e^{-b_T^4/b_{\max}^4}}{1 - e^{-b_T^4/b_{\min}^4}} \right)^{1/4}$$

$$b_{\max} = 2e^{-\gamma_E}$$

$$b_{\min} = \frac{2e^{-\gamma_E}}{Q}$$

$$\mu_b = 2e^{-\gamma_E}/b_*$$



μ_b never bigger than Q nor smaller than 1 GeV

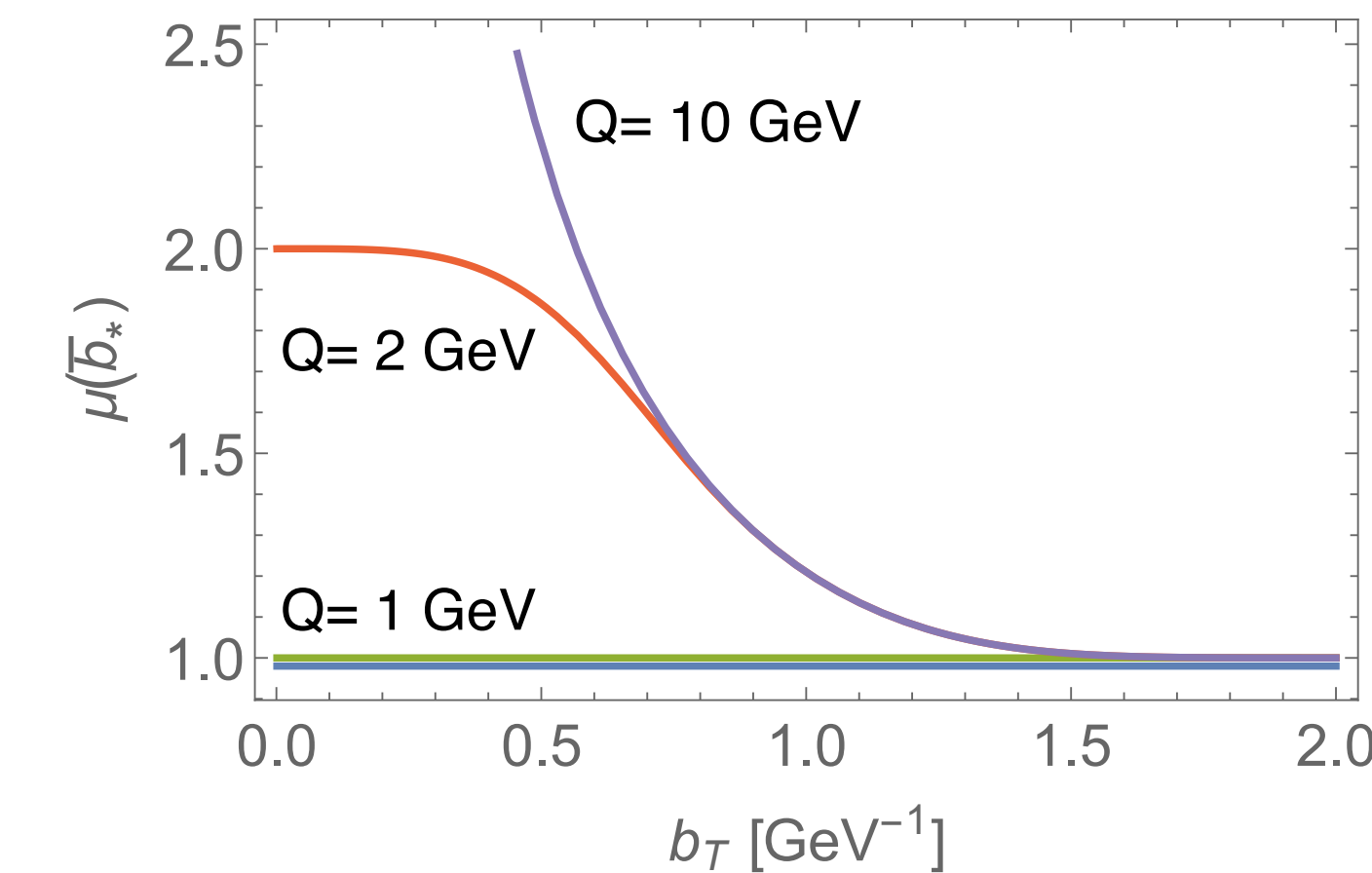
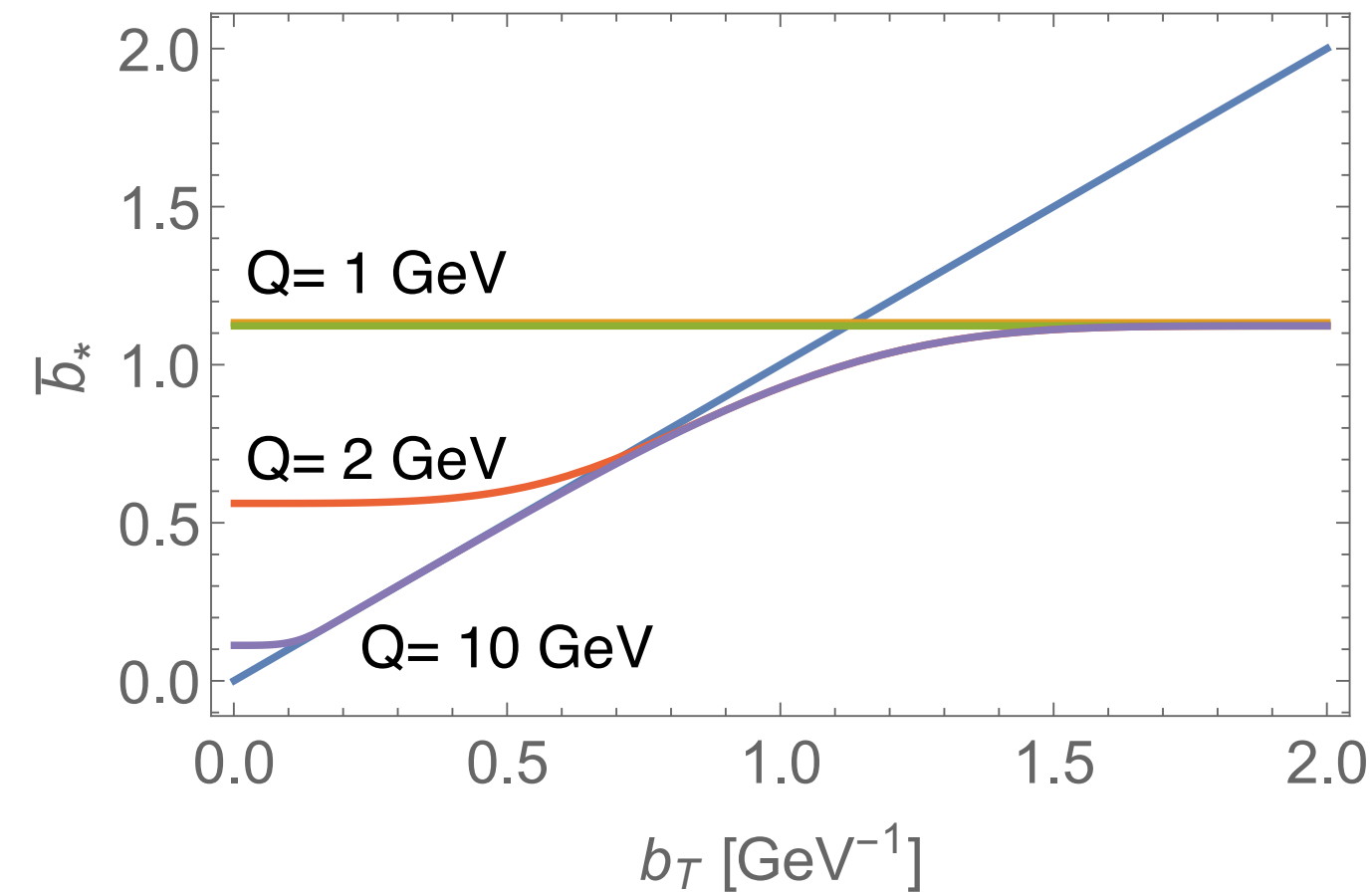
Effects of b_* prescription

$$\bar{b}_* \equiv b_{\max} \left(\frac{1 - e^{-b_T^4/b_{\max}^4}}{1 - e^{-b_T^4/b_{\min}^4}} \right)^{1/4}$$

$$b_{\max} = 2e^{-\gamma_E}$$

$$b_{\min} = \frac{2e^{-\gamma_E}}{Q}$$

$$\mu_b = 2e^{-\gamma_E}/b_*$$



μ_b never bigger than Q nor smaller than 1 GeV

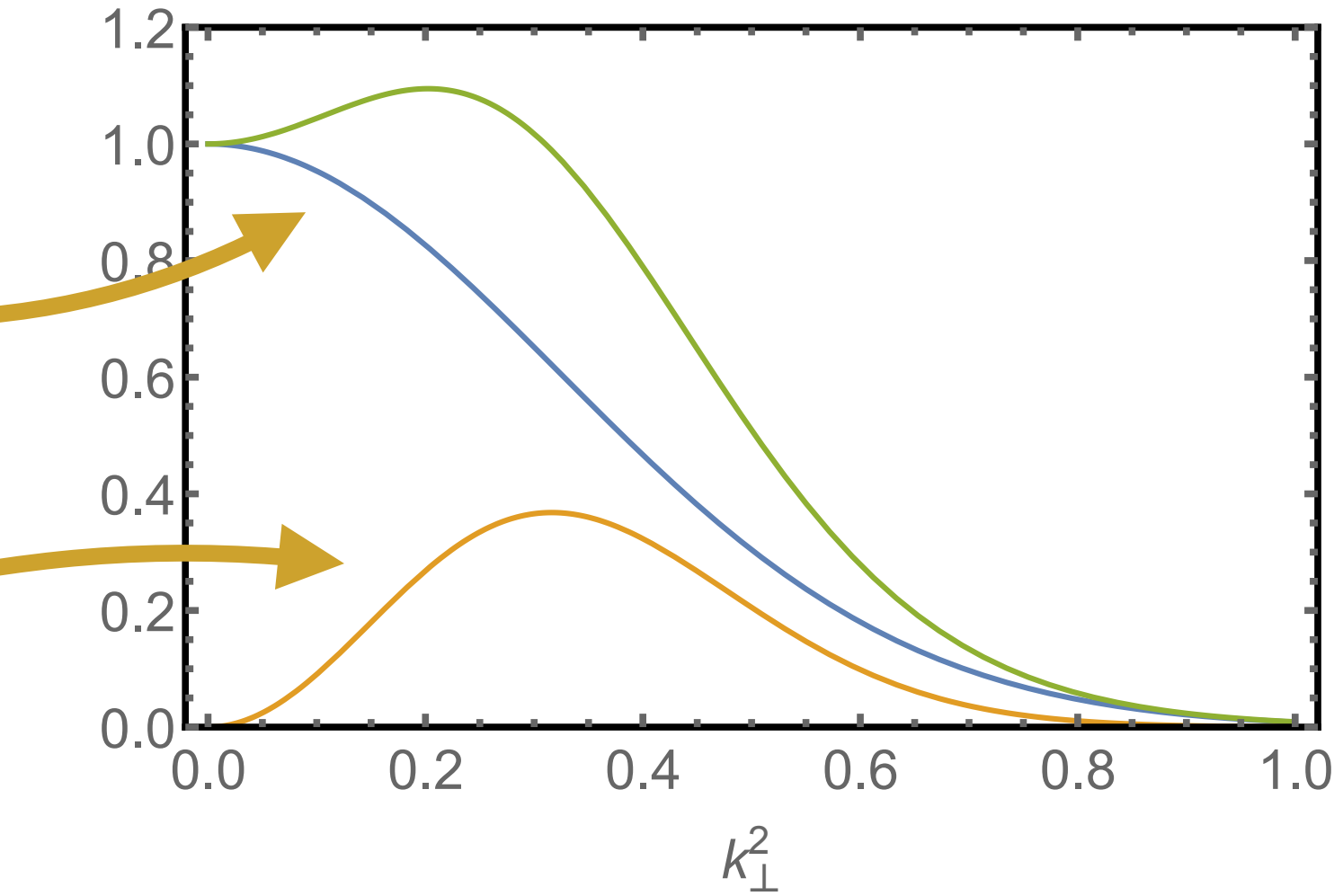
No significant effect at high Q , but large effect at low Q (inhibits gluon radiation)

Functional form of TMDs at 1 GeV

$$\hat{f}_{\text{NP}}^a = \text{F.T. of} \left(e^{-\frac{k_\perp^2}{\langle k_{\perp,a}^2 \rangle}} + \lambda k_\perp^2 e^{-\frac{k_\perp^2}{\langle k_{\perp,a}^2 \rangle'}} \right)$$

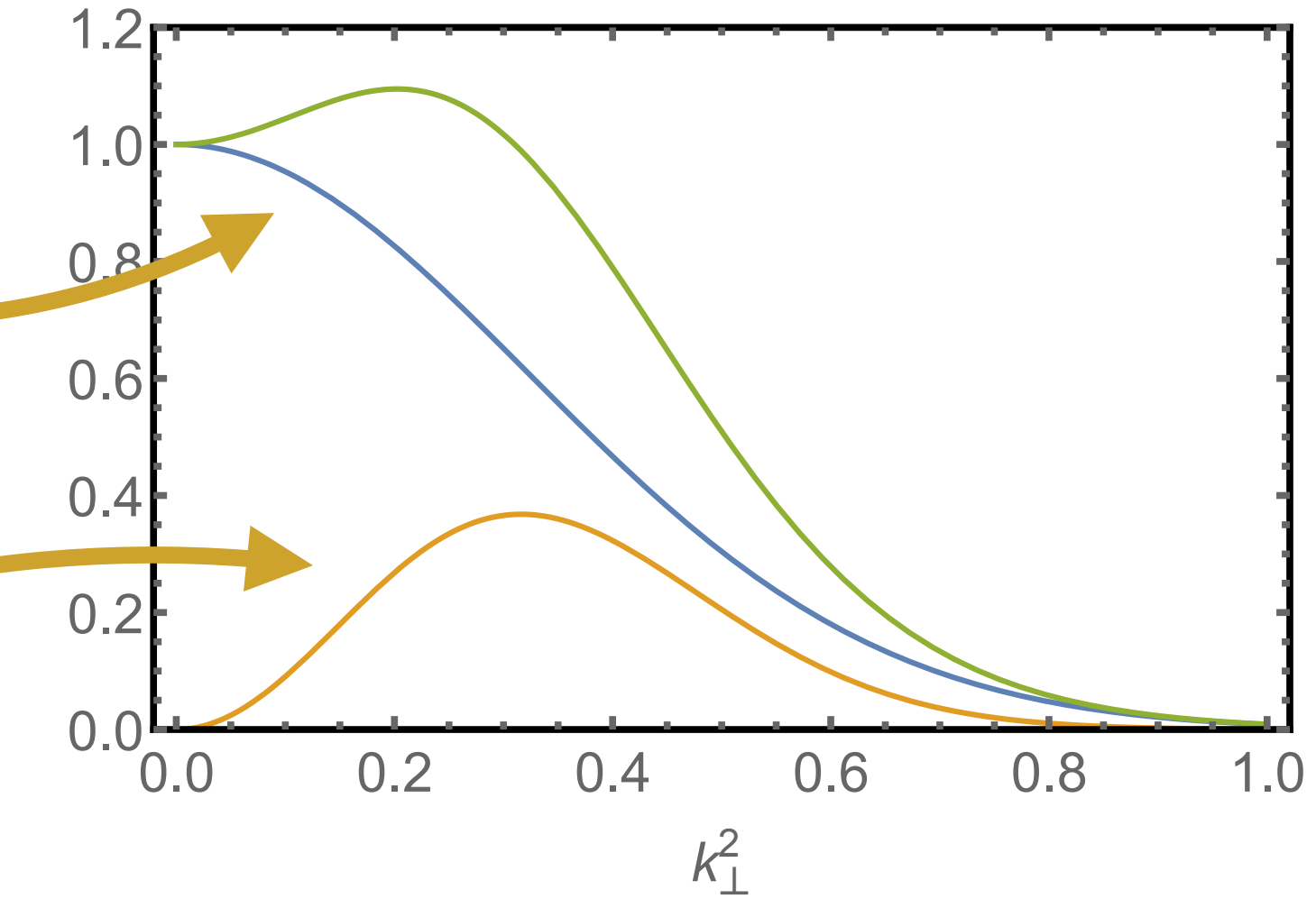
Functional form of TMDs at 1 GeV

$$\hat{f}_{\text{NP}}^a = \text{F.T. of} \left(e^{-\frac{k_\perp^2}{\langle k_{\perp,a}^2 \rangle}} + \lambda k_\perp^2 e^{-\frac{k_\perp^2}{\langle k_{\perp,a}^2 \rangle'}} \right)$$



Functional form of TMDs at 1 GeV

$$\hat{f}_{\text{NP}}^a = \text{F.T. of} \left(e^{-\frac{k_\perp^2}{\langle k_{\perp,a}^2 \rangle}} + \lambda k_\perp^2 e^{-\frac{k_\perp^2}{\langle k_{\perp,a}^2 \rangle'}} \right)$$

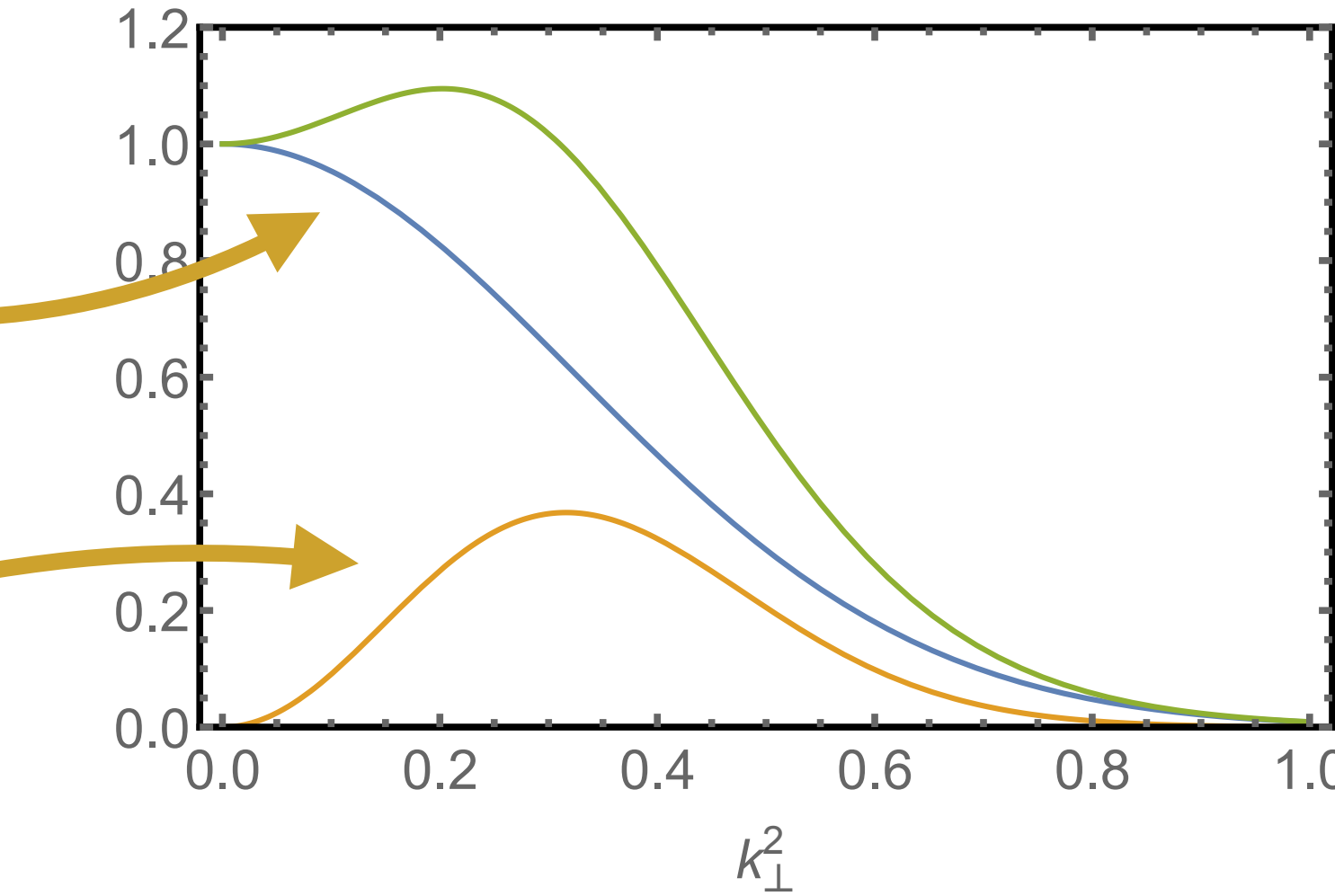


x-dependent width $\langle \mathbf{k}_{\perp,a}^2 \rangle(x) = \langle \hat{\mathbf{k}}_{\perp,a}^2 \rangle \frac{(1-x)^\alpha x^\sigma}{(1-\hat{x})^\alpha \hat{x}^\sigma}$,

where $\langle \hat{\mathbf{k}}_{\perp,a}^2 \rangle \equiv \langle \mathbf{k}_{\perp,a}^2 \rangle(\hat{x})$, and $\hat{x} = 0.1$.

Functional form of TMDs at 1 GeV

$$\hat{f}_{\text{NP}}^a = \text{F.T. of} \left(e^{-\frac{k_\perp^2}{\langle k_{\perp,a}^2 \rangle}} + \lambda k_\perp^2 e^{-\frac{k_\perp^2}{\langle k_{\perp,a}^2 \rangle'}} \right)$$



x-dependent width $\langle \mathbf{k}_{\perp,a}^2 \rangle(x) = \langle \hat{\mathbf{k}}_{\perp,a}^2 \rangle \frac{(1-x)^\alpha x^\sigma}{(1-\hat{x})^\alpha \hat{x}^\sigma}$, where $\langle \hat{\mathbf{k}}_{\perp,a}^2 \rangle \equiv \langle \mathbf{k}_{\perp,a}^2 \rangle(\hat{x})$, and $\hat{x} = 0.1$.

Fragmentation function is similar
Including TMD PDFs and FFs, in total: 11 free parameters
(4 for TMD PDFs, 6 for TMD FFs, 1 for TMD evolution)

Data selection

$$Q^2 > 1.4 \text{ GeV}^2$$

$$0.2 < z < 0.7$$

$$P_{hT}, q_T < \text{Min}[0.2 Q, 0.7 Qz] + 0.5 \text{ GeV}$$

Data selection

$$Q^2 > 1.4 \text{ GeV}^2$$

$$0.2 < z < 0.7$$

$$P_{hT}, q_T < \text{Min}[0.2 Q, 0.7 Qz] + 0.5 \text{ GeV}$$

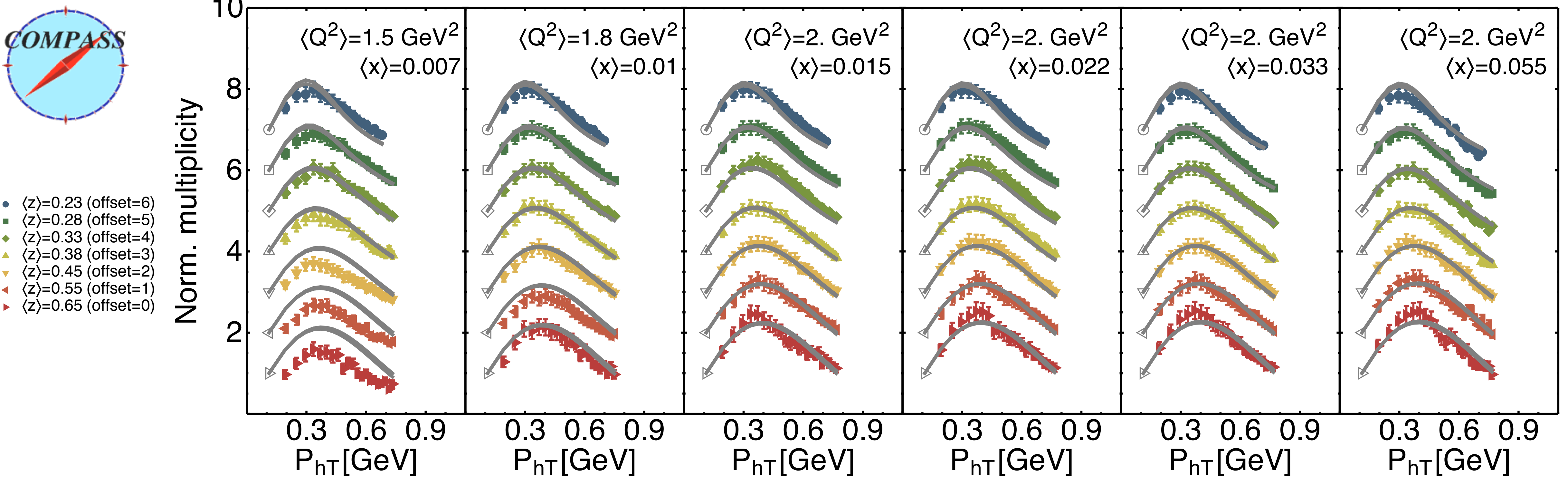
Total number of data points: 8059

Total $\chi^2/\text{dof} = 1.52$

Preliminary

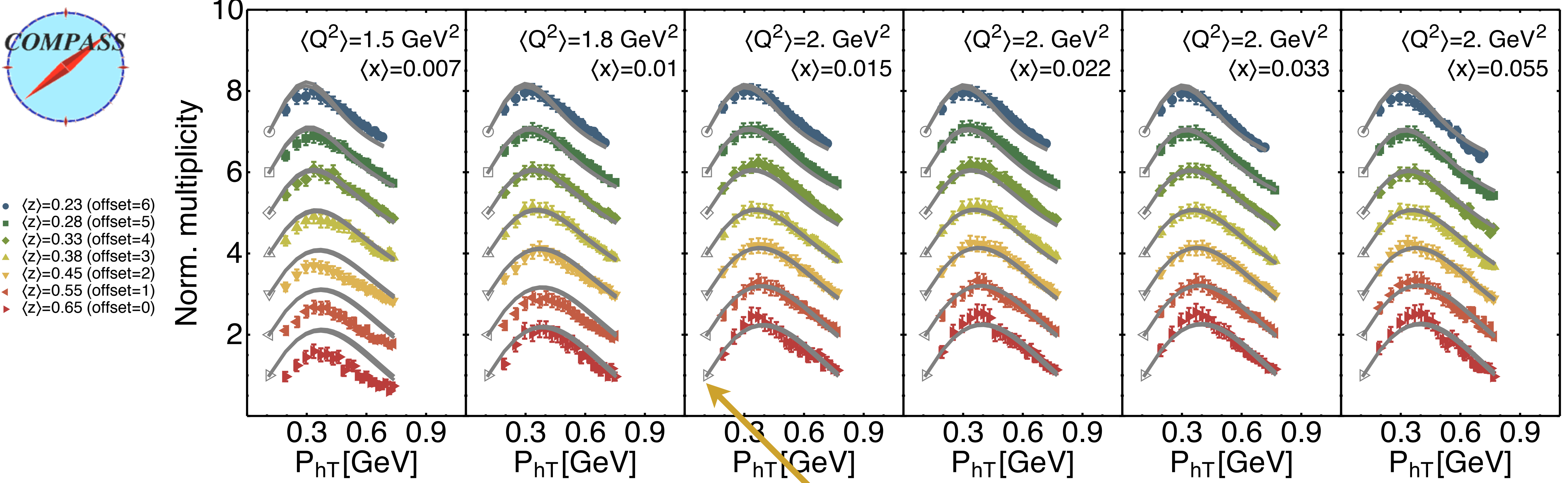
Data vs. theory plots

COMPASS selected bins



Deuteron h- $\chi^2/\text{dof} = 1.58$

COMPASS selected bins



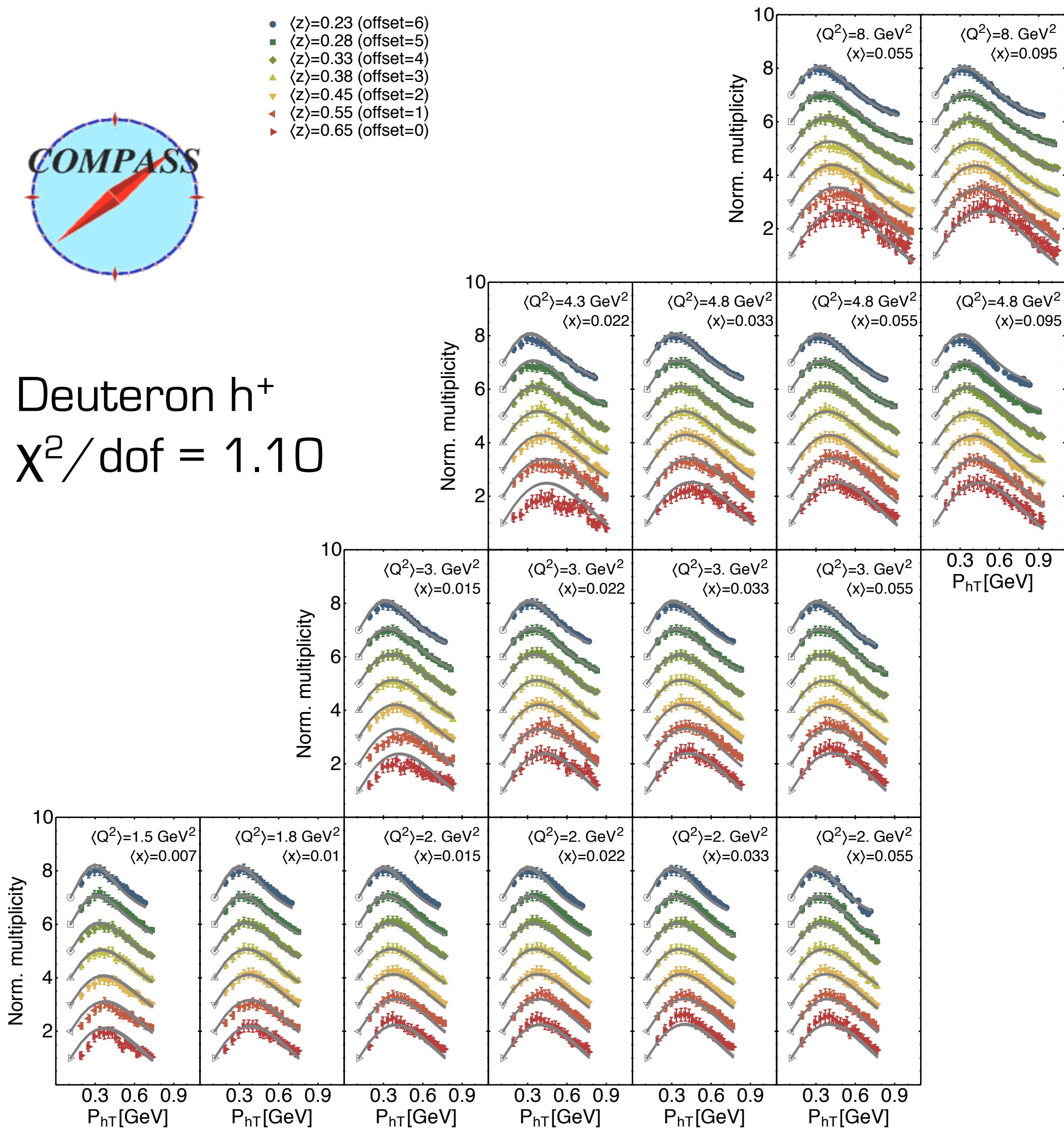
Deuteron h-

$\chi^2/\text{dof} = 1.58$

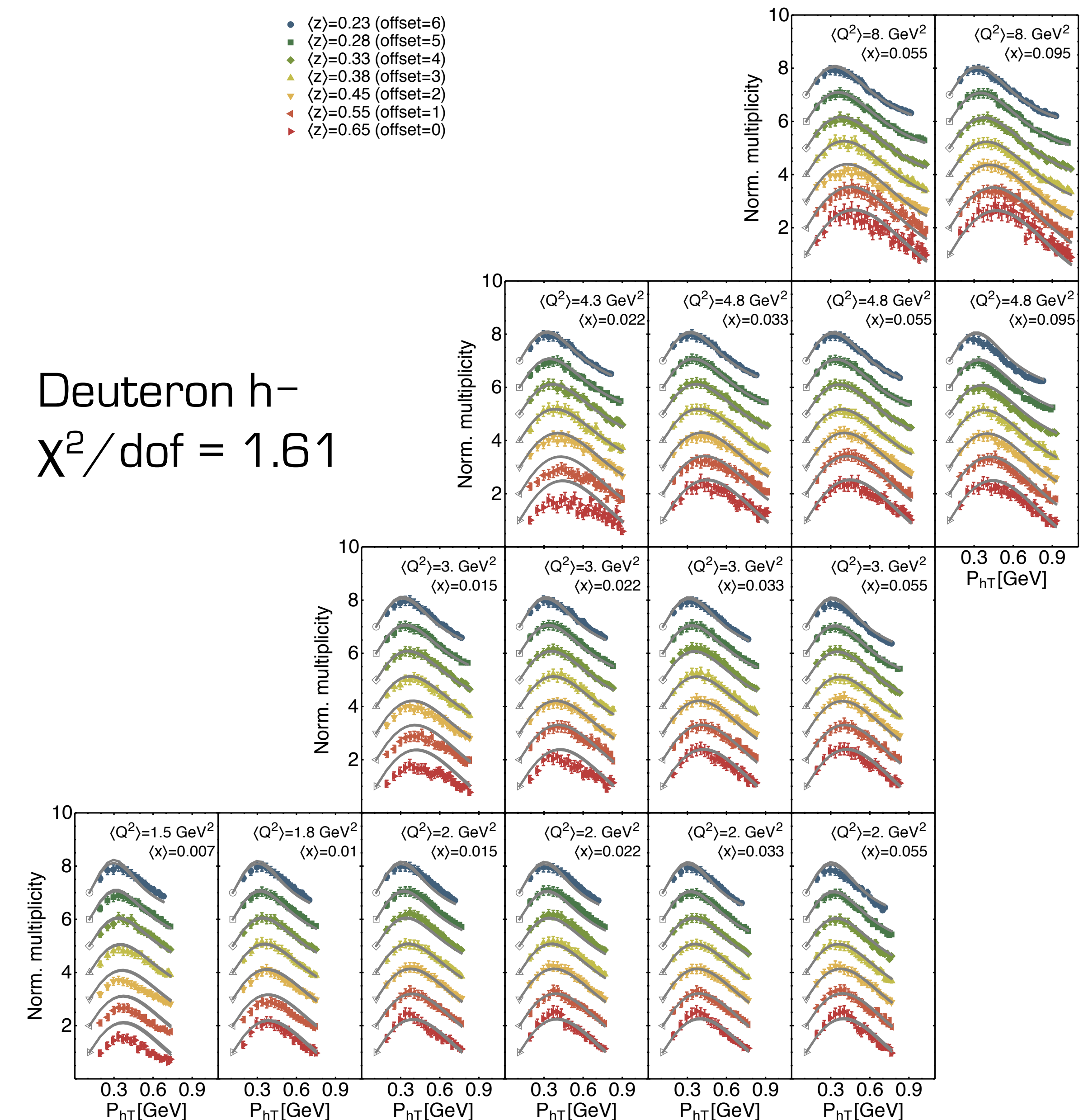
First points are not fitted, but used as normalization



Deuteron h⁺
 $\chi^2/\text{dof} = 1.10$

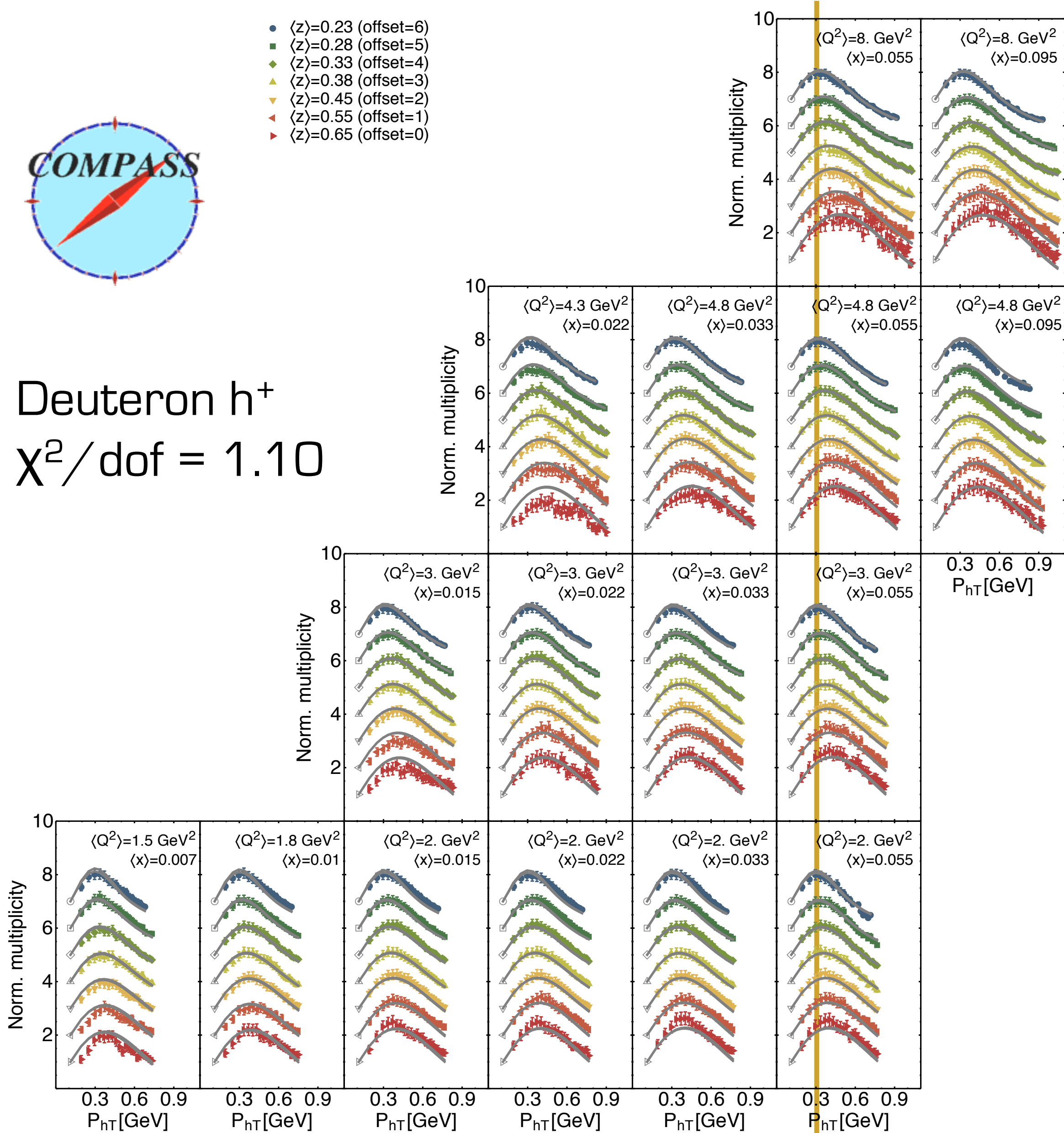


Deuteron h⁻
 $\chi^2/\text{dof} = 1.61$

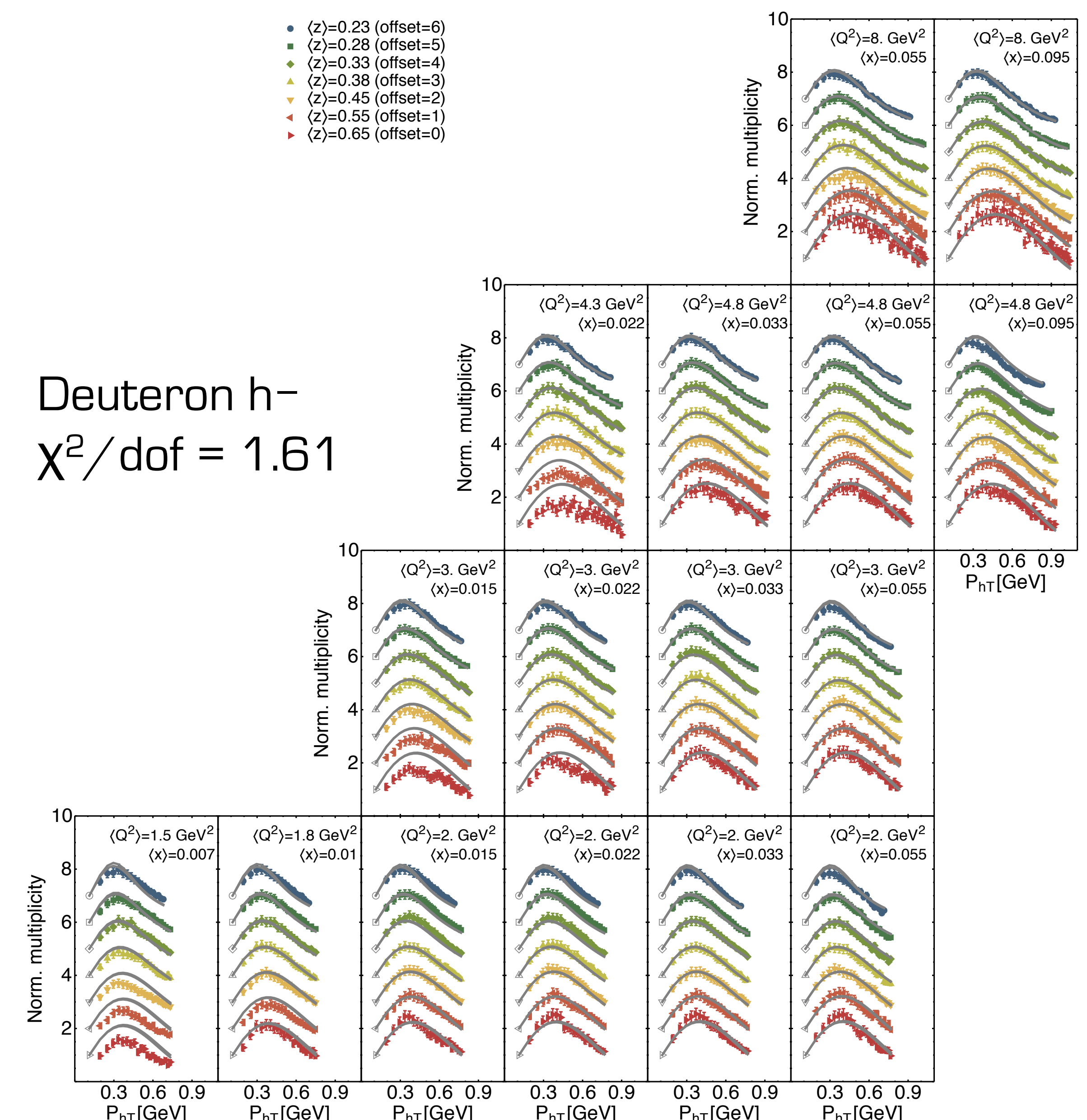




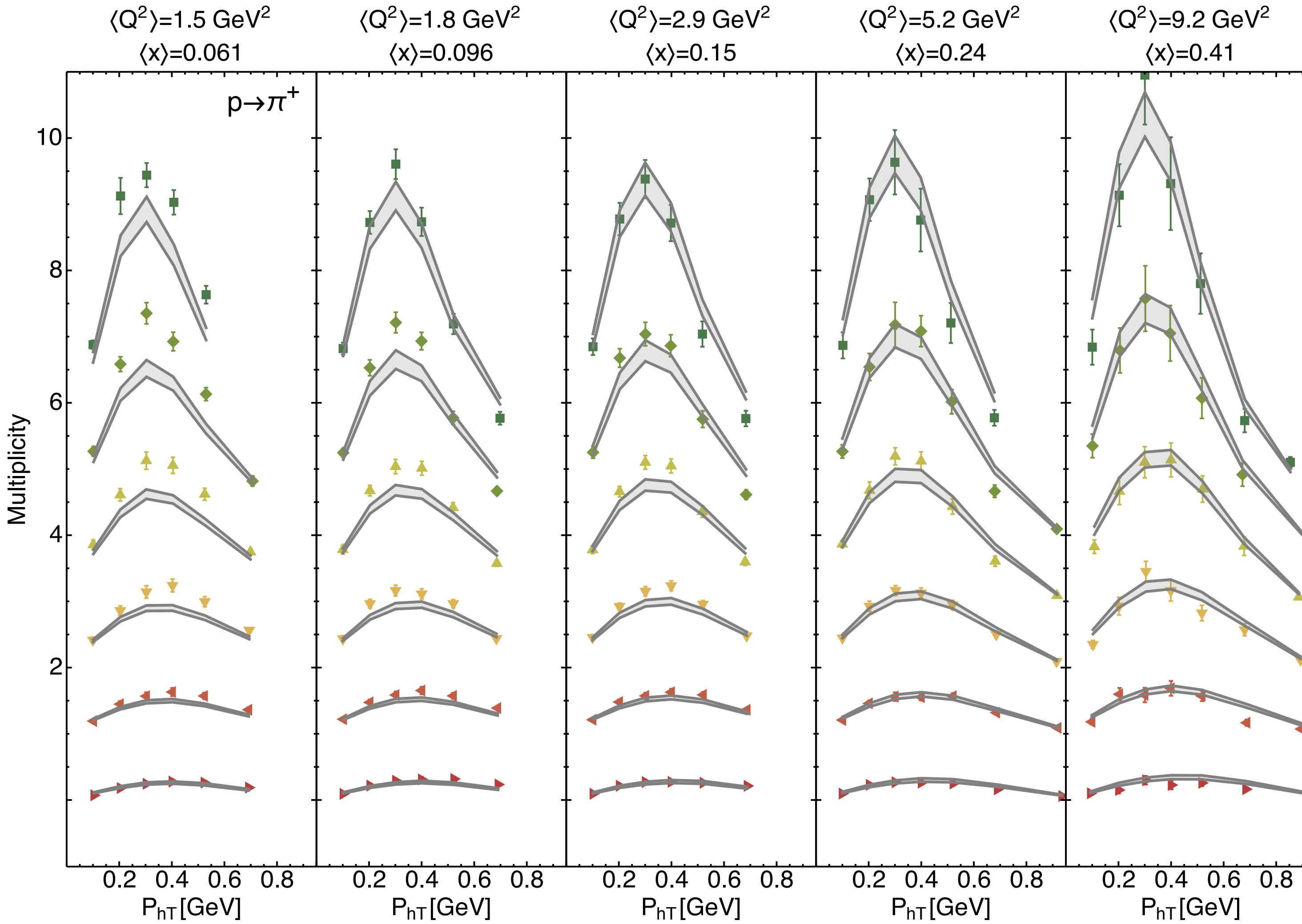
Deuteron h⁺
 $\chi^2/\text{dof} = 1.10$



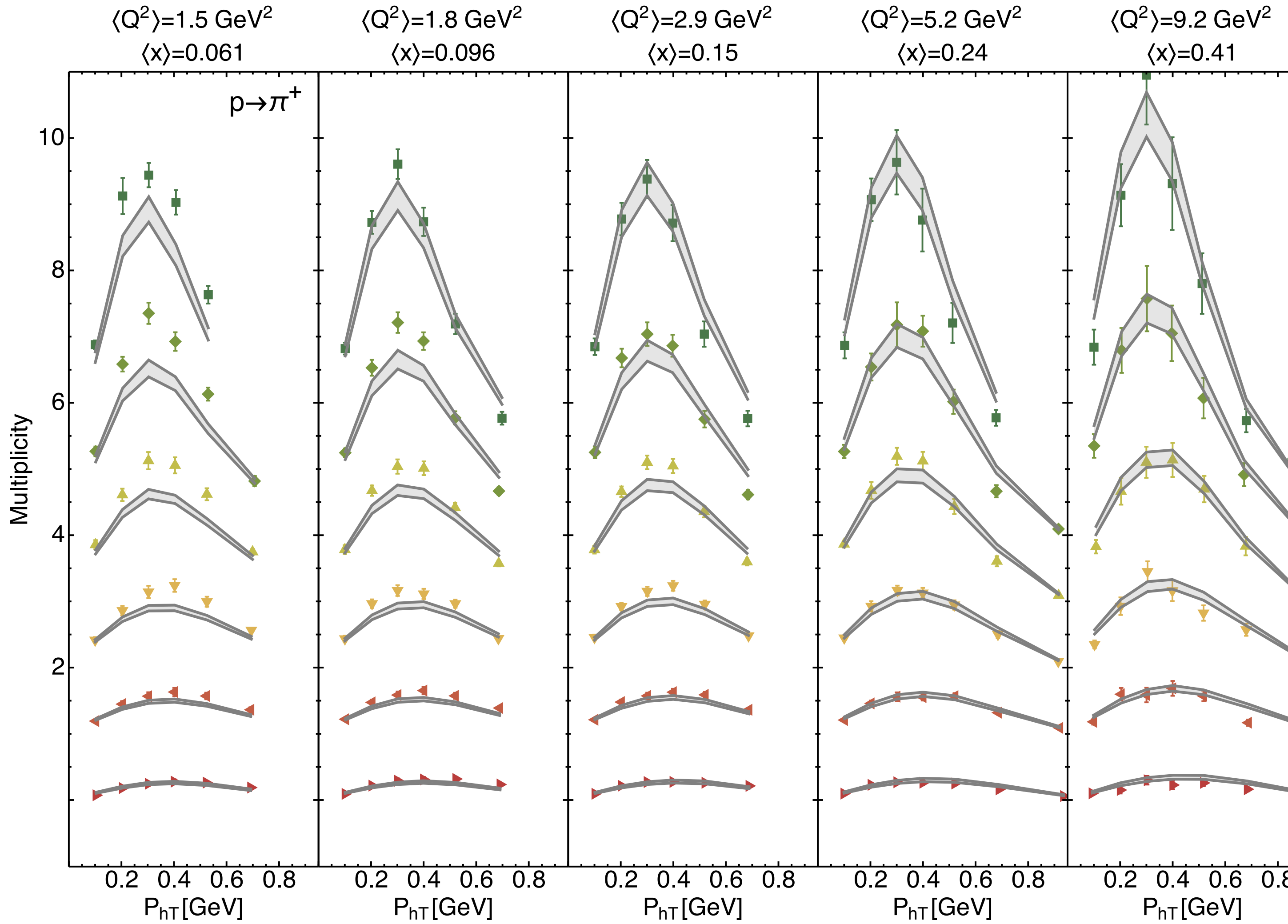
Deuteron h⁻
 $\chi^2/\text{dof} = 1.61$



HERMES, selected bins



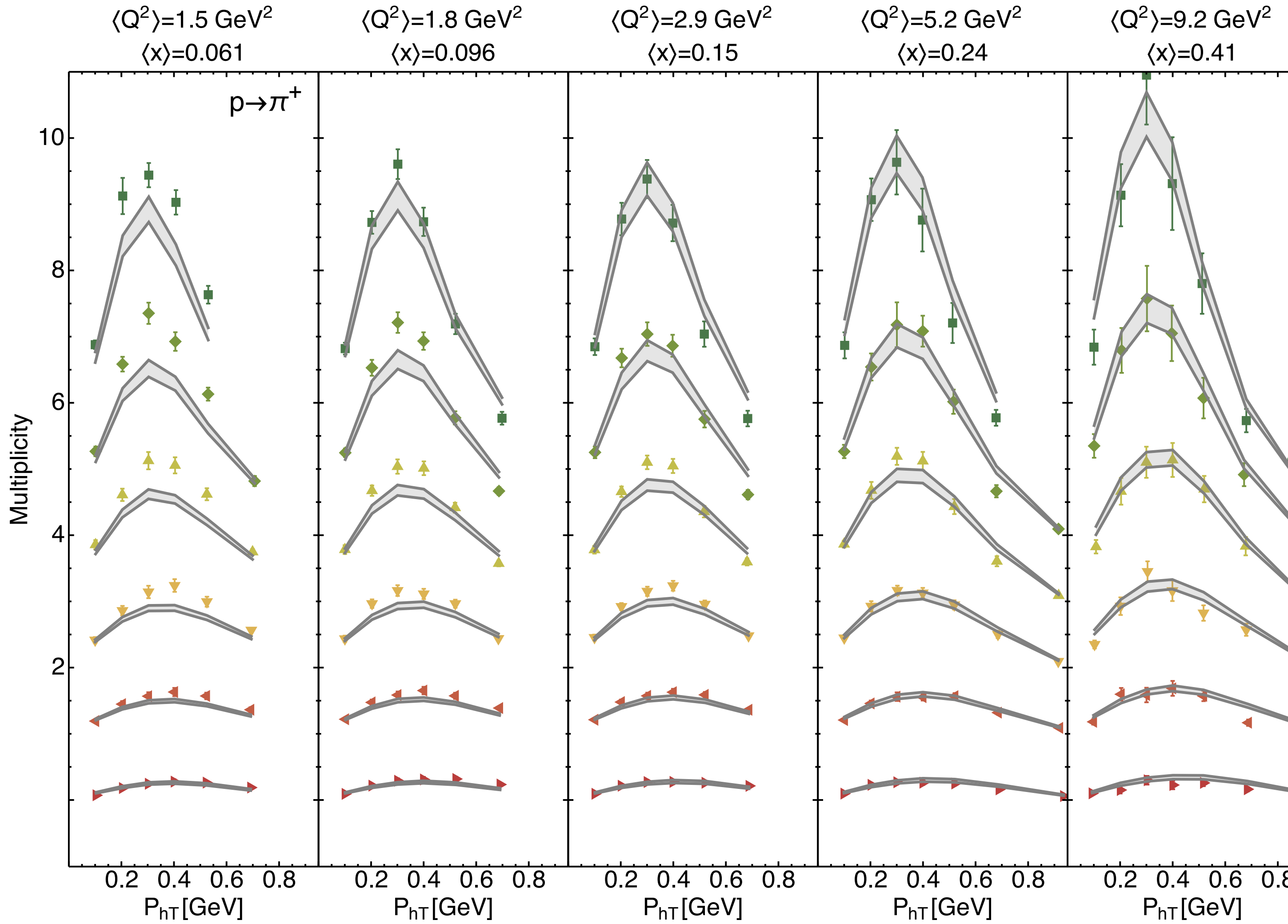
HERMES, selected bins



$\chi^2/\text{dof} = 4.80$

The worst of all channels...

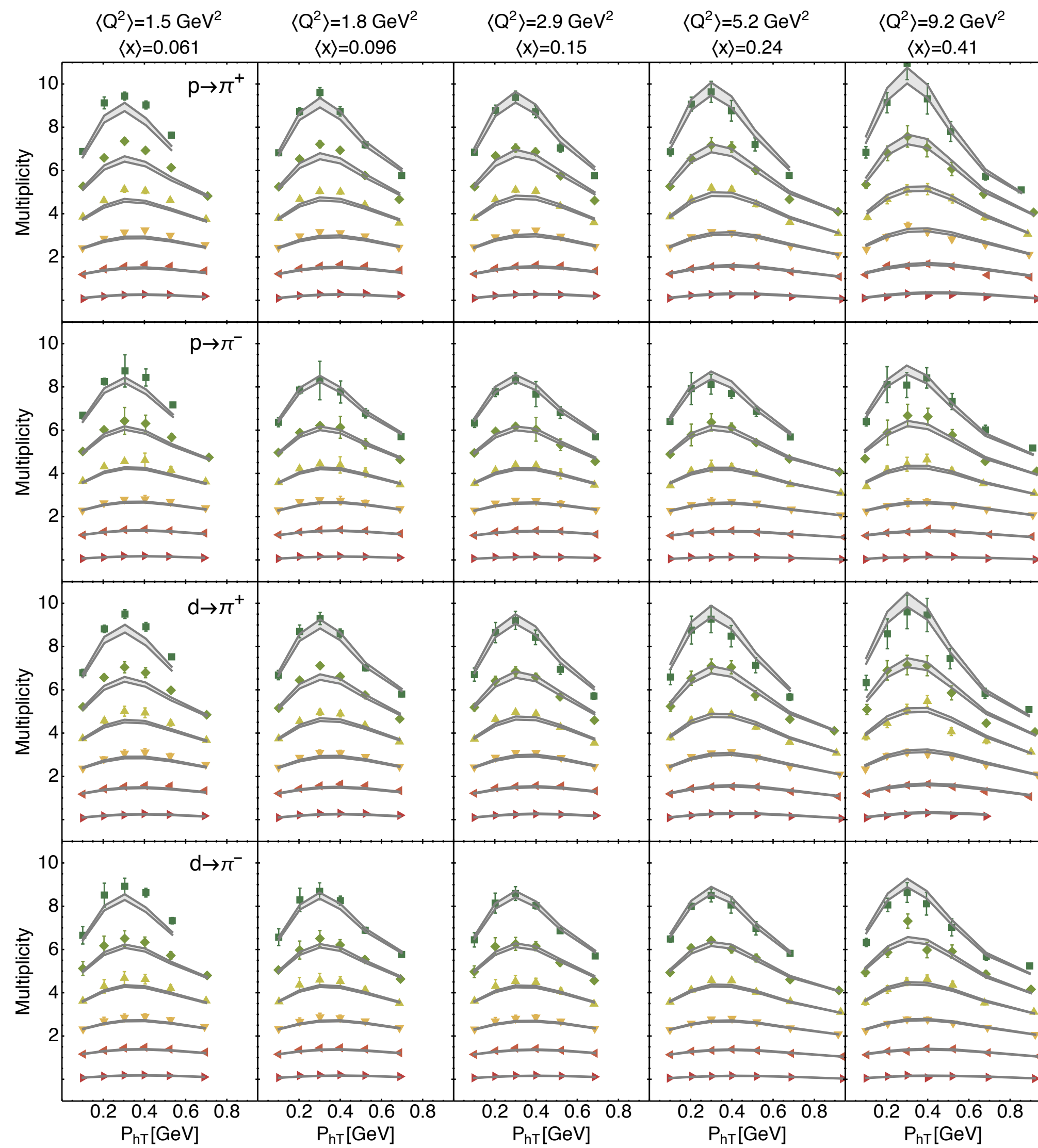
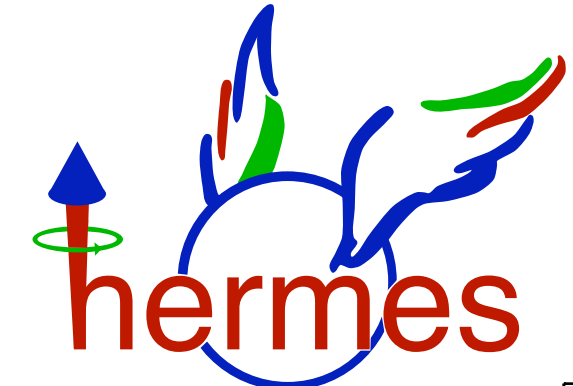
HERMES, selected bins



$\chi^2/\text{dof} = 4.80$

The worst of all channels...

However normalizing the theory
curves to the first bin, without
changing the parameters of the fit,
 χ^2/dof becomes good



χ^2/dof

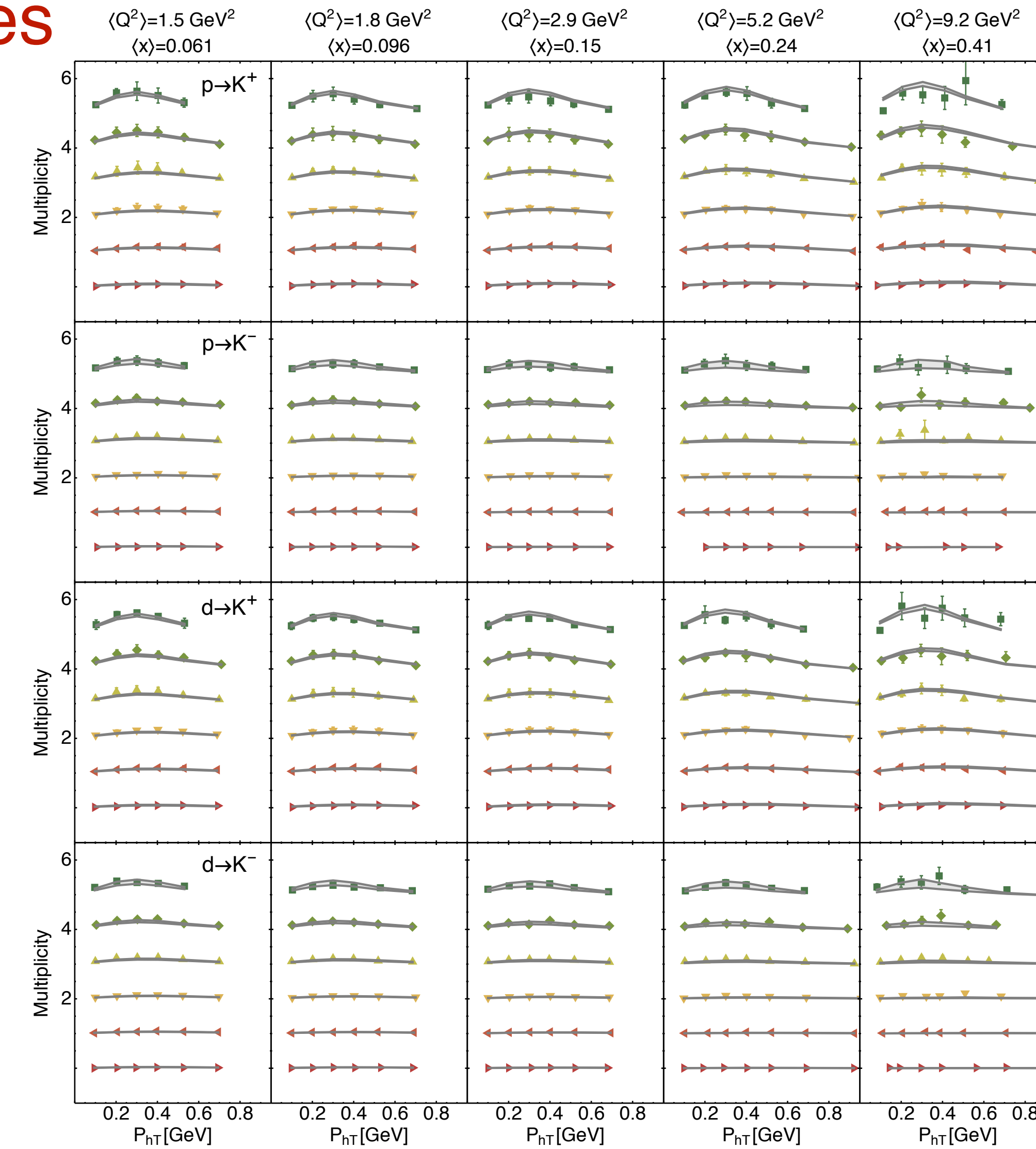
4.8

2.5

3.5

2.0

- $\langle z \rangle = 0.24 \text{ (offset=5)}$
- ◆ $\langle z \rangle = 0.28 \text{ (offset=4)}$
- ▲ $\langle z \rangle = 0.34 \text{ (offset=3)}$
- ▼ $\langle z \rangle = 0.43 \text{ (offset=2)}$
- $\langle z \rangle = 0.54 \text{ (offset=1)}$
- $\langle z \rangle = 0.70 \text{ (offset=0)}$



χ^2/dof

0.9

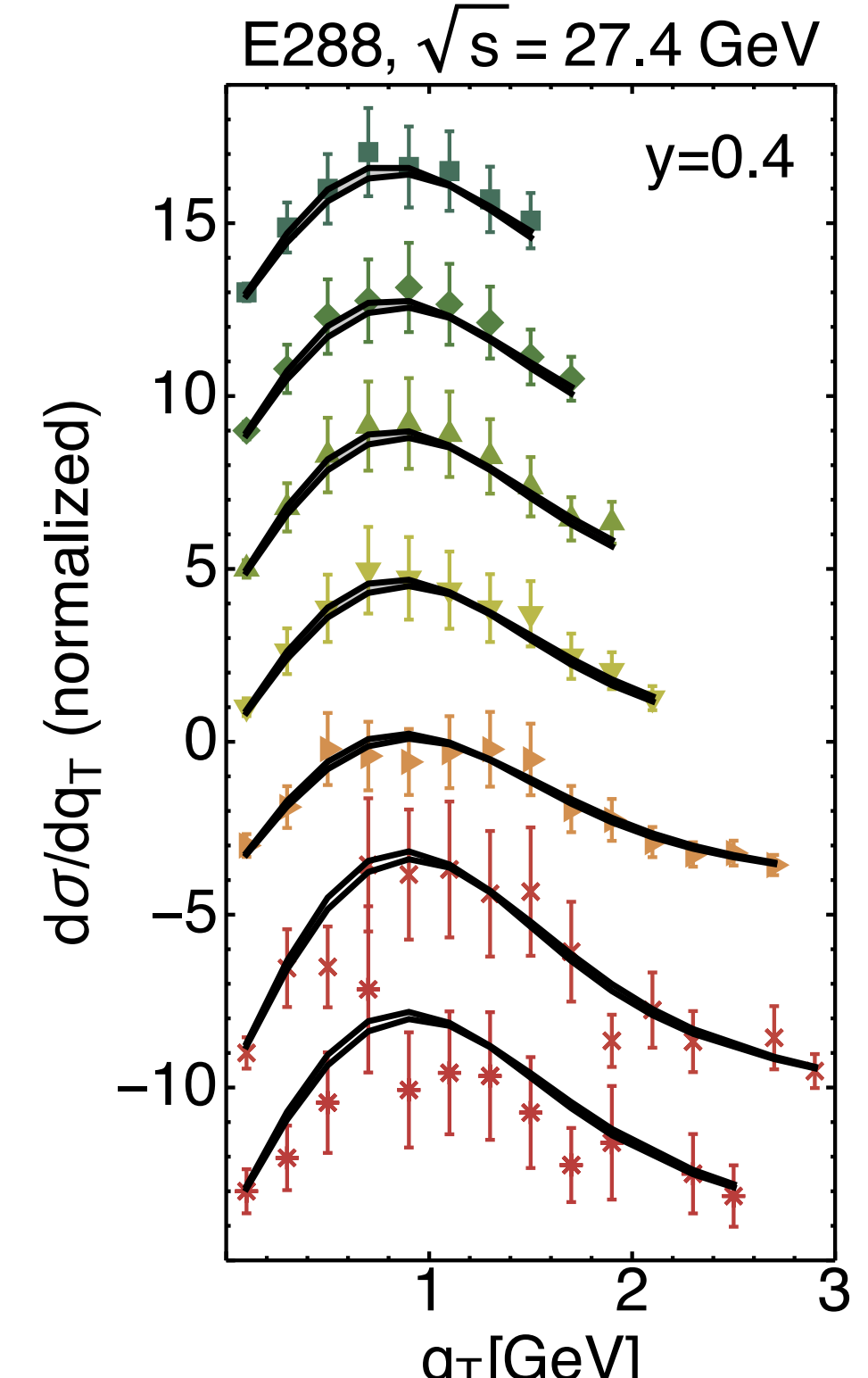
0.8

1.3

2.5

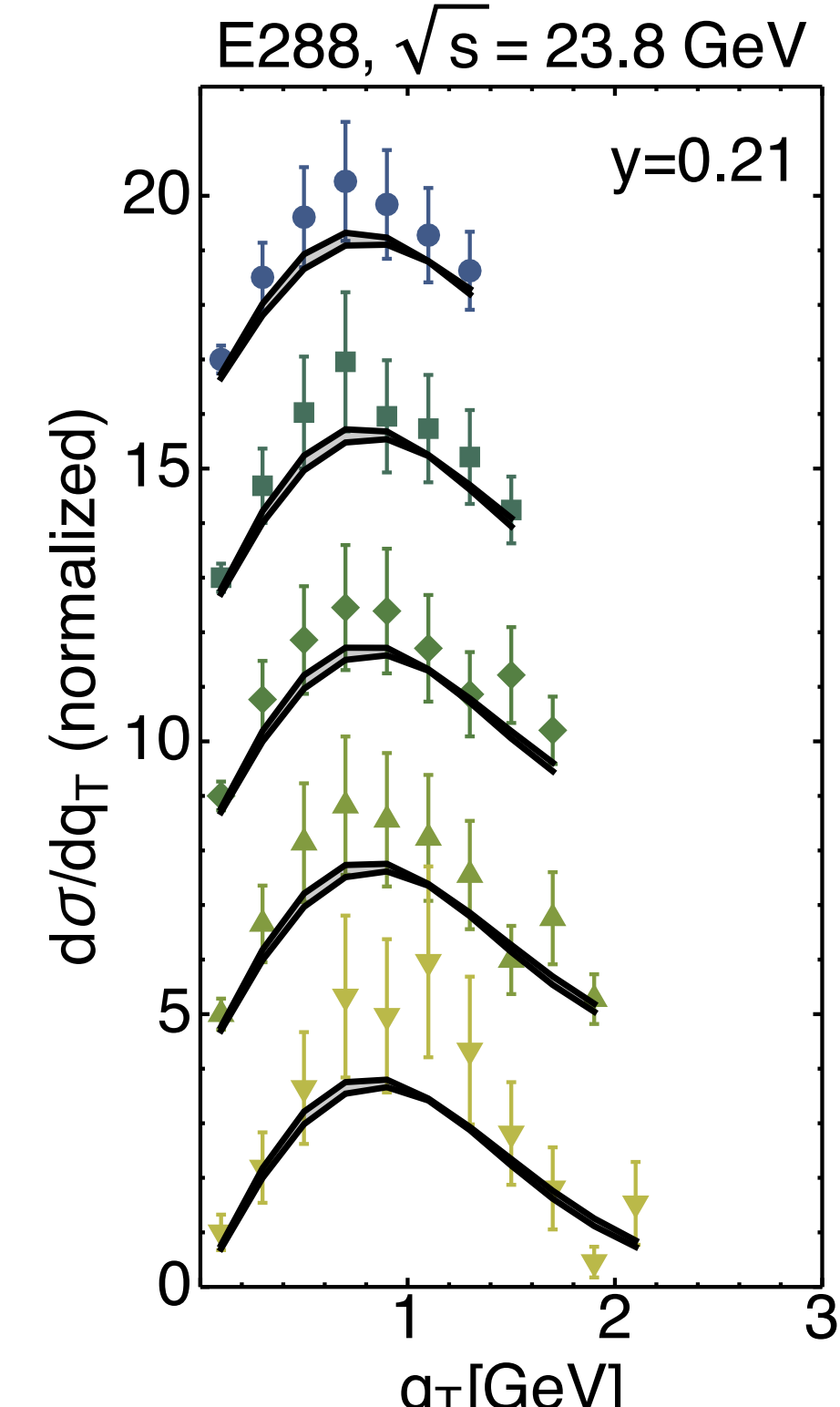
Drell-Yan data

- $\langle Q \rangle = 4.5 \text{ GeV}$ (offset = 16)
- $\langle Q \rangle = 5.5 \text{ GeV}$ (offset = 12)
- ◆ $\langle Q \rangle = 6.5 \text{ GeV}$ (offset = 8)
- ▲ $\langle Q \rangle = 7.5 \text{ GeV}$ (offset = 4)
- ▼ $\langle Q \rangle = 8.5 \text{ GeV}$ (offset = 0)
- ▷ $\langle Q \rangle = 11.0 \text{ GeV}$ (offset = -4)
- ▷ $\langle Q \rangle = 11.5 \text{ GeV}$ (offset = -4)
- ×
- * $\langle Q \rangle = 13.5 \text{ GeV}$ (offset = -14)

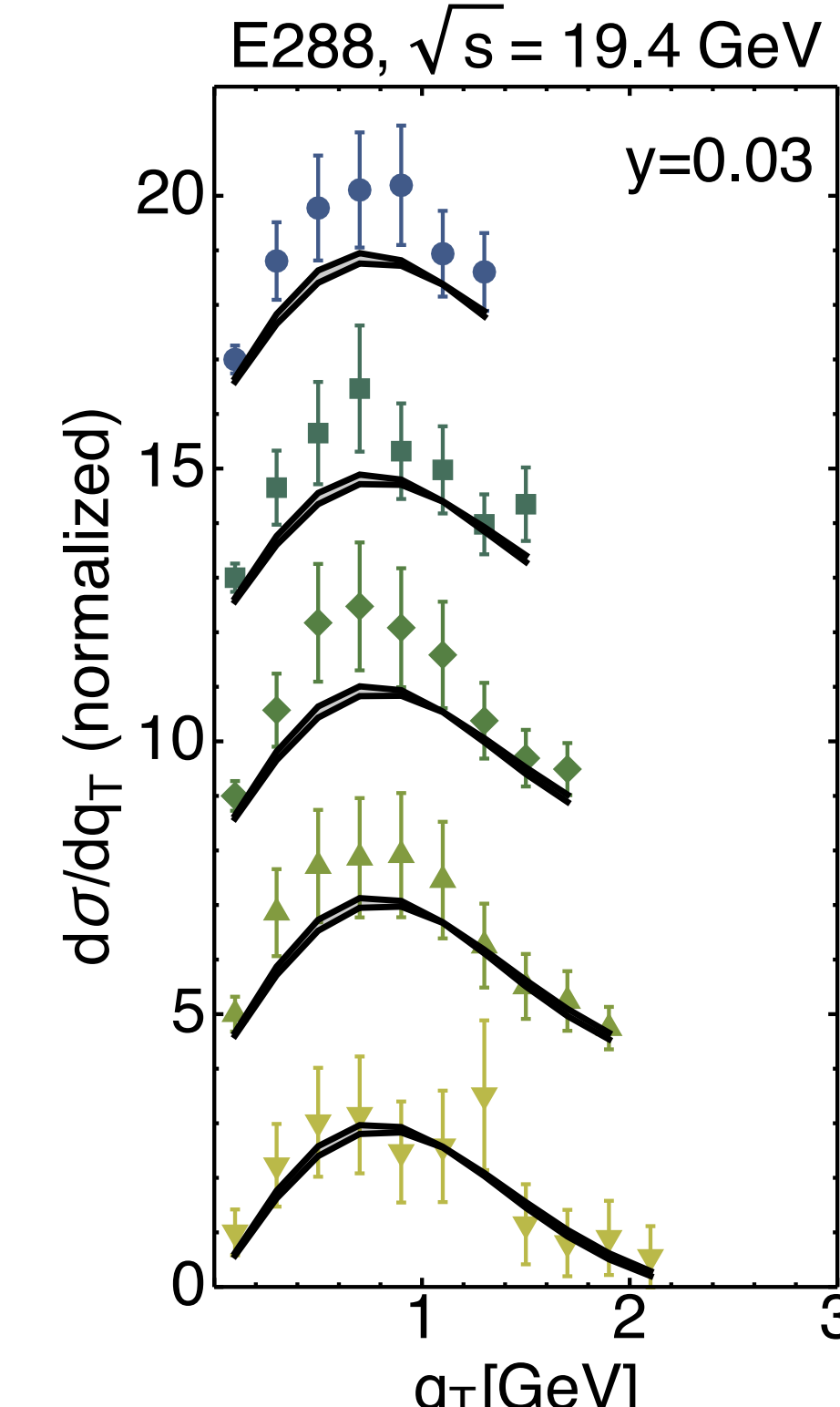


χ^2/dof

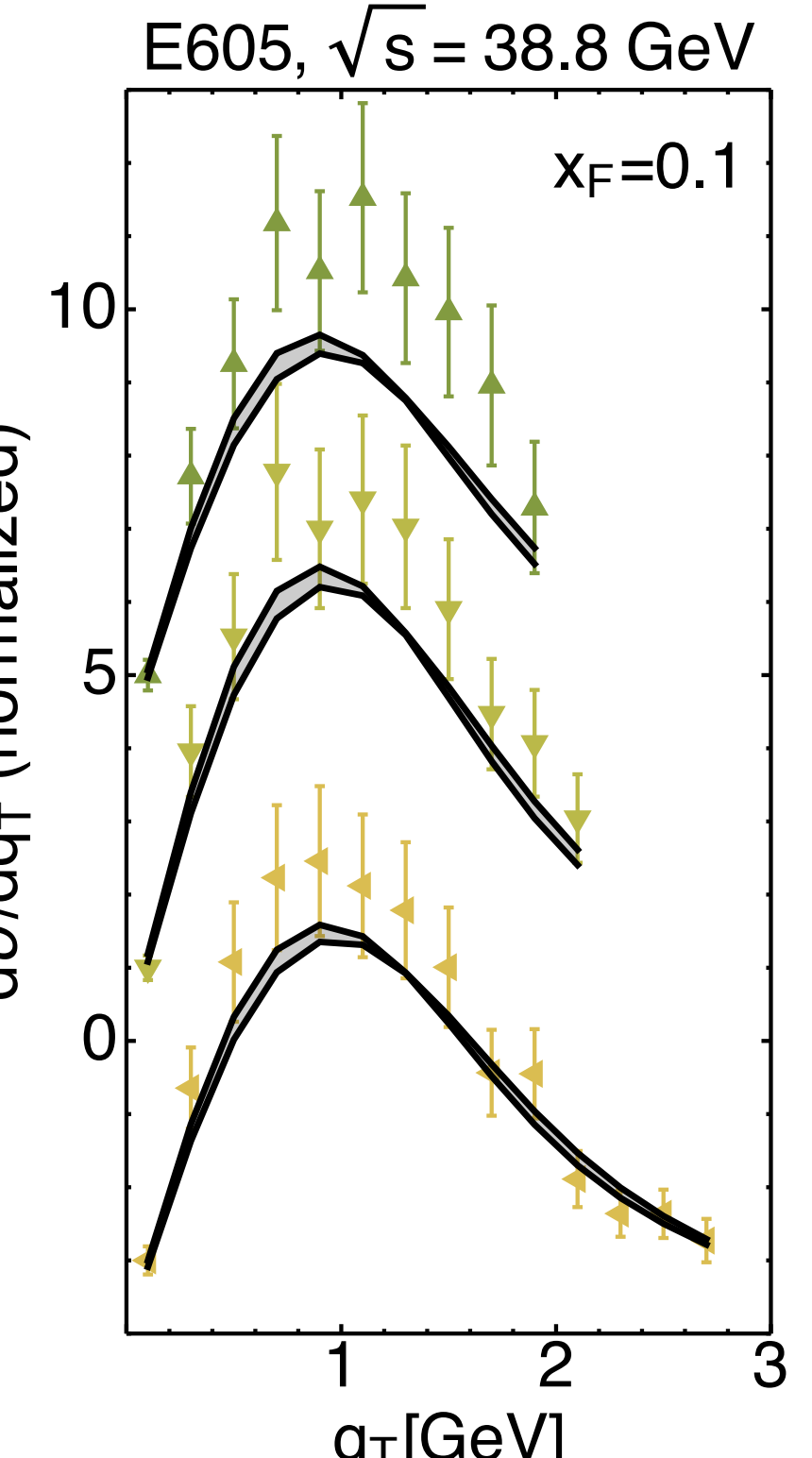
0.32



0.84



0.99

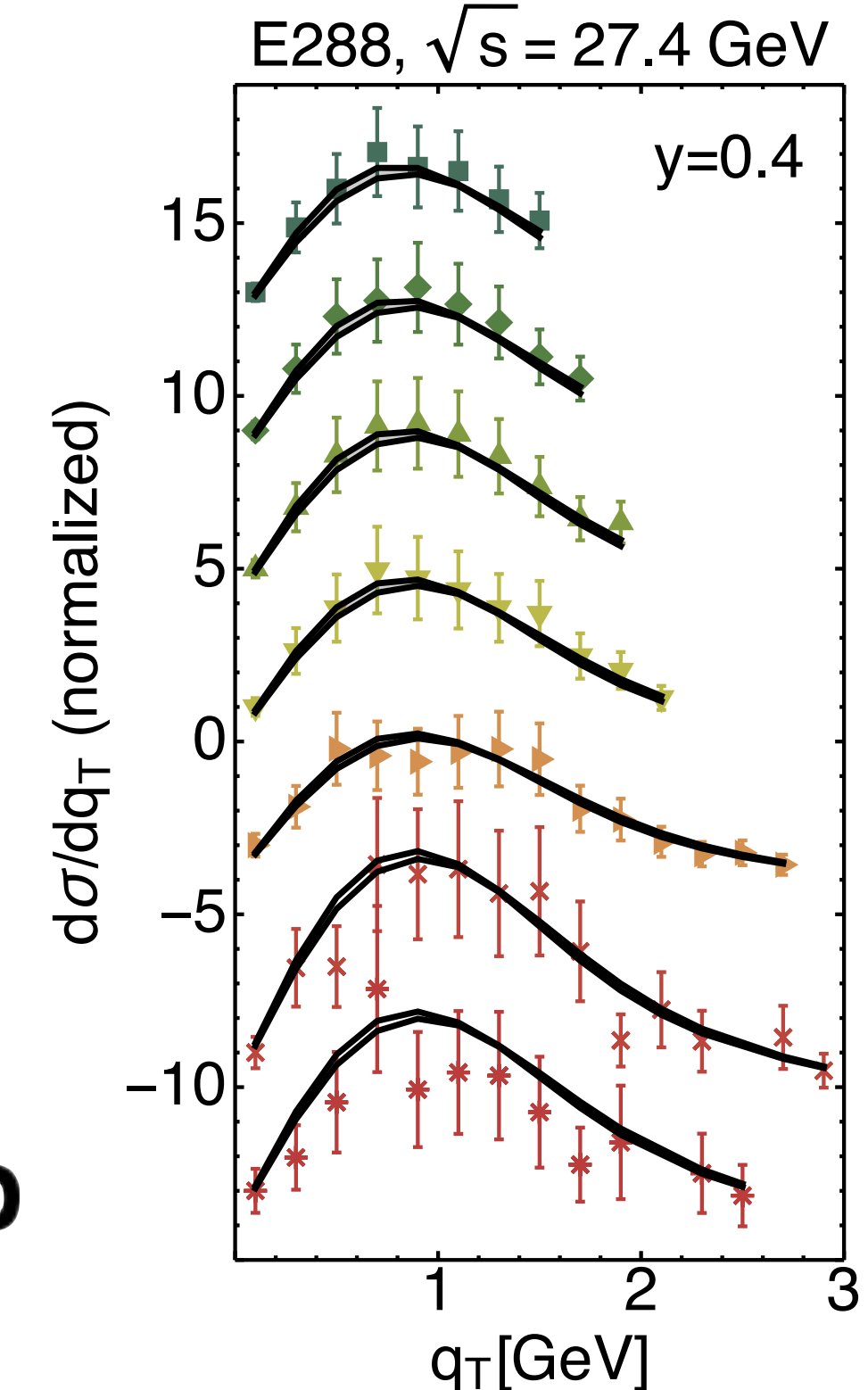


1.13

Drell-Yan data

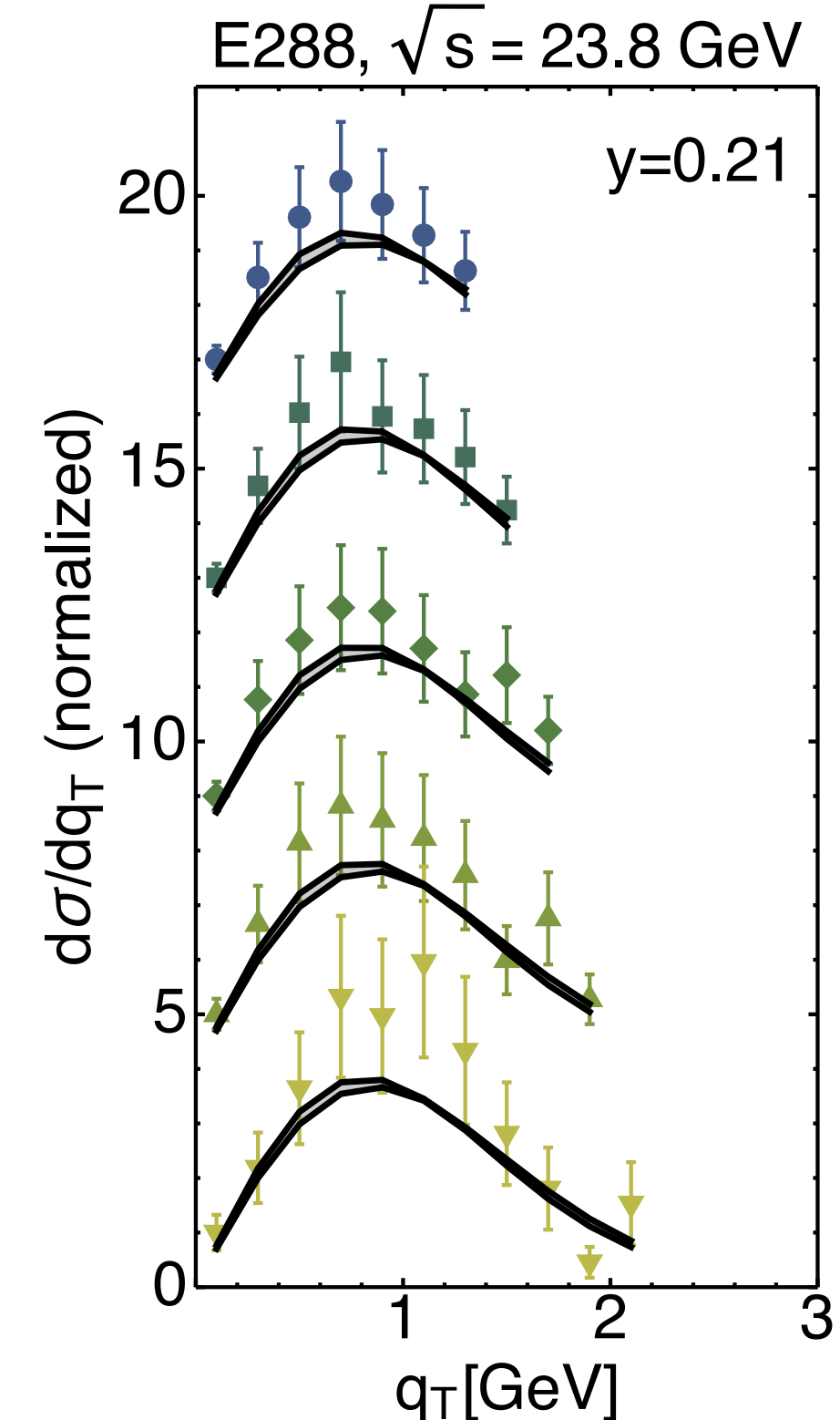
- $\langle Q \rangle = 4.5 \text{ GeV}$ (offset = 16)
- $\langle Q \rangle = 5.5 \text{ GeV}$ (offset = 12)
- ◆ $\langle Q \rangle = 6.5 \text{ GeV}$ (offset = 8)
- ▲ $\langle Q \rangle = 7.5 \text{ GeV}$ (offset = 4)
- ▼ $\langle Q \rangle = 8.5 \text{ GeV}$ (offset = 0)
- ▷ $\langle Q \rangle = 11.0 \text{ GeV}$ (offset = -4)
- ▷ $\langle Q \rangle = 11.5 \text{ GeV}$ (offset = -4)
- ×
- * $\langle Q \rangle = 13.5 \text{ GeV}$ (offset = -14)

Fermilab

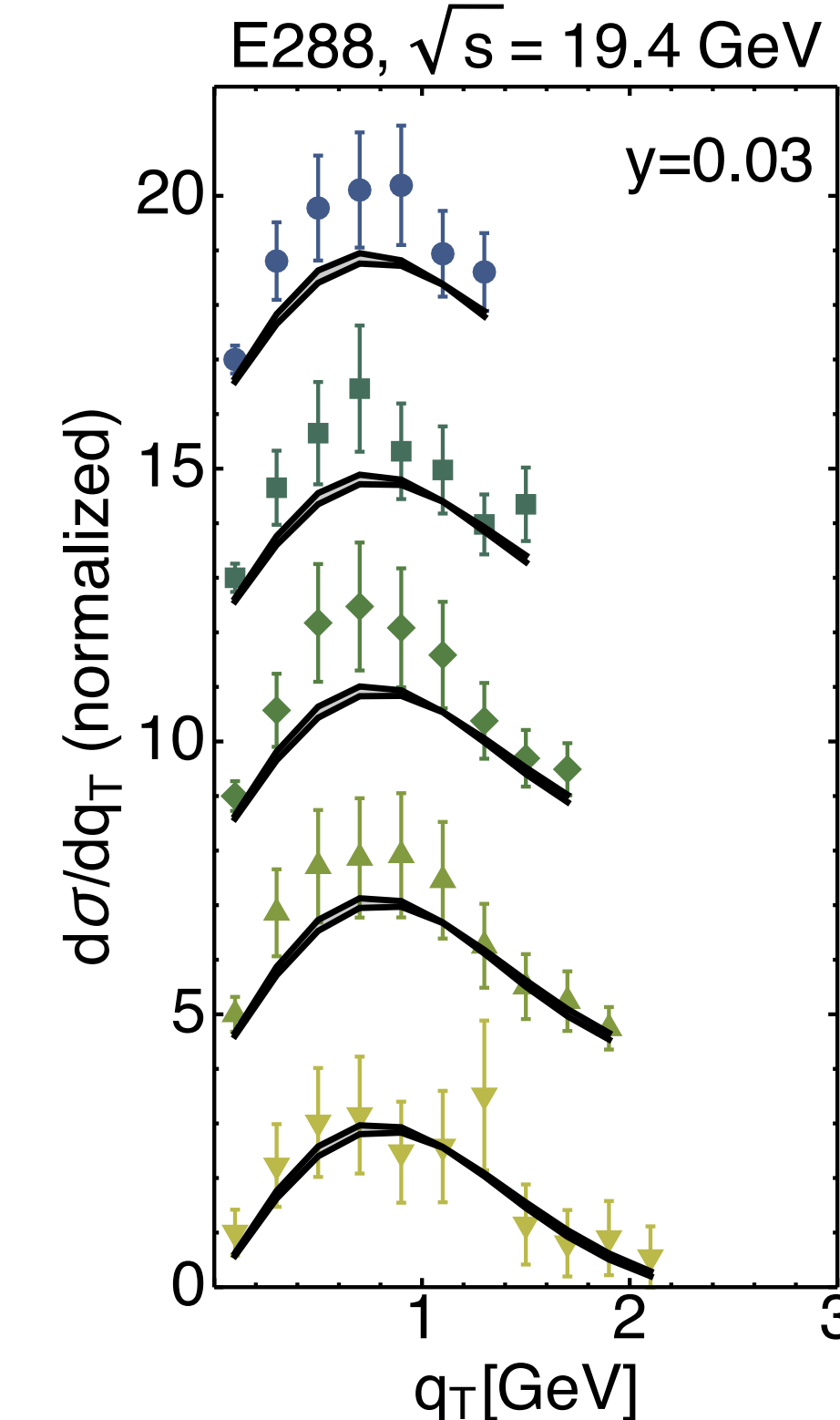


χ^2/dof

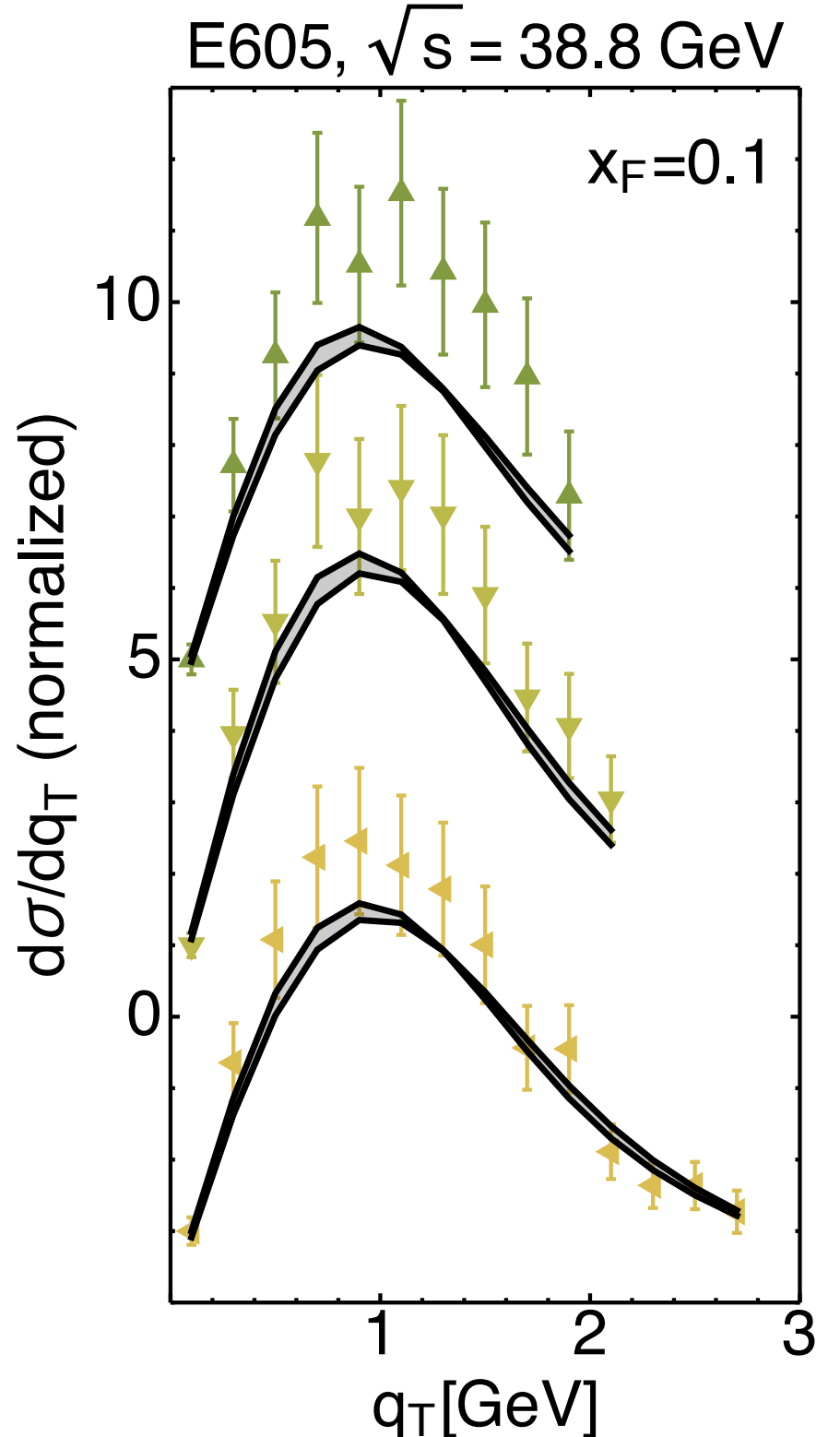
0.32



0.84



0.99

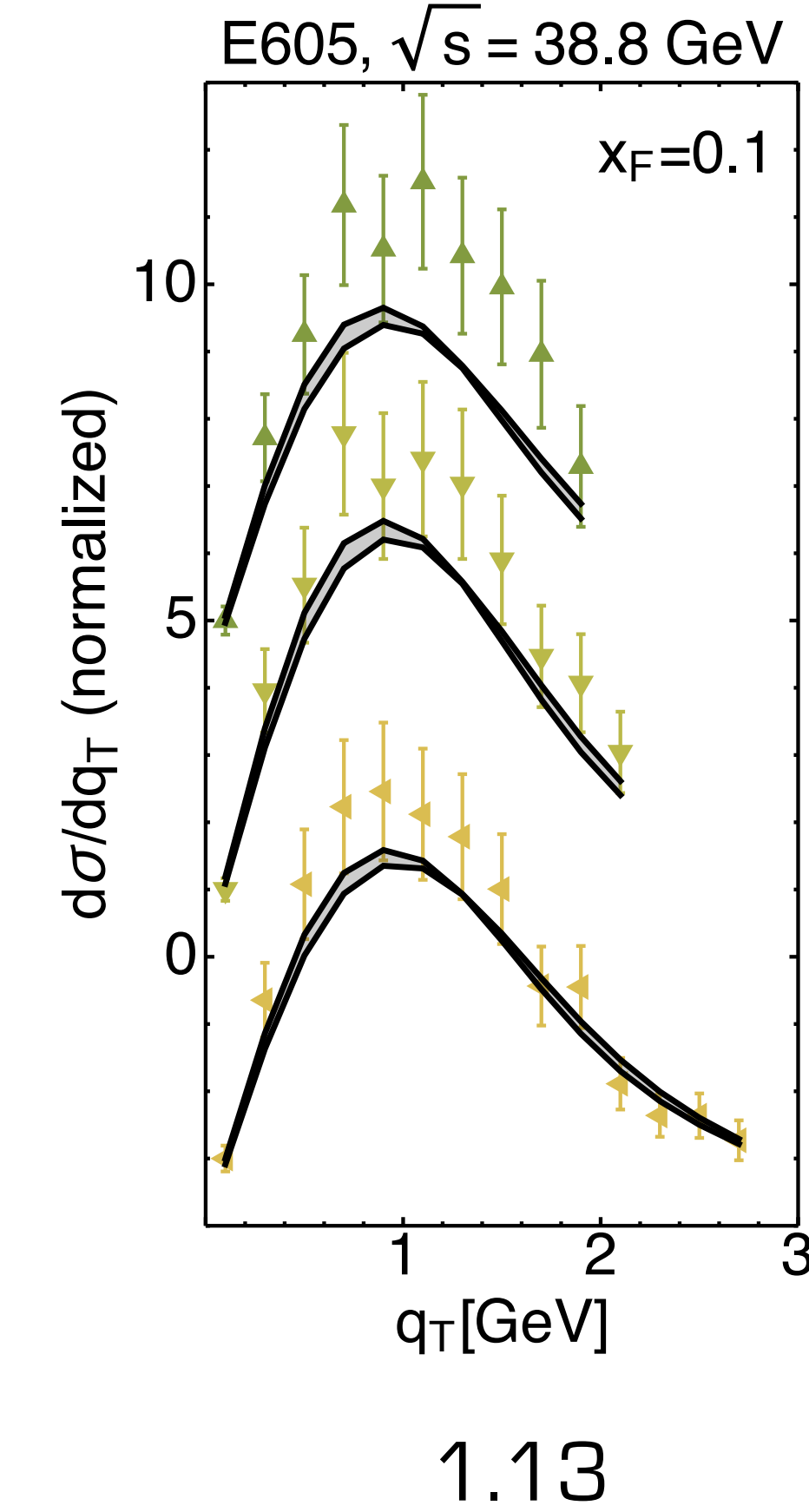
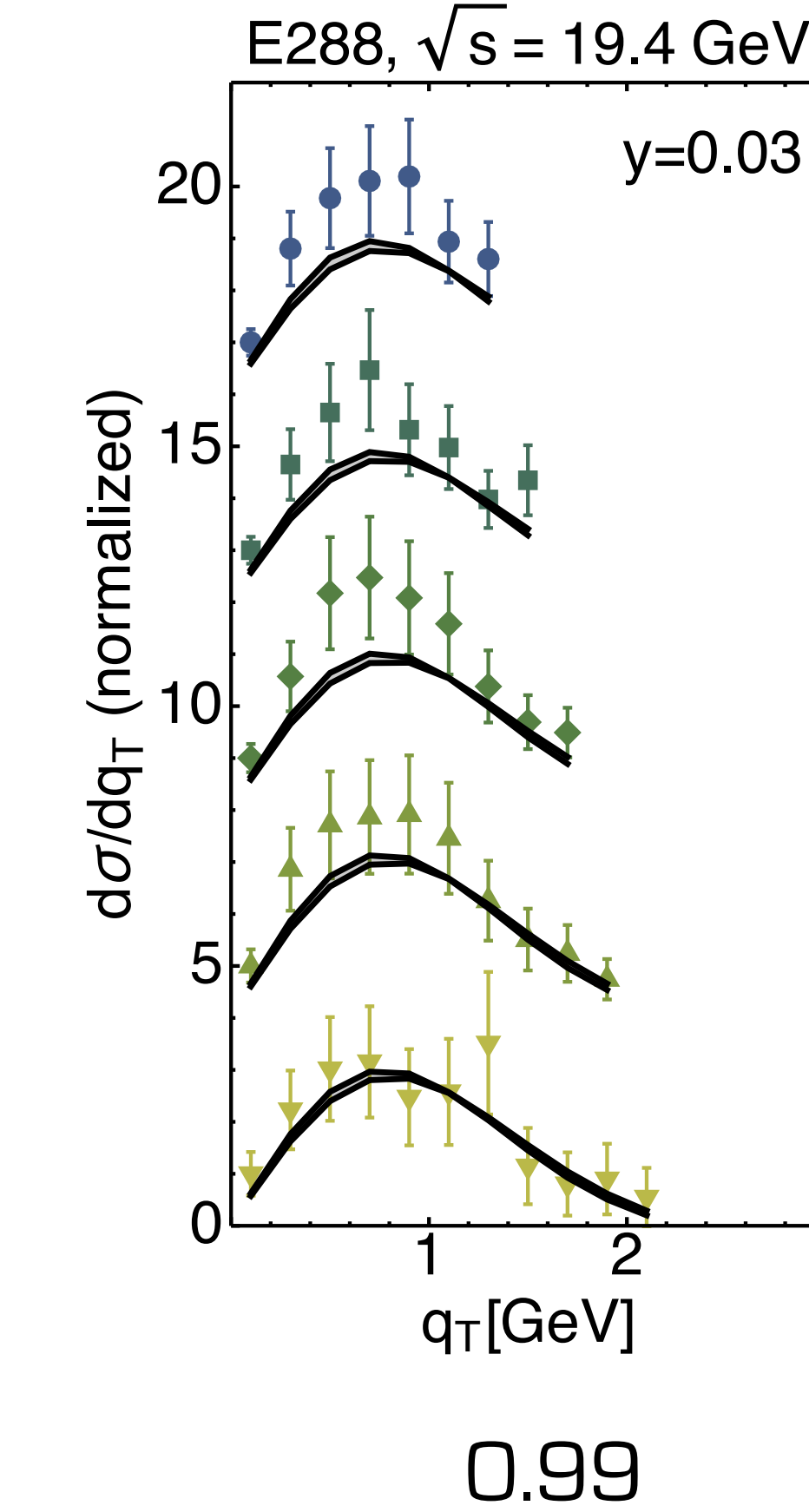
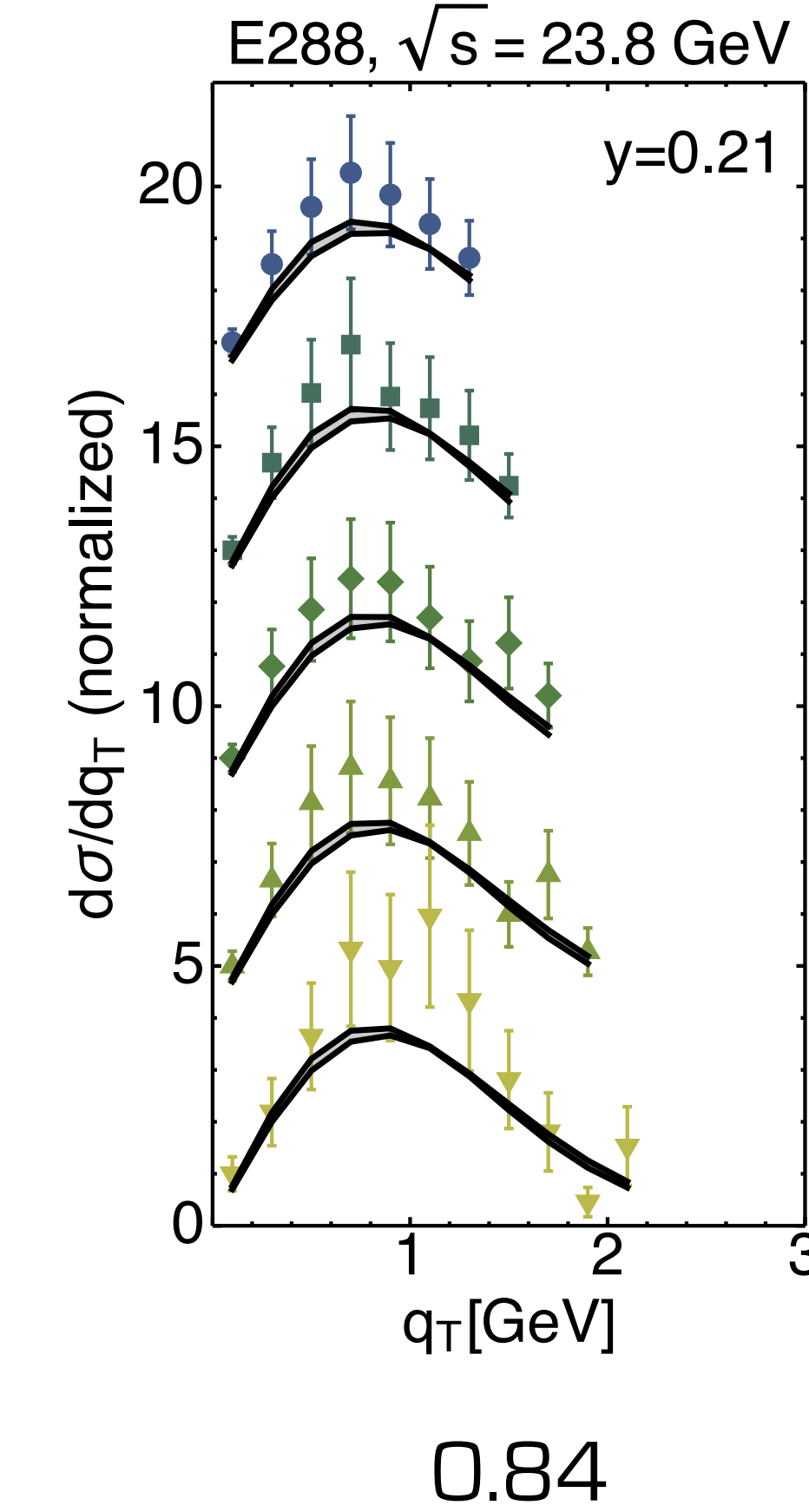
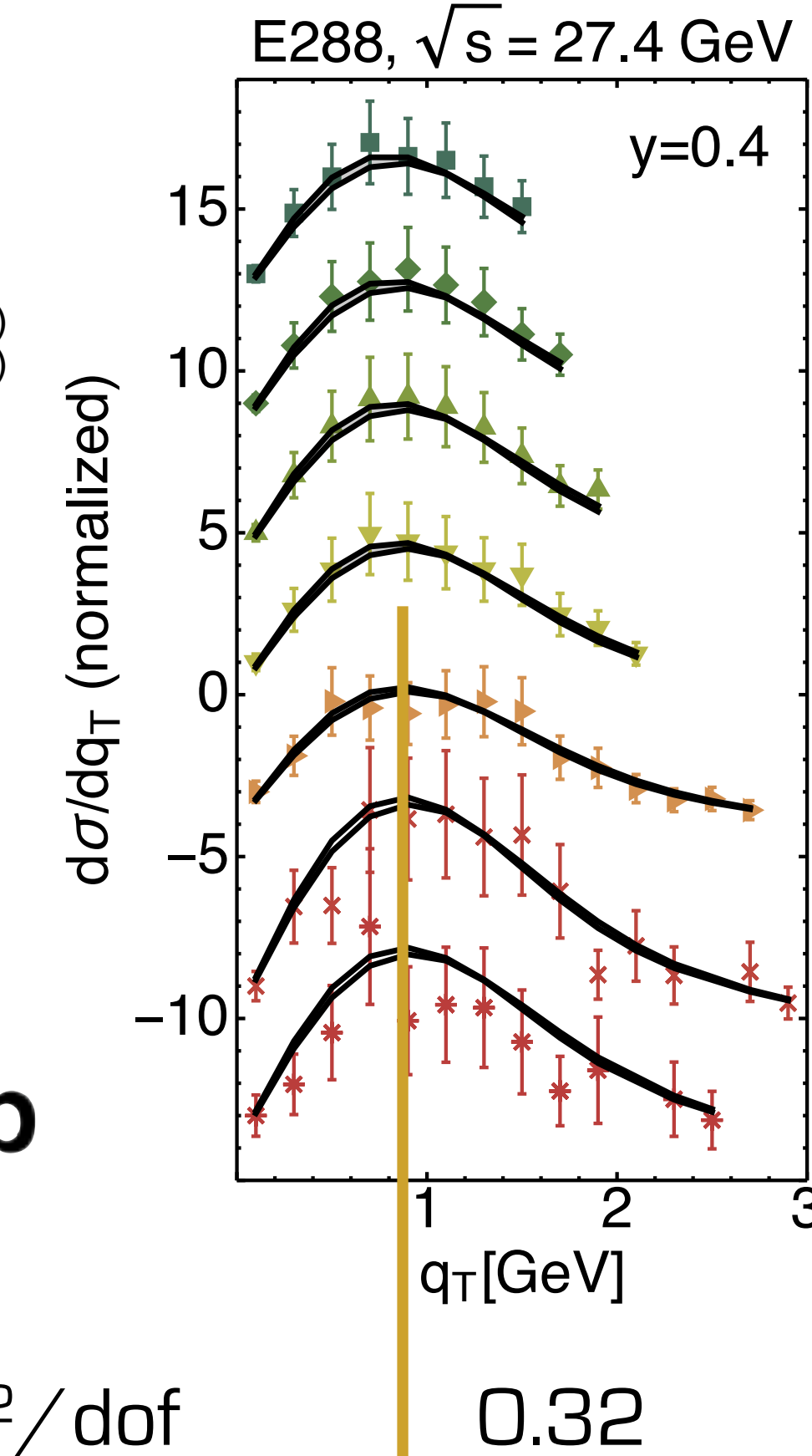


1.13

Drell-Yan data

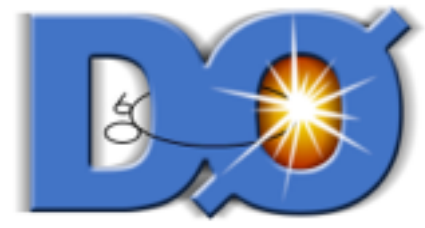
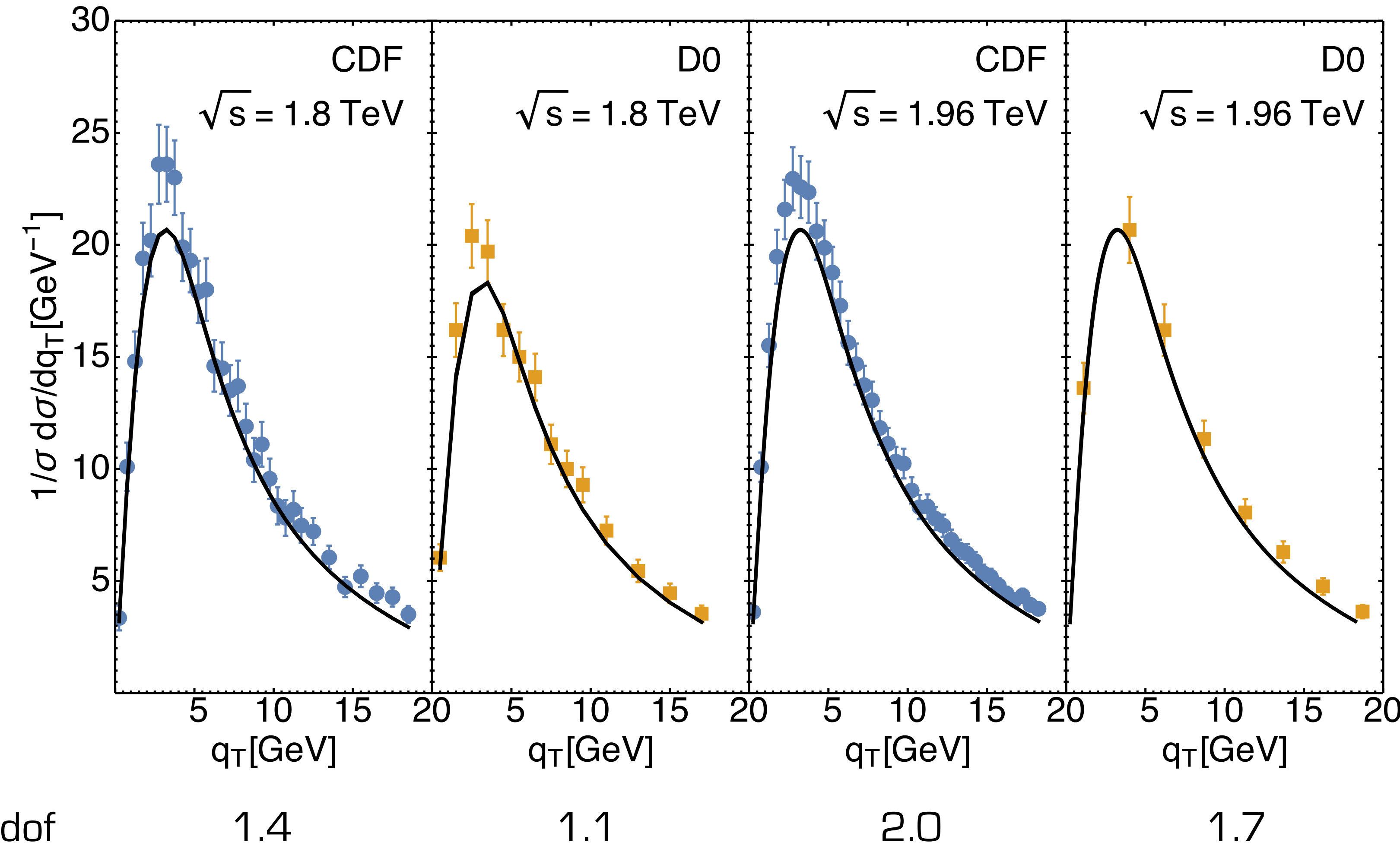
- $\langle Q \rangle = 4.5 \text{ GeV}$ (offset = 16)
- $\langle Q \rangle = 5.5 \text{ GeV}$ (offset = 12)
- ◆ $\langle Q \rangle = 6.5 \text{ GeV}$ (offset = 8)
- ▲ $\langle Q \rangle = 7.5 \text{ GeV}$ (offset = 4)
- ▼ $\langle Q \rangle = 8.5 \text{ GeV}$ (offset = 0)
- ▷ $\langle Q \rangle = 11.0 \text{ GeV}$ (offset = -4)
- ▷ $\langle Q \rangle = 11.5 \text{ GeV}$ (offset = -4)
- ×
- * $\langle Q \rangle = 13.5 \text{ GeV}$ (offset = -14)

Fermilab

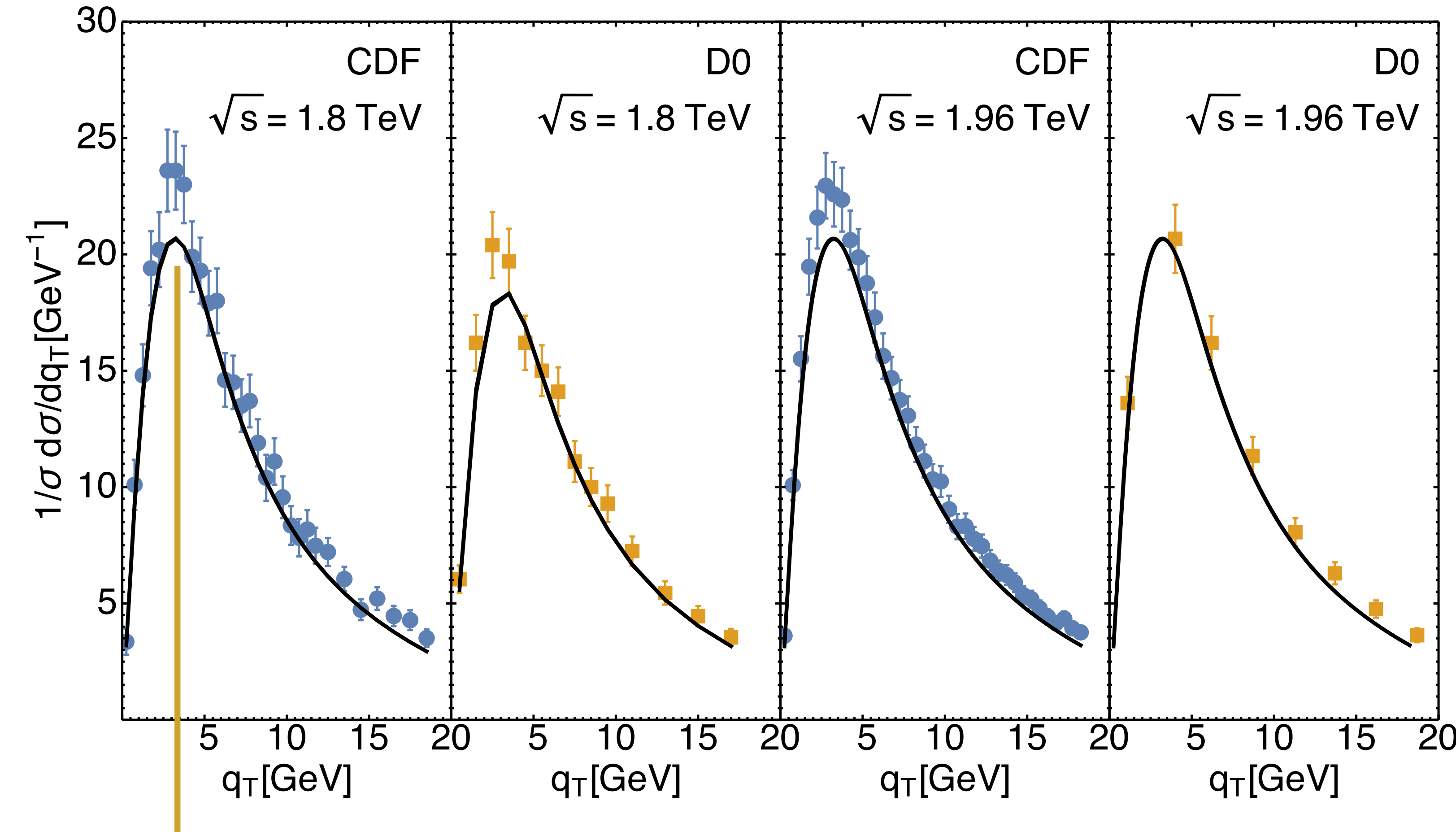


the peak was at 0.4 GeV and now is at 1 GeV

Z-boson data



Z-boson data



χ^2/dof

1.4

1.1

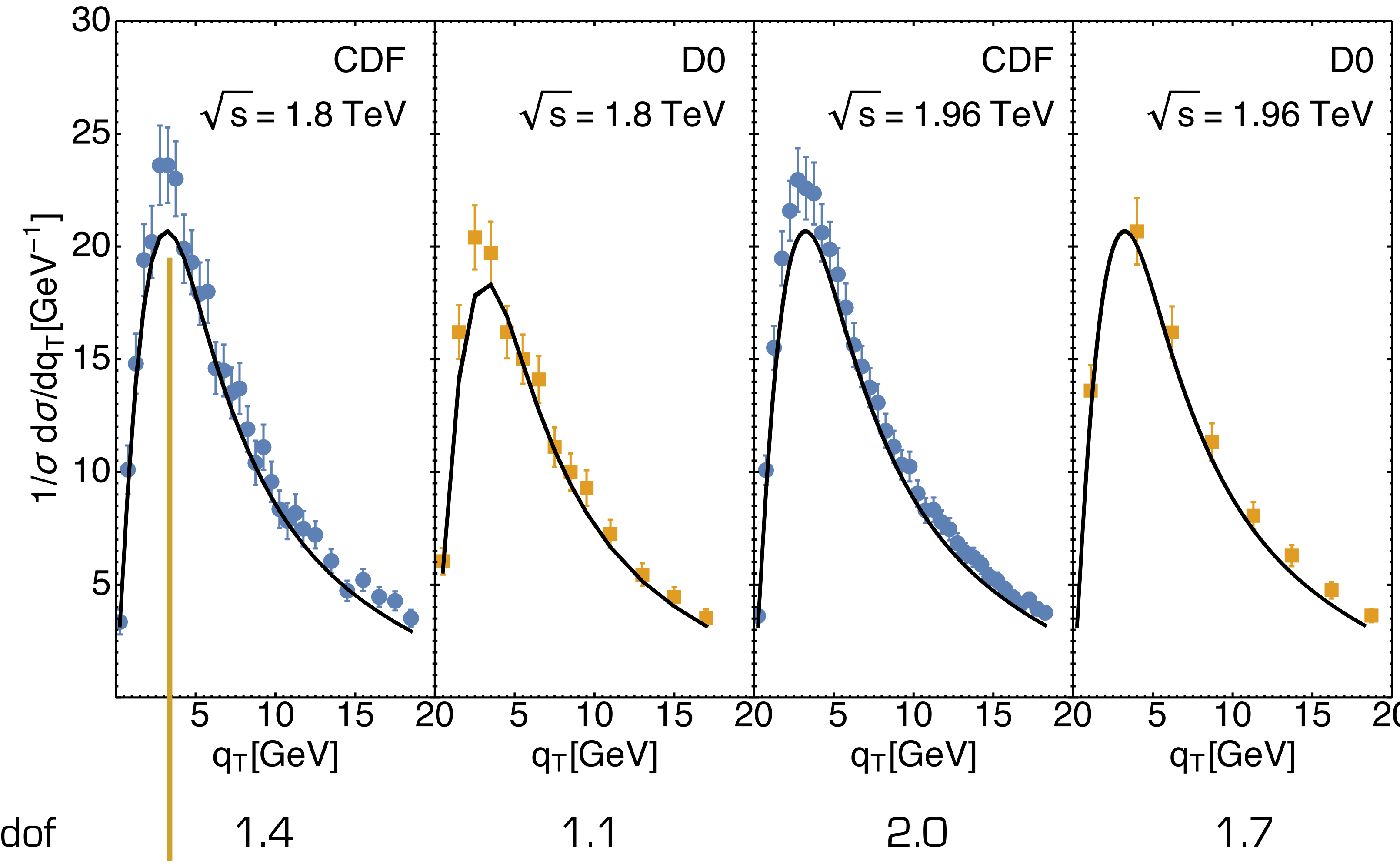
2.0

1.7

the peak now is at 4 GeV

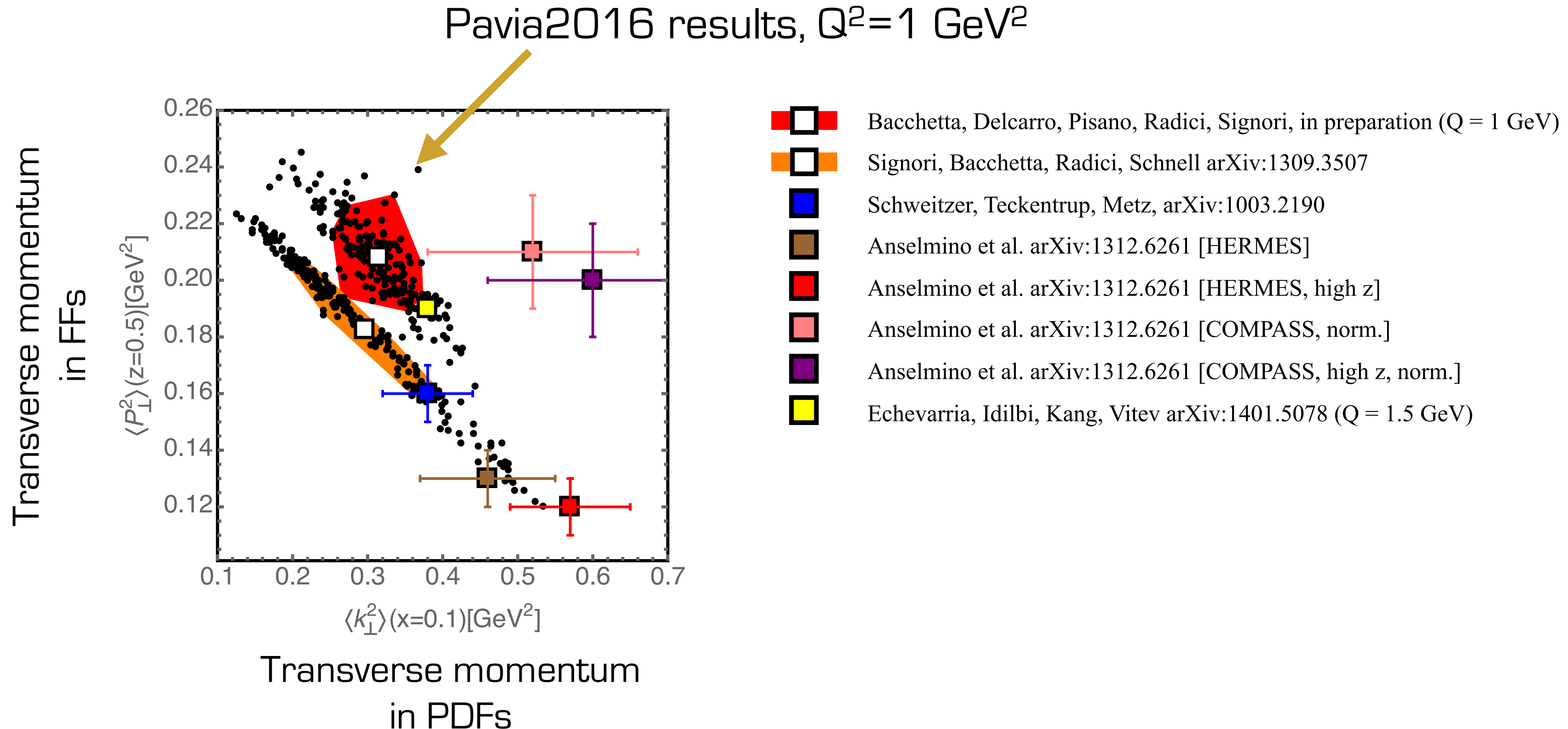


Z-boson data

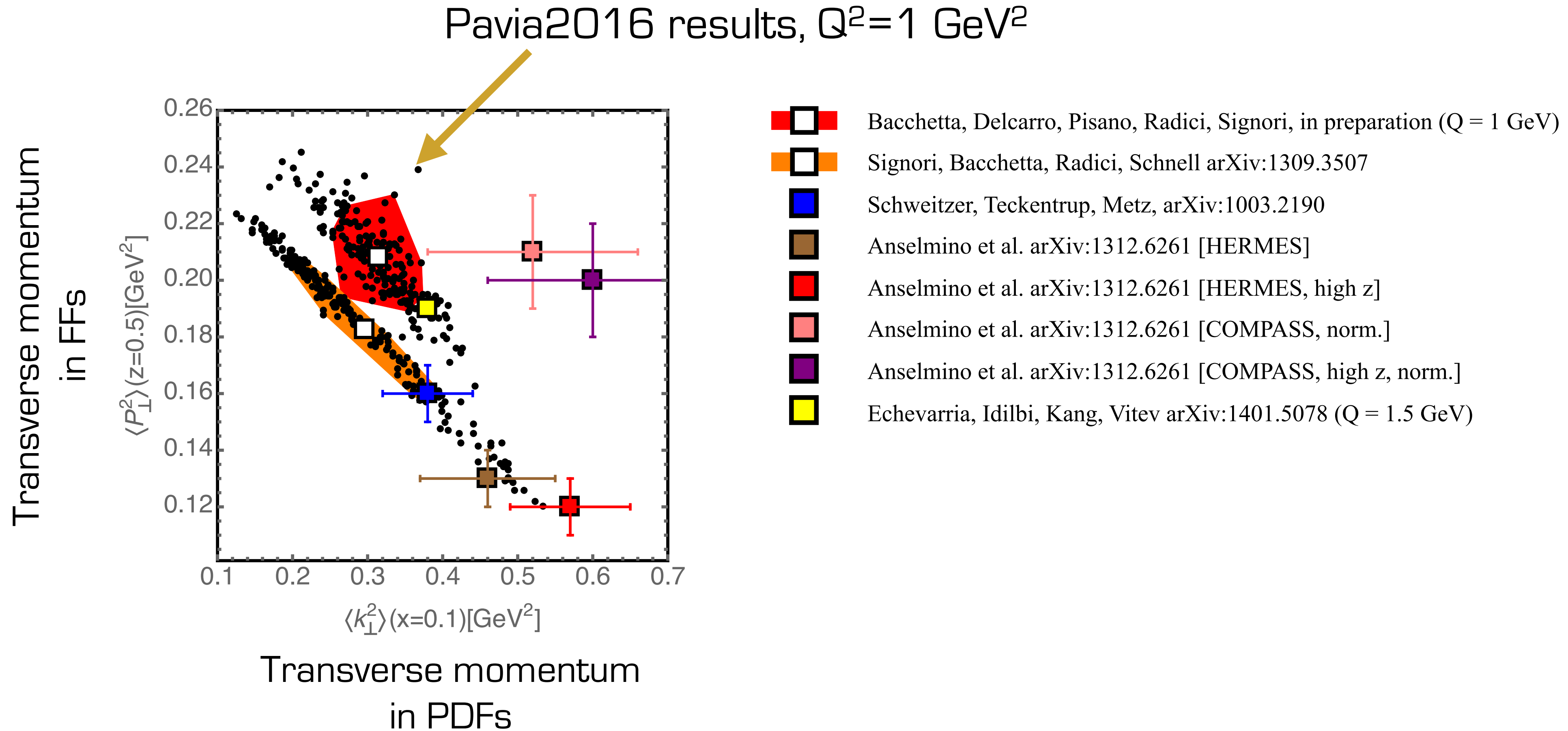


Some outcomes

Mean transverse momentum squared

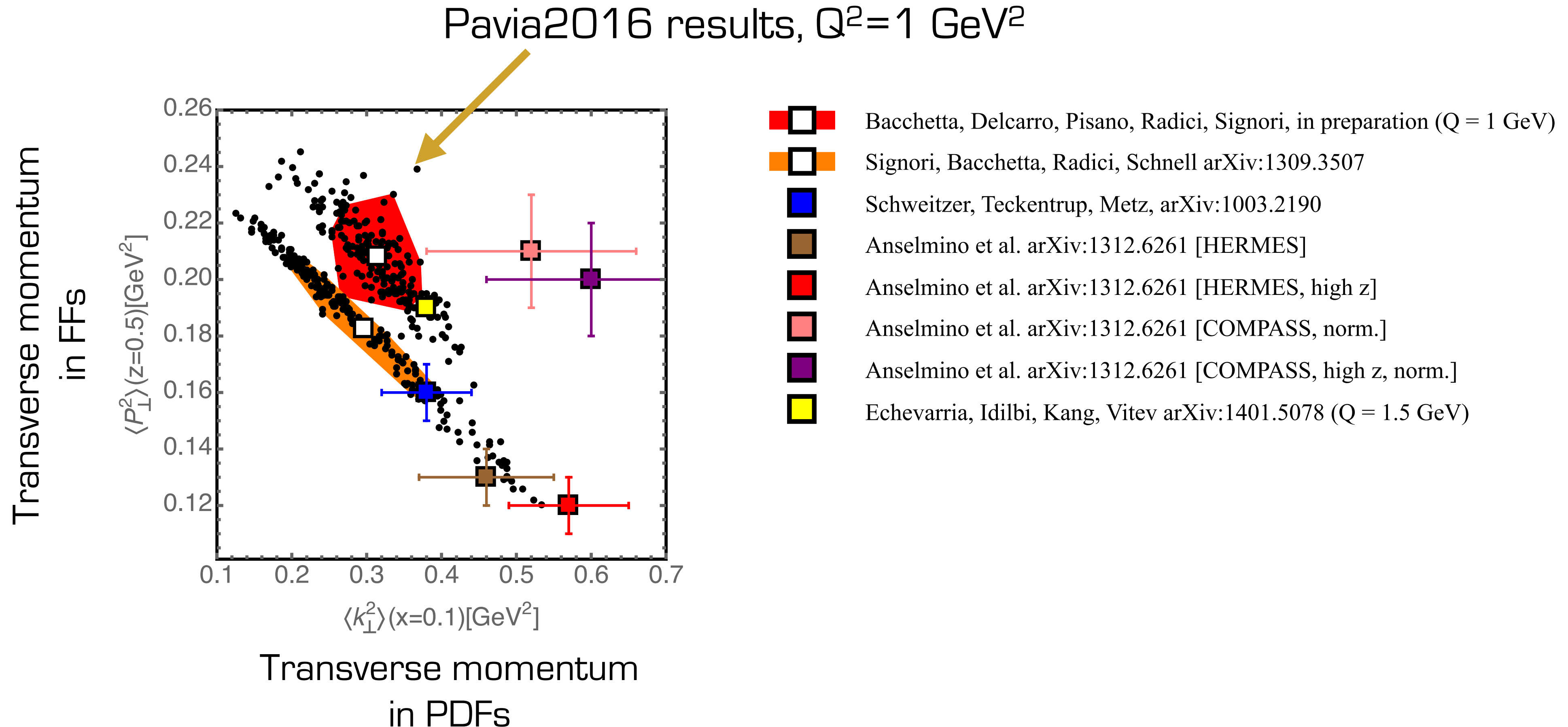


Mean transverse momentum squared



CAVEAT: intrinsic transverse momentum depends on TMD evolution “scheme” and its parameters

Mean transverse momentum squared

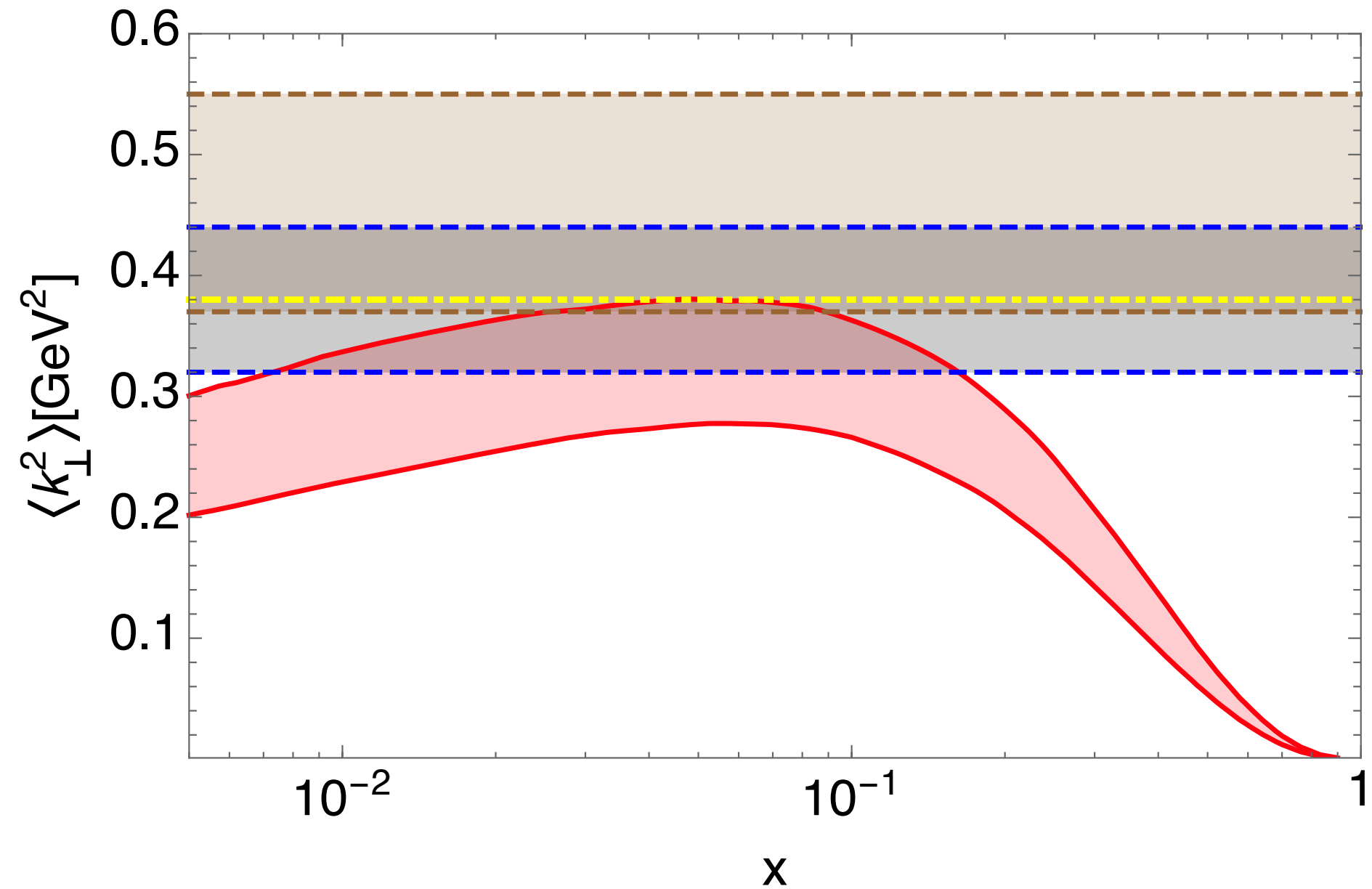


CAVEAT: intrinsic transverse momentum depends on TMD evolution “scheme” and its parameters

Anti correlation between transverse momentum in TMD PDFs and in TMD FFs, in spite of Drell-Yan data

Mean transverse momentum squared

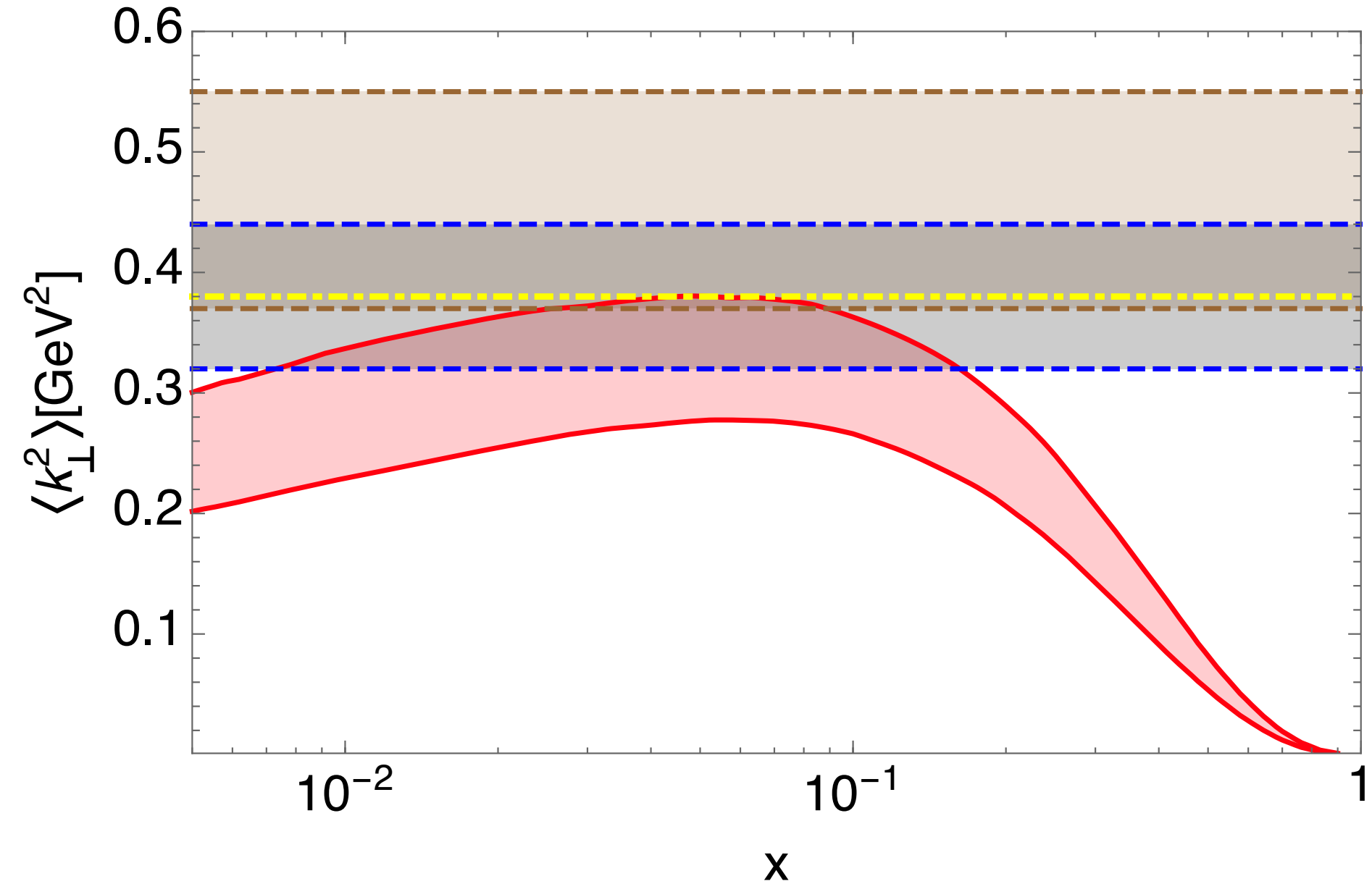
same color coding as previous slide



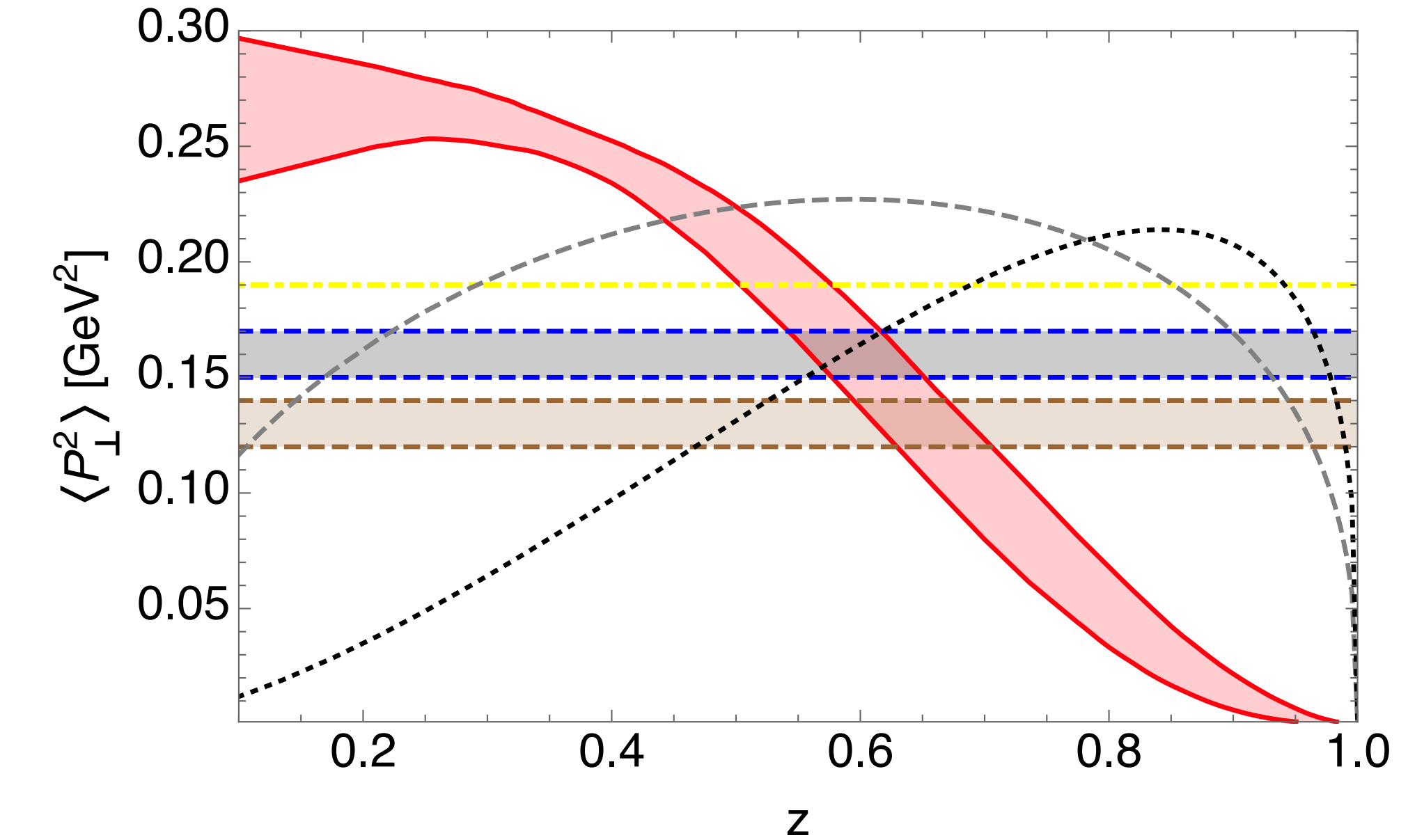
In TMD distribution functions

Mean transverse momentum squared

same color coding as previous slide



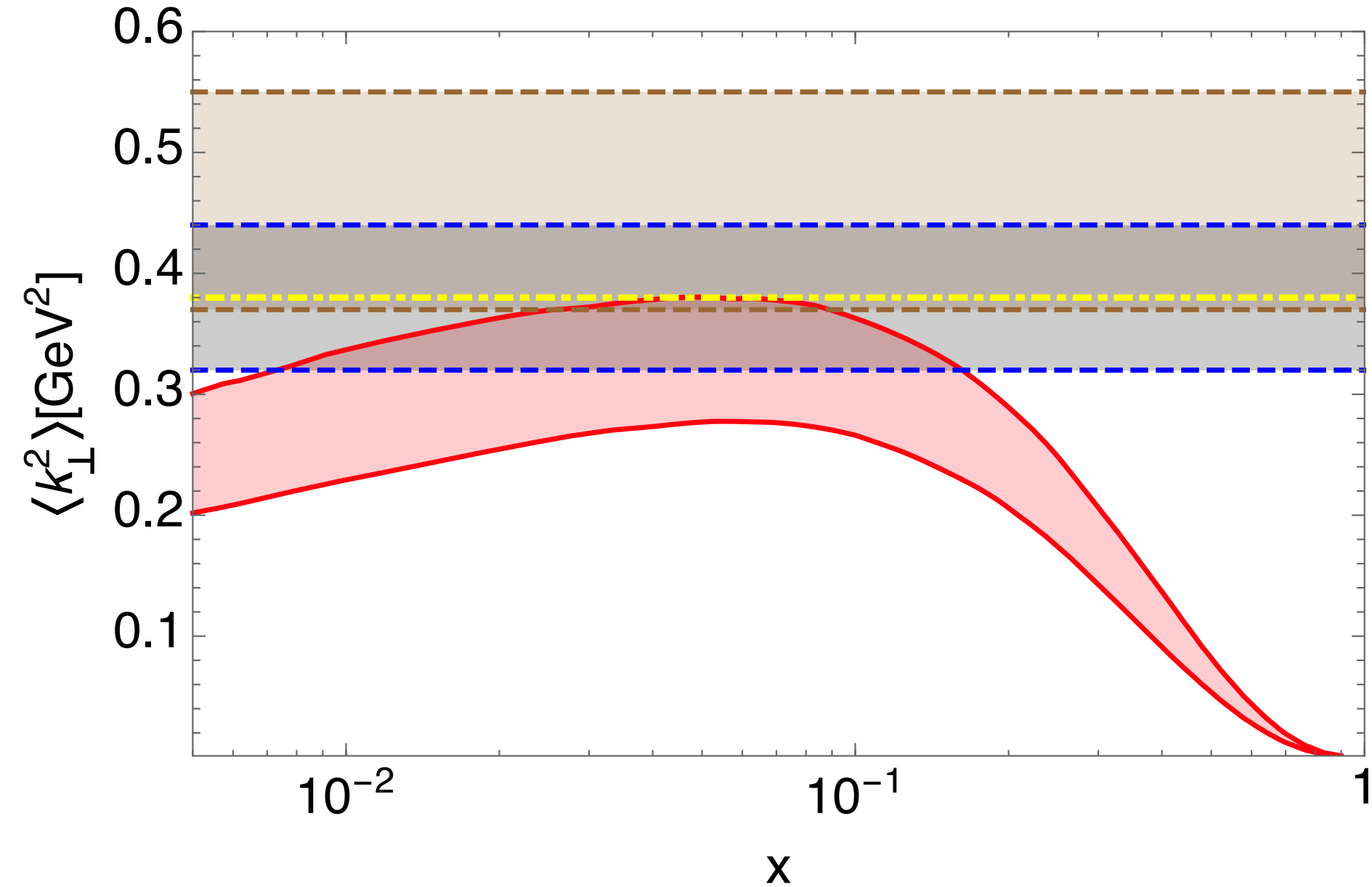
In TMD distribution functions



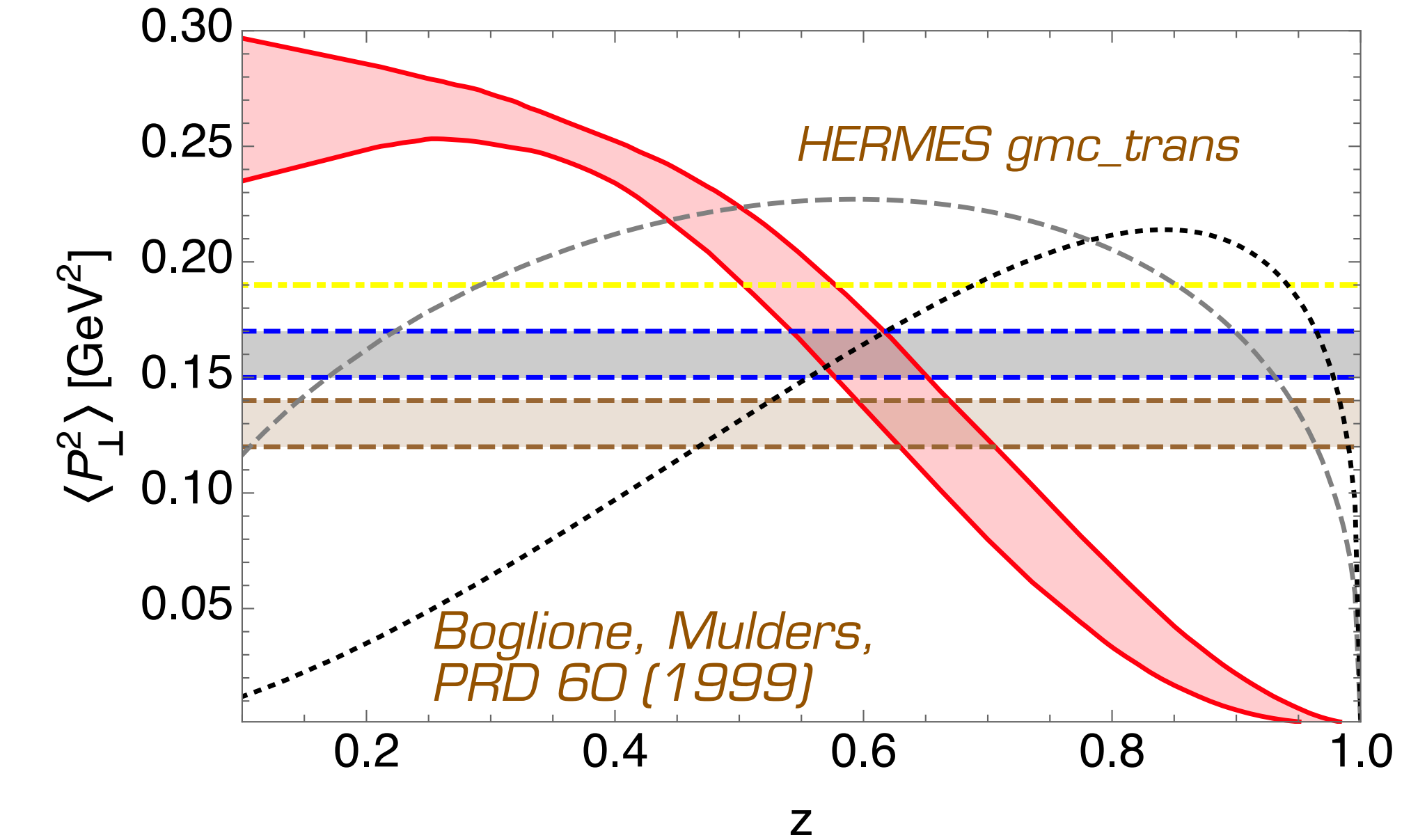
In TMD fragmentation functions

Mean transverse momentum squared

same color coding as previous slide



In TMD distribution functions



In TMD fragmentation functions

Nonperturbative evolution parameters

TMD evolution is not uniquely determined by pQCD calculations. Nonperturbative input is needed to determine evolution precisely. Different schemes may behave differently.

	$g_2 \text{ (GeV}^2\text{)}$	$b_{\max}(\text{GeV}^{-1})$
BLNY 2003	0.68 ± 0.02	0.5
KN 2006	0.184 ± 0.018	1.5
EIKV 2014	0.18	1.5
Pavia 2016	0.12 ± 0.01	1.123

Nonperturbative evolution parameters

TMD evolution is not uniquely determined by pQCD calculations. Nonperturbative input is needed to determine evolution precisely. Different schemes may behave differently.

	$g_2 \text{ (GeV}^2\text{)}$	$b_{\max}(\text{GeV}^{-1})$
BLNY 2003	0.68 ± 0.02	0.5
KN 2006	0.184 ± 0.018	1.5
EIKV 2014	0.18	1.5
Pavia 2016	0.12 ± 0.01	1.123

Faster evolution: transverse momentum increases faster due to gluon radiation

Nonperturbative evolution parameters

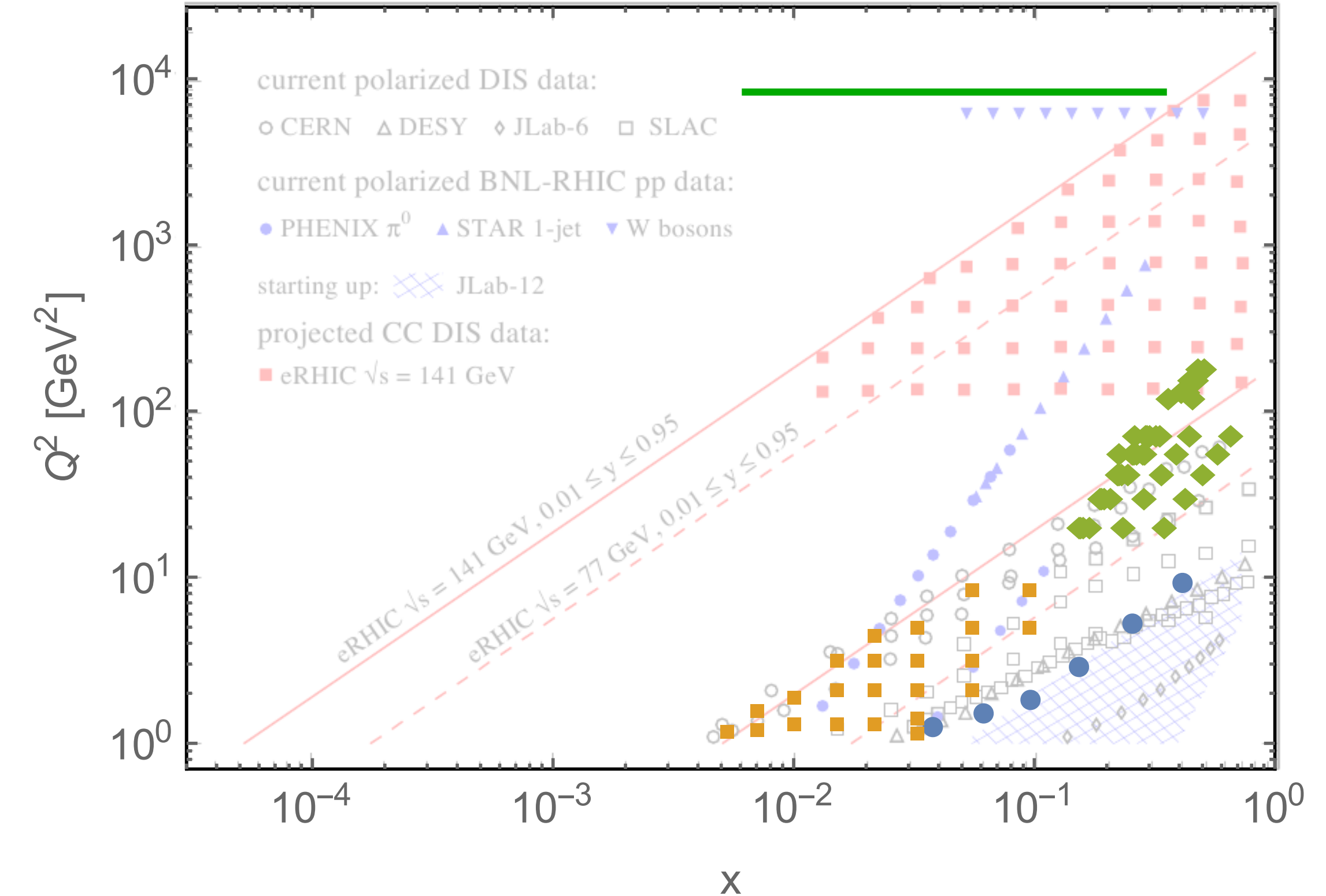
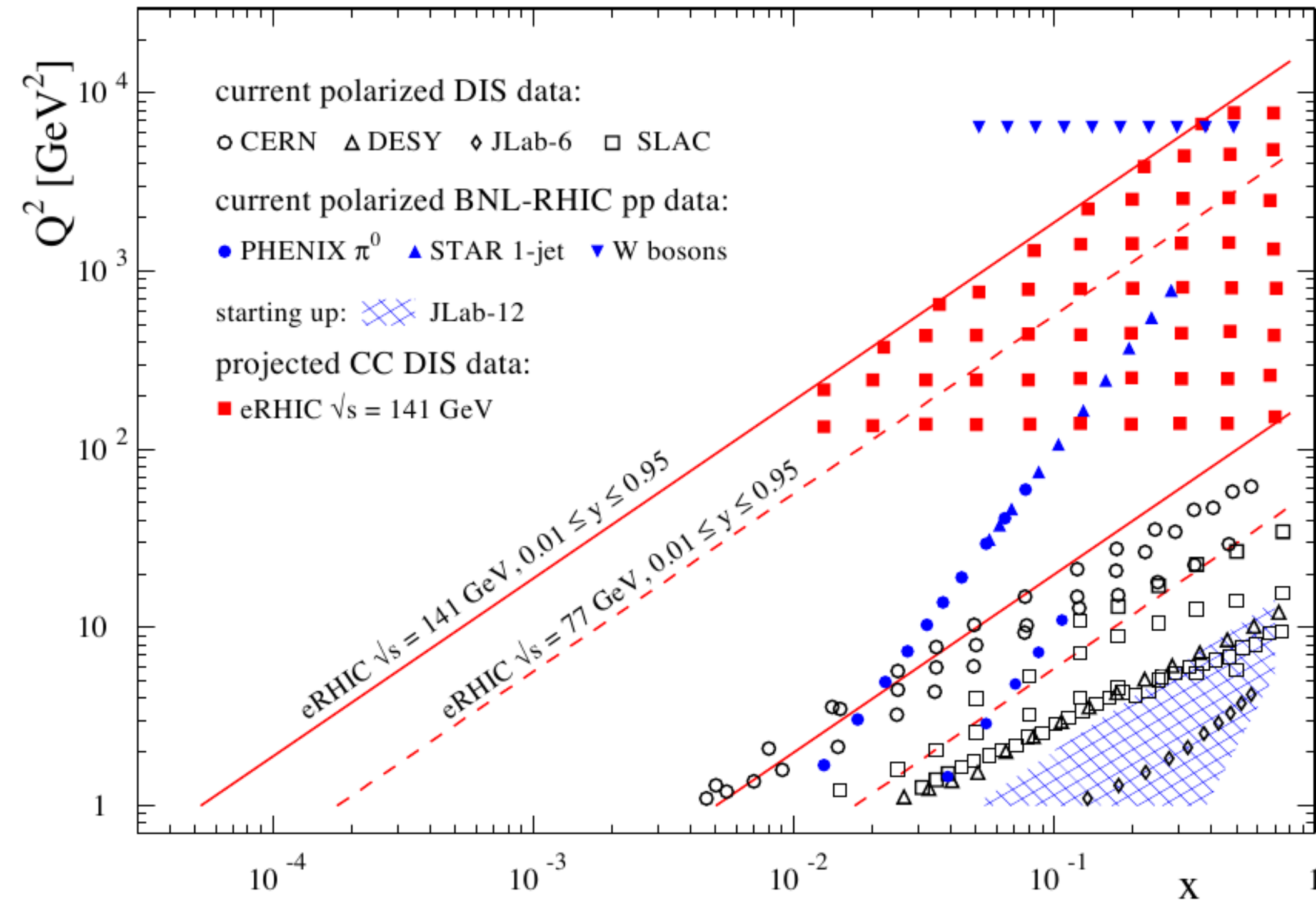
TMD evolution is not uniquely determined by pQCD calculations. Nonperturbative input is needed to determine evolution precisely. Different schemes may behave differently.

	$g_2 \text{ (GeV}^2\text{)}$	$b_{\max}(\text{GeV}^{-1})$
BLNY 2003	0.68 ± 0.02	0.5
KN 2006	0.184 ± 0.018	1.5
EIKV 2014	0.18	1.5
Pavia 2016	0.12 ± 0.01	1.123

Faster evolution: transverse momentum increases faster due to gluon radiation

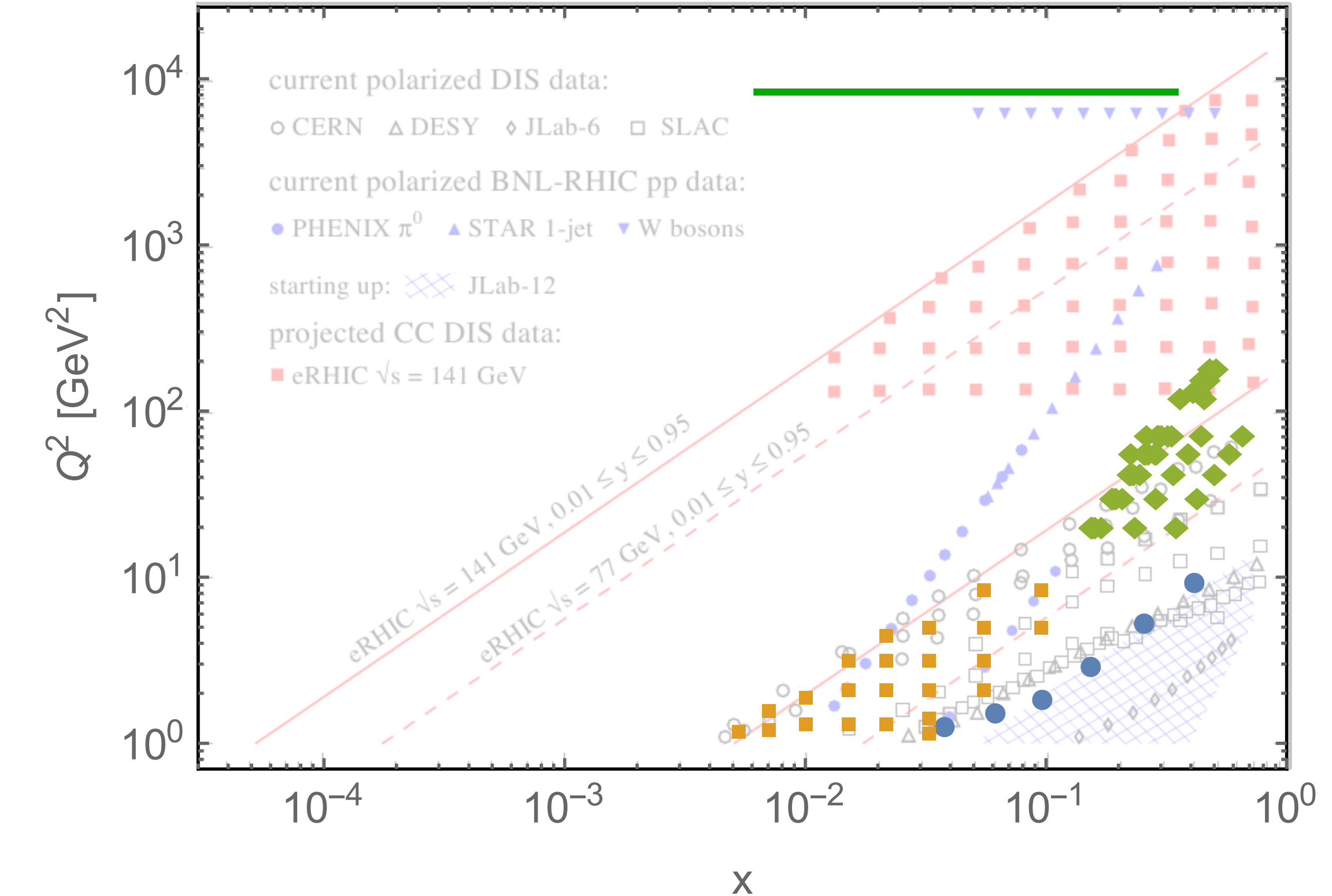
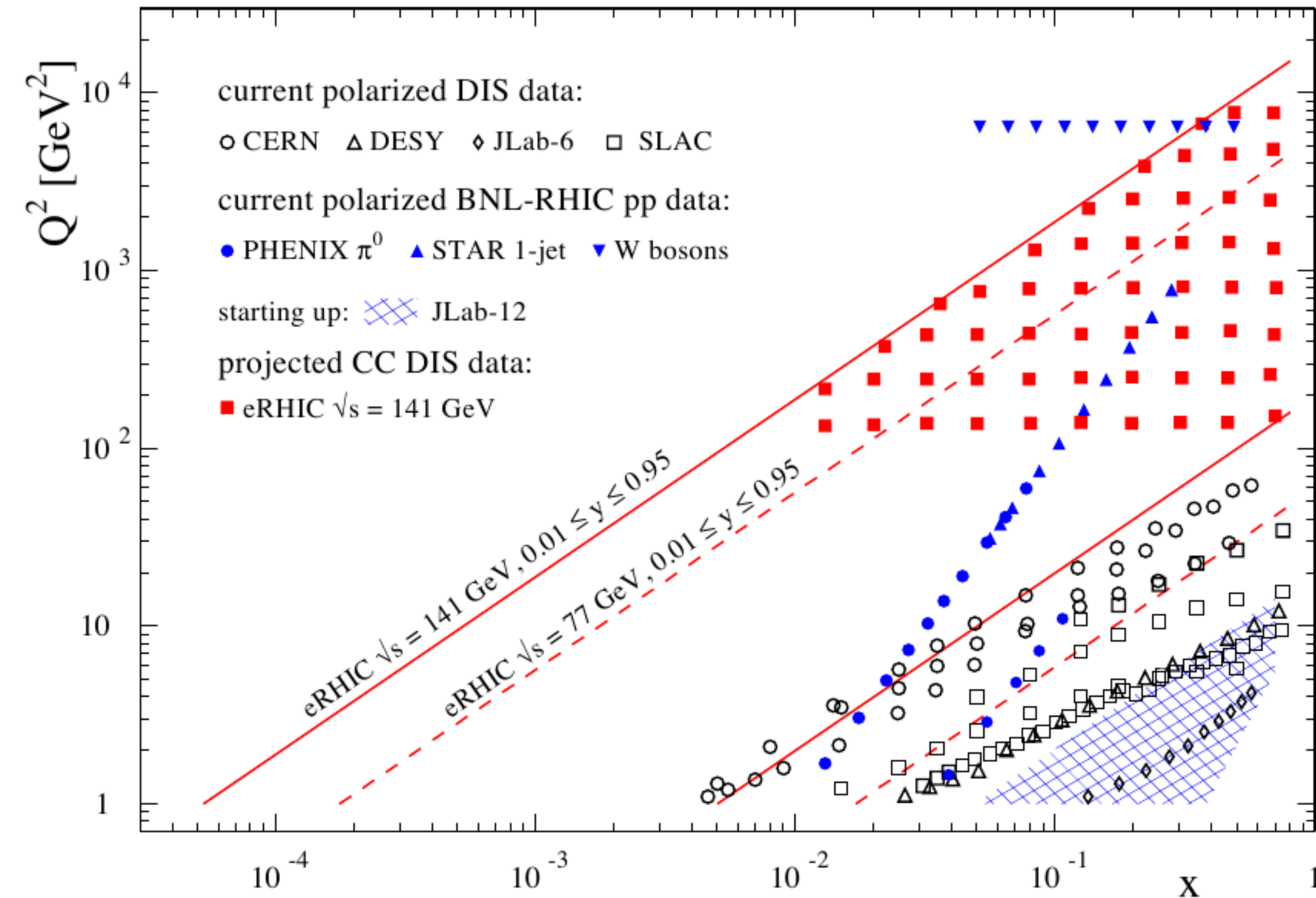
Slower evolution: the effect of gluon radiation is weaker

Comparison with future perspectives



from EIC white paper EPJA 52 (2016)

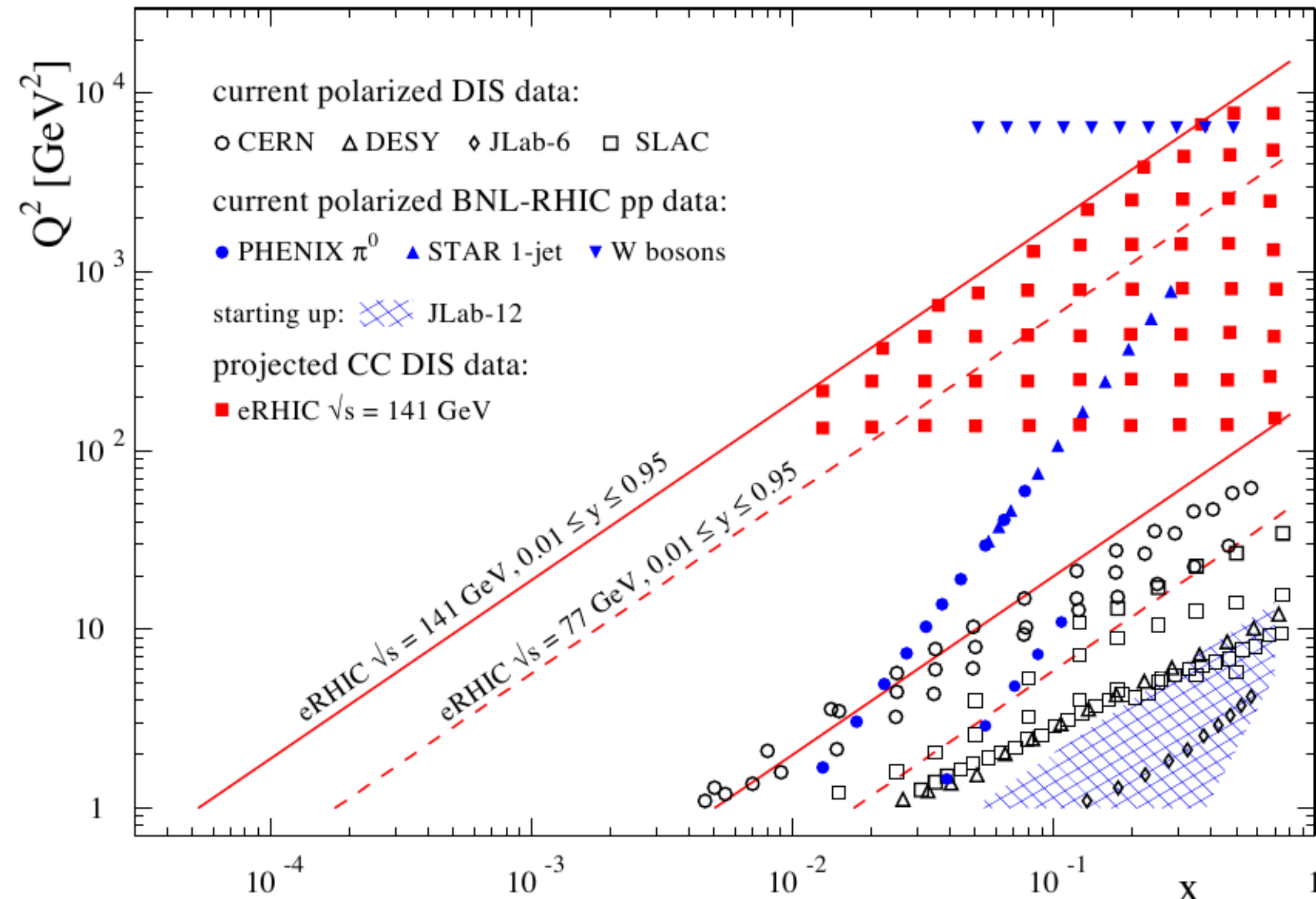
Comparison with future perspectives



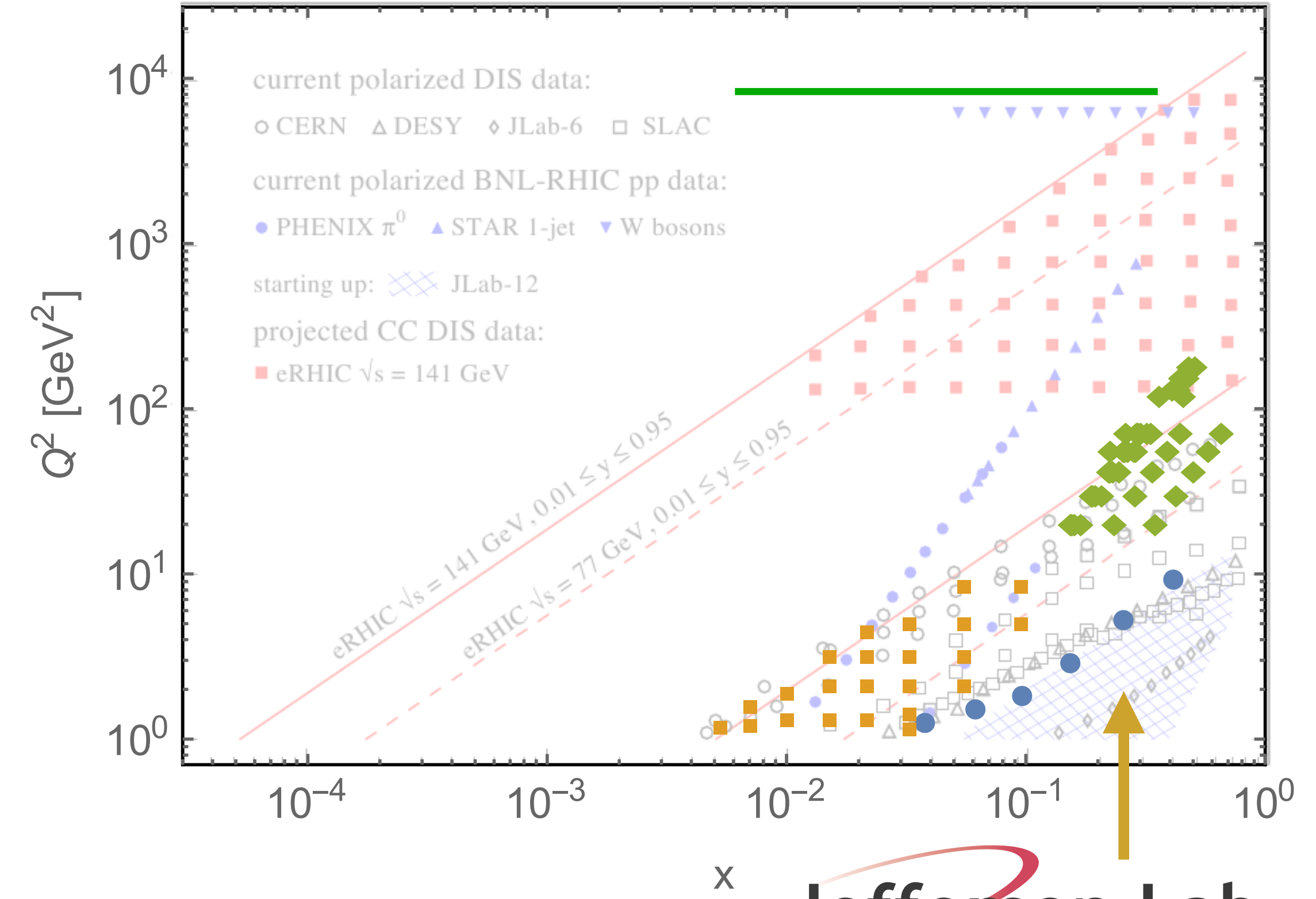
from EIC white paper EPJA 52 (2016)

To test the formalism, we would need more data covering the same x range and spanning over a large range in Q^2 . Data from JLab and Drell-Yan would be very important.

Comparison with future perspectives

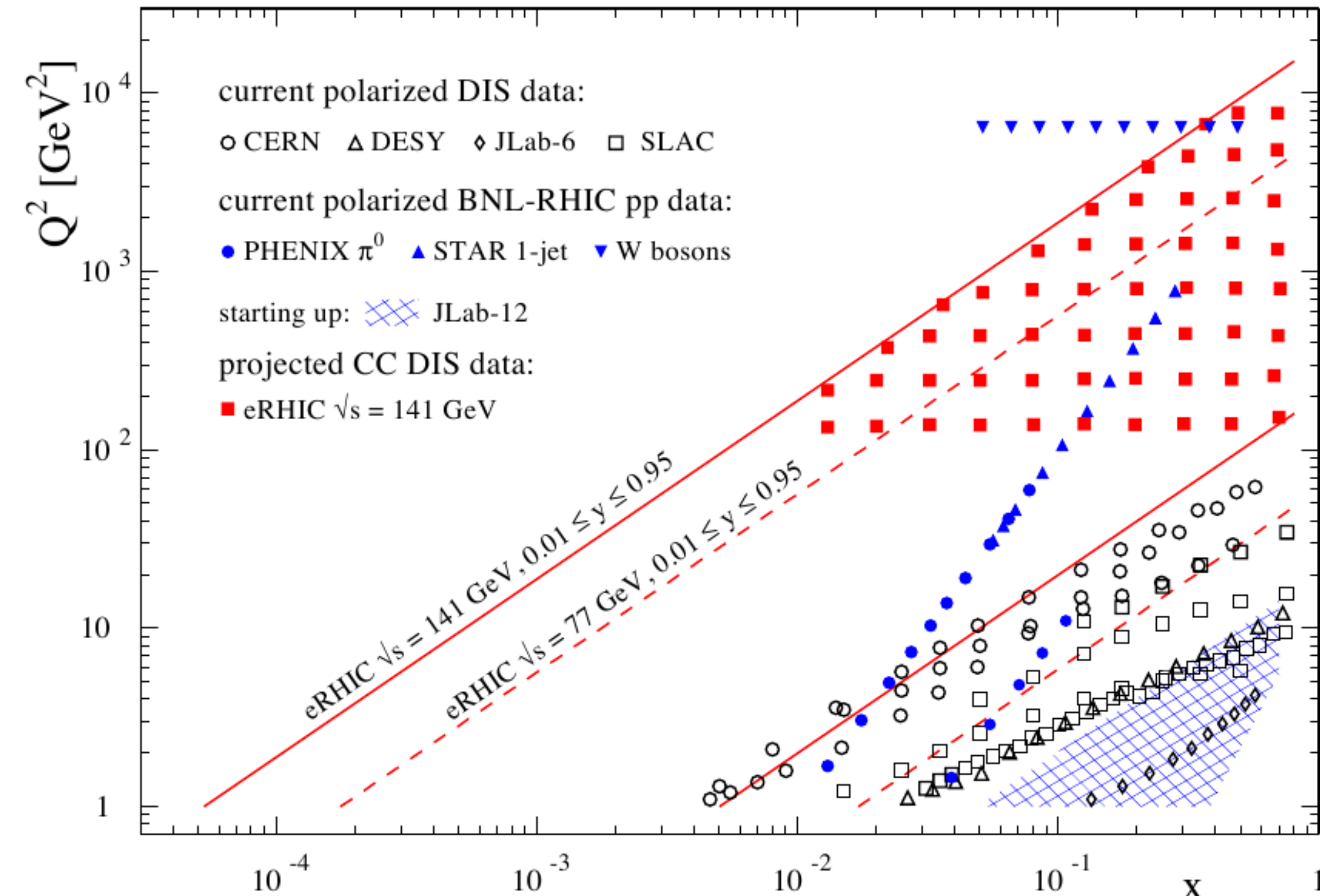


from EIC white paper EPJA 52 (2016)

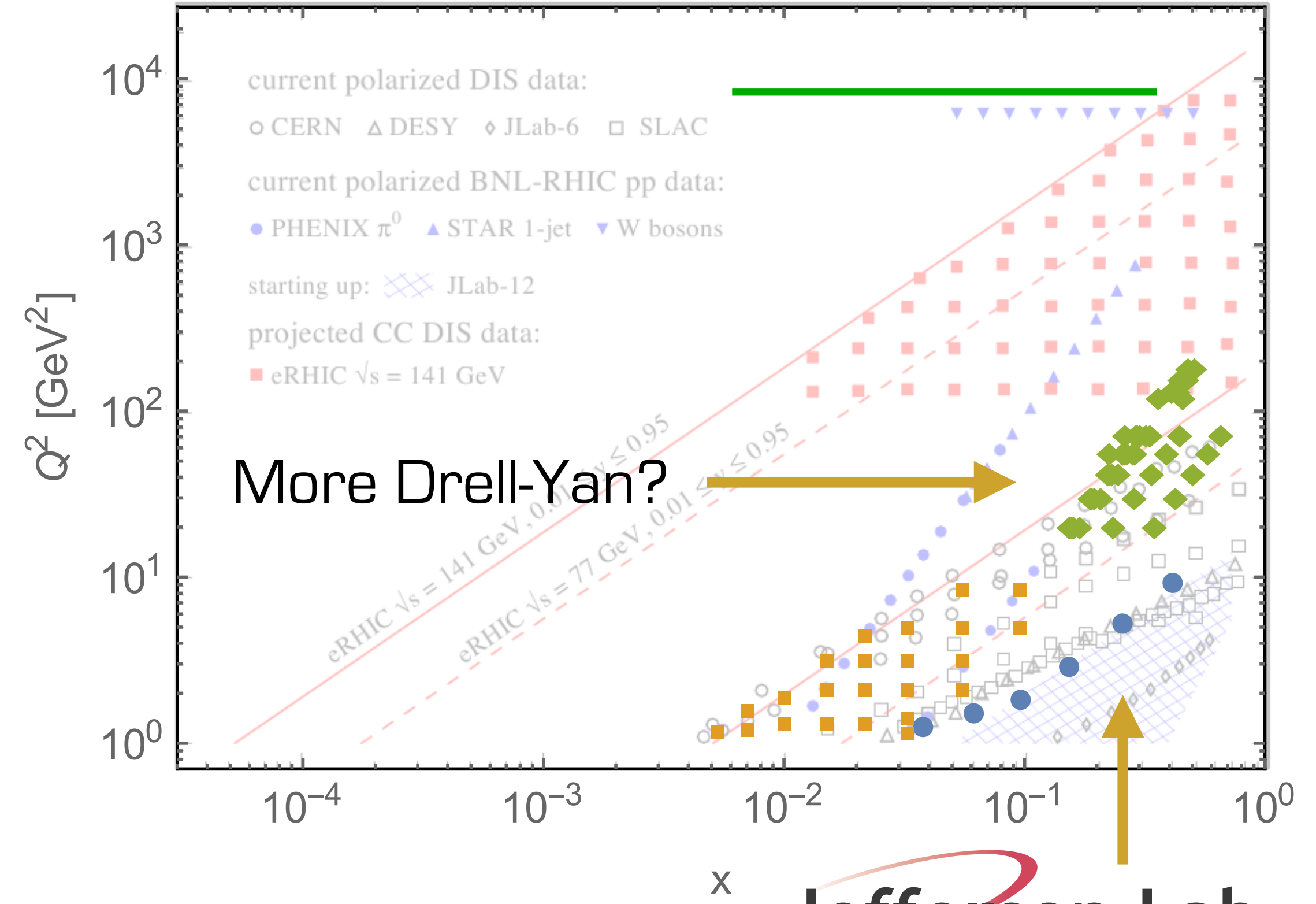


To test the formalism, we would need more data covering the same x range and spanning over a large range in Q^2 . Data from JLab and Drell-Yan would be very important.

Comparison with future perspectives

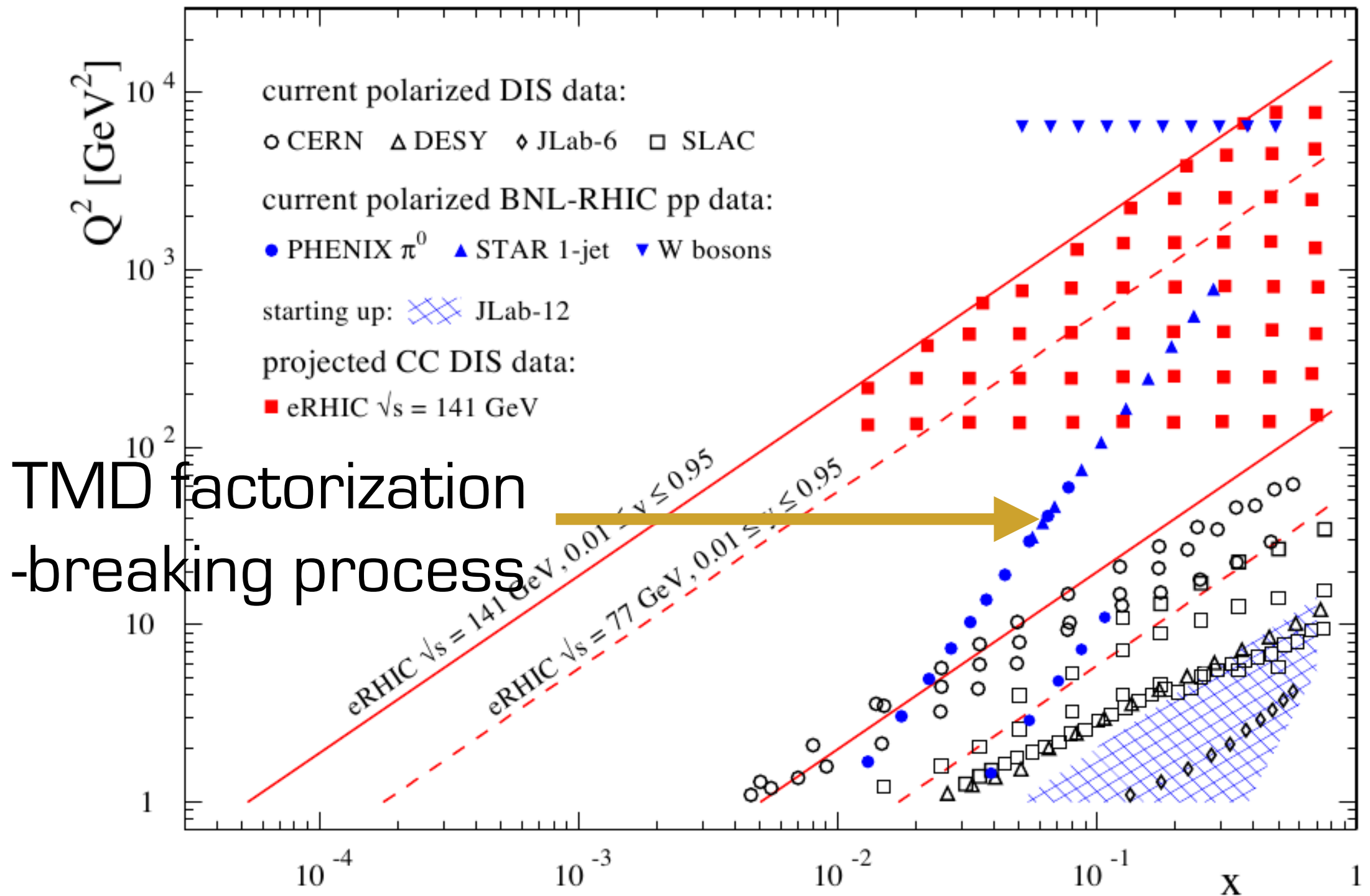


from EIC white paper EPJA 52 (2016)

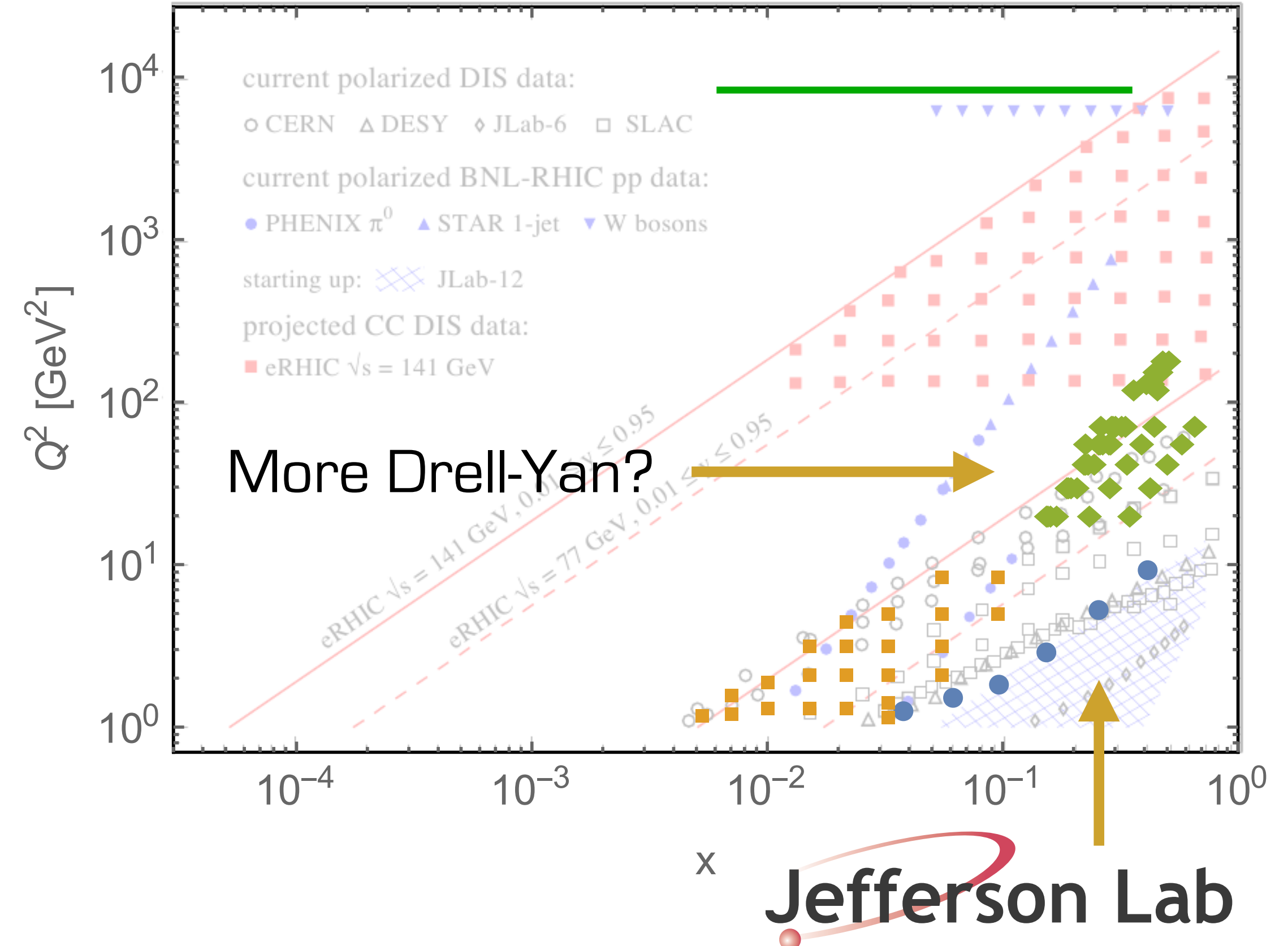


To test the formalism, we would need more data covering the same x range and spanning over a large range in Q^2 . Data from JLab and Drell-Yan would be very important.

Comparison with future perspectives

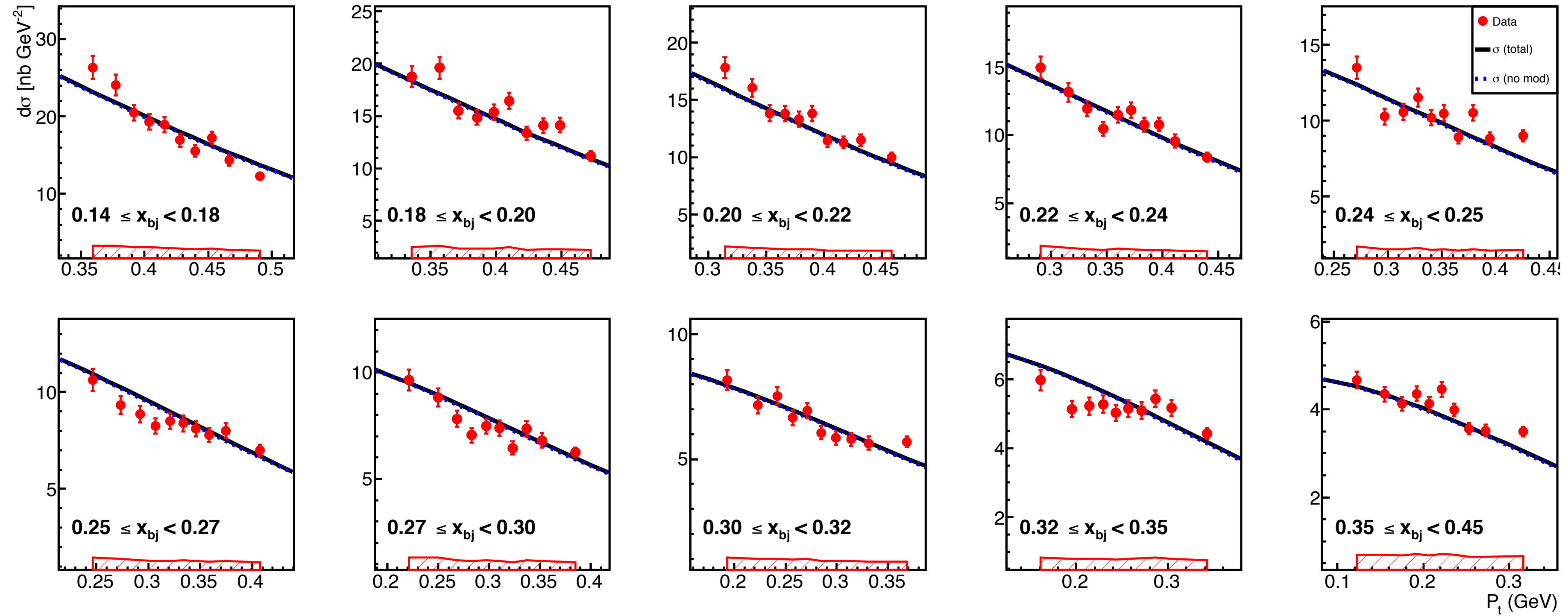


from EIC white paper EPJA 52 (2016)



To test the formalism, we would need more data covering the same x range and spanning over a large range in Q^2 . Data from JLab and Drell-Yan would be very important.

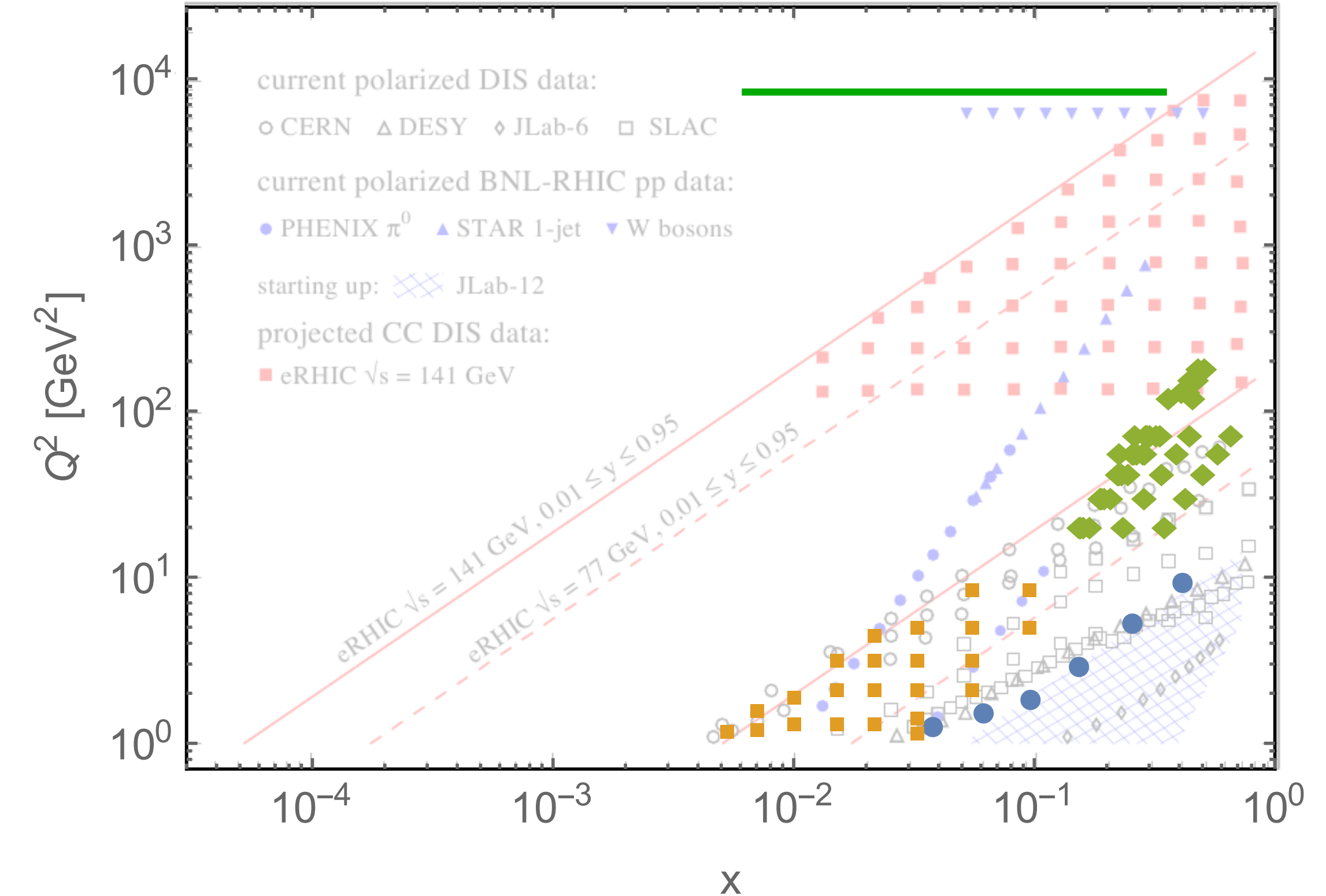
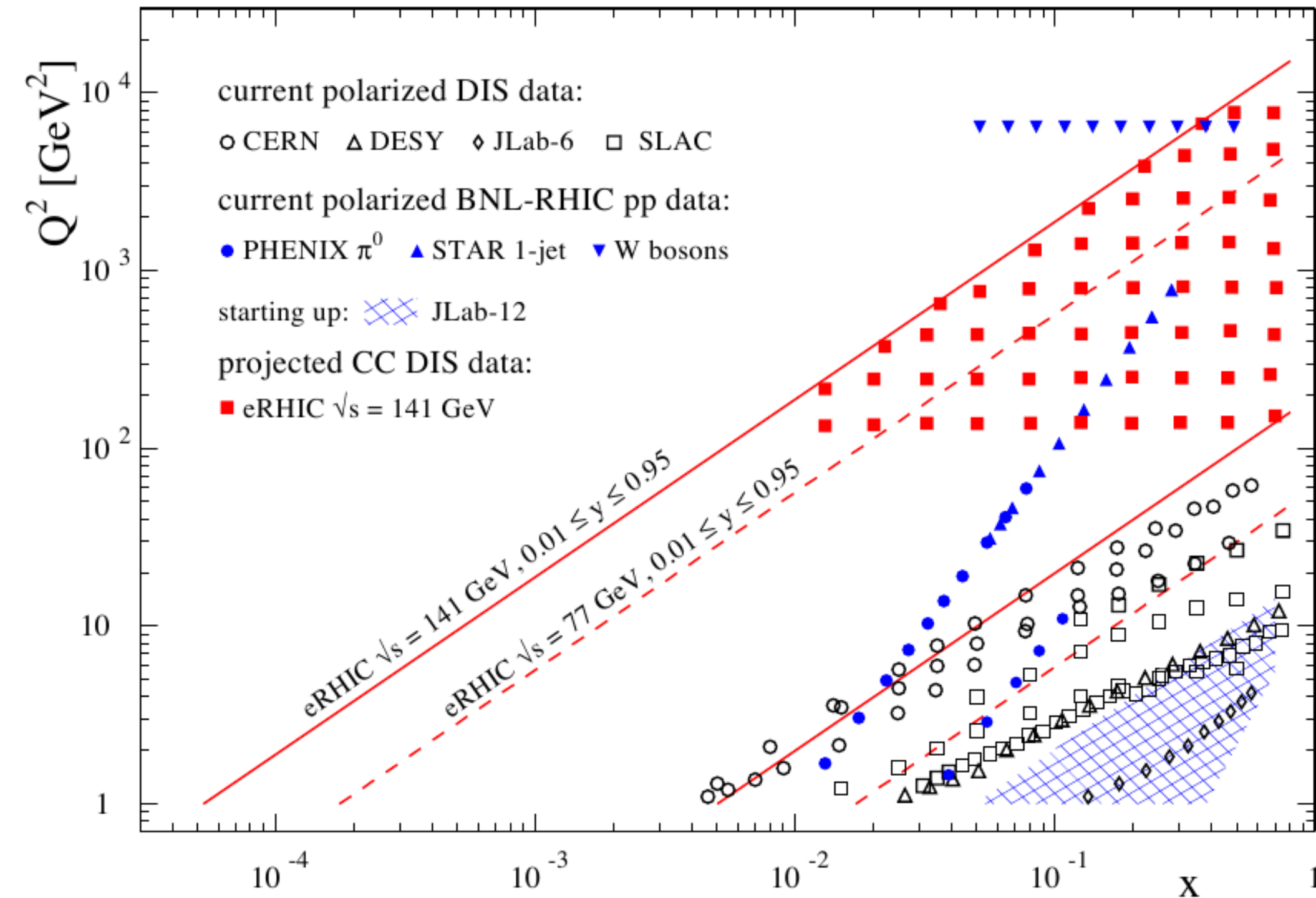
Recent ${}^3\text{He}$ data from JLab Hall A



Yan et al., arXiv:1610.02350

Not included in the present fits on the ground that it is at 6 GeV: needs to be checked!

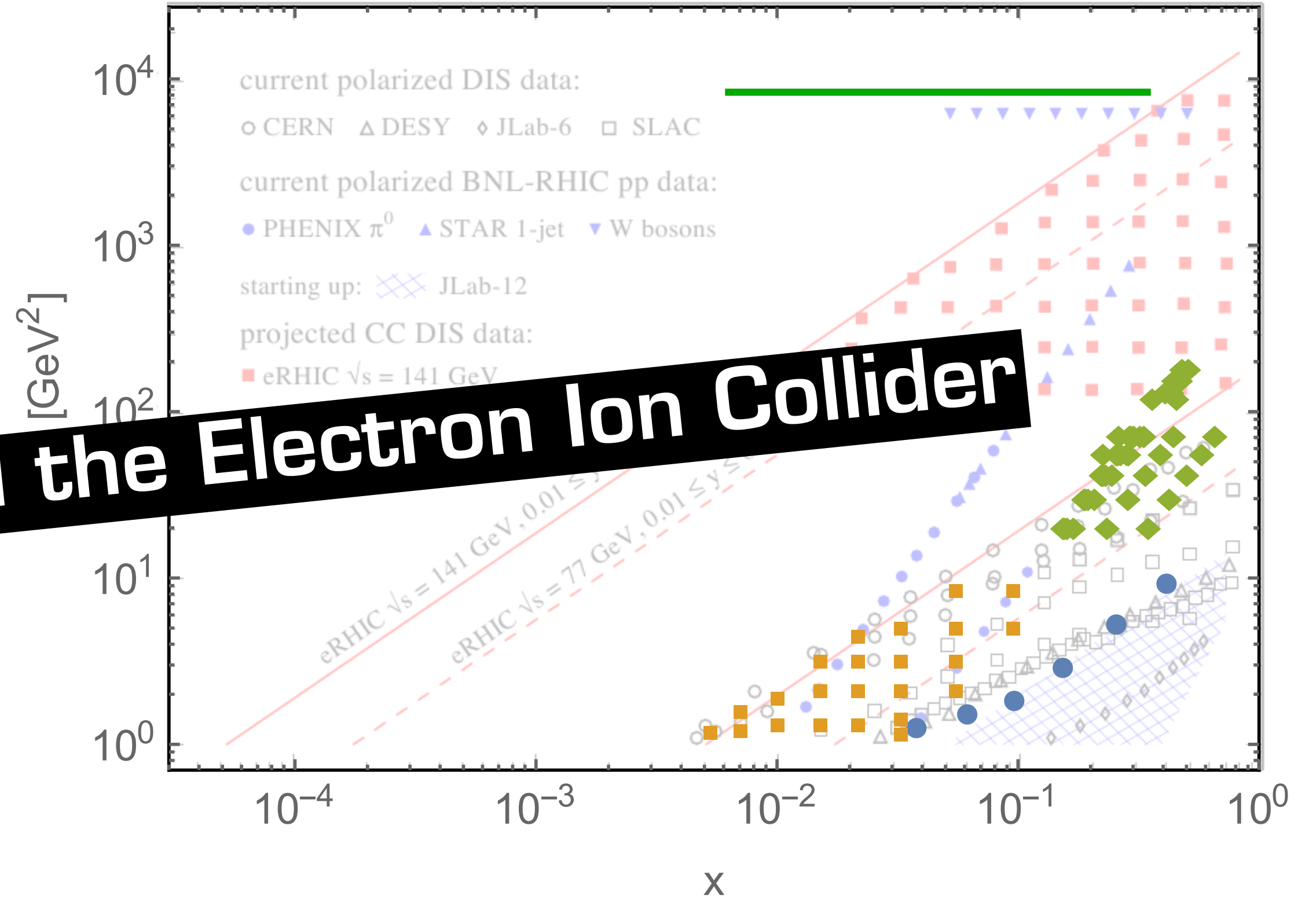
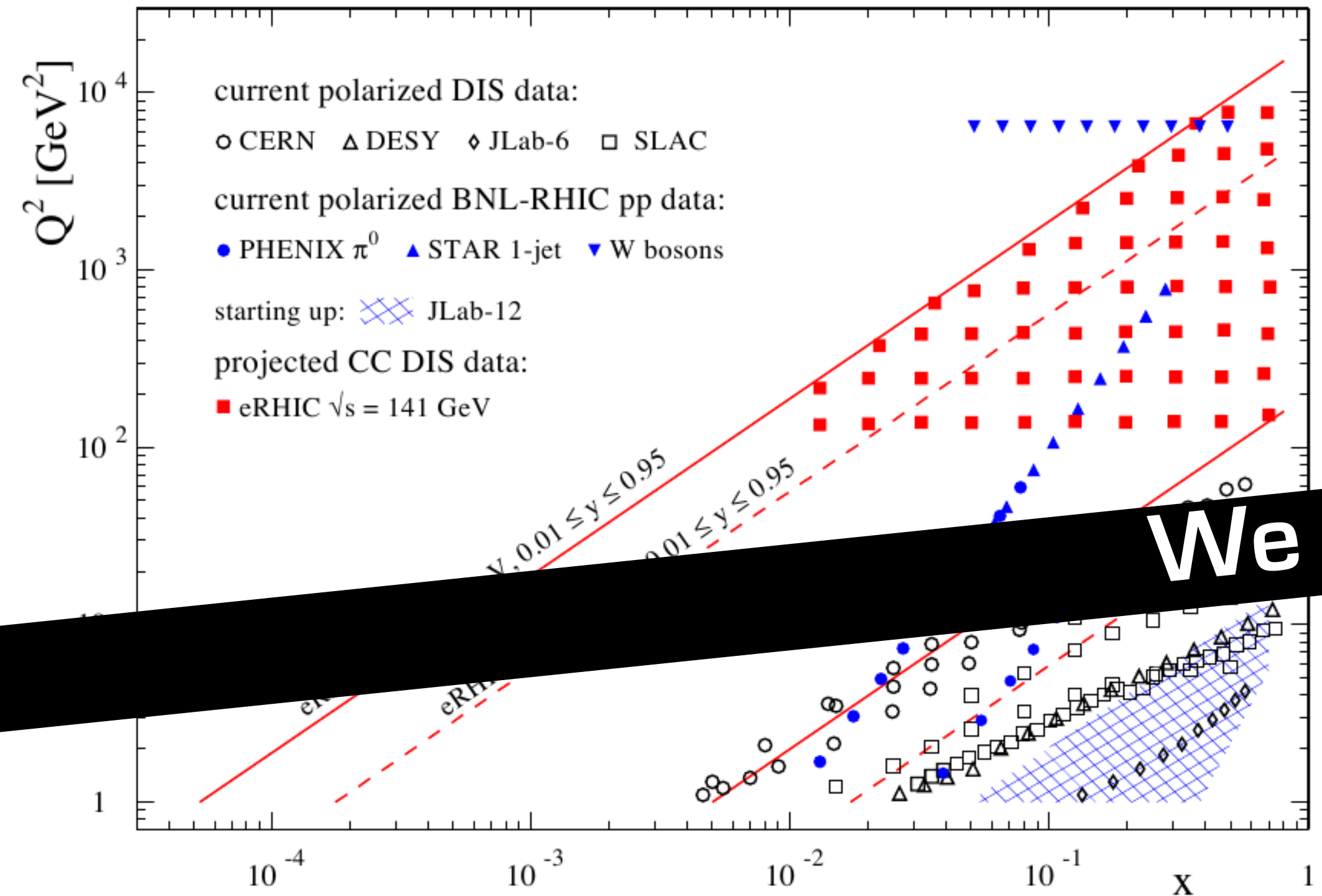
Comparison with future perspectives



from EIC white paper EPJA 52 (2016)

To test the formalism, we would need more data covering the same x range and spanning over a large range in Q^2 . Data from JLab and Drell-Yan would be very important.

Comparison with future perspectives



from EIC white paper EPJA 52 (2016)

To test the formalism, we would need more data covering the same x range and spanning over a large range in Q^2 . Data from JLab and Drell-Yan would be very important.

Conclusions

Conclusions

- We demonstrated for the first time that it is possible to fit simultaneously SIDIS, DY, and Z boson data

Conclusions

- We demonstrated for the first time that it is possible to fit simultaneously SIDIS, DY, and Z boson data
- We extracted unpolarized TMDs using several thousand data points

Conclusions

- We demonstrated for the first time that it is possible to fit simultaneously SIDIS, DY, and Z boson data
- We extracted unpolarized TMDs using several thousand data points
- The TMD framework seems to hold pretty well

Conclusions

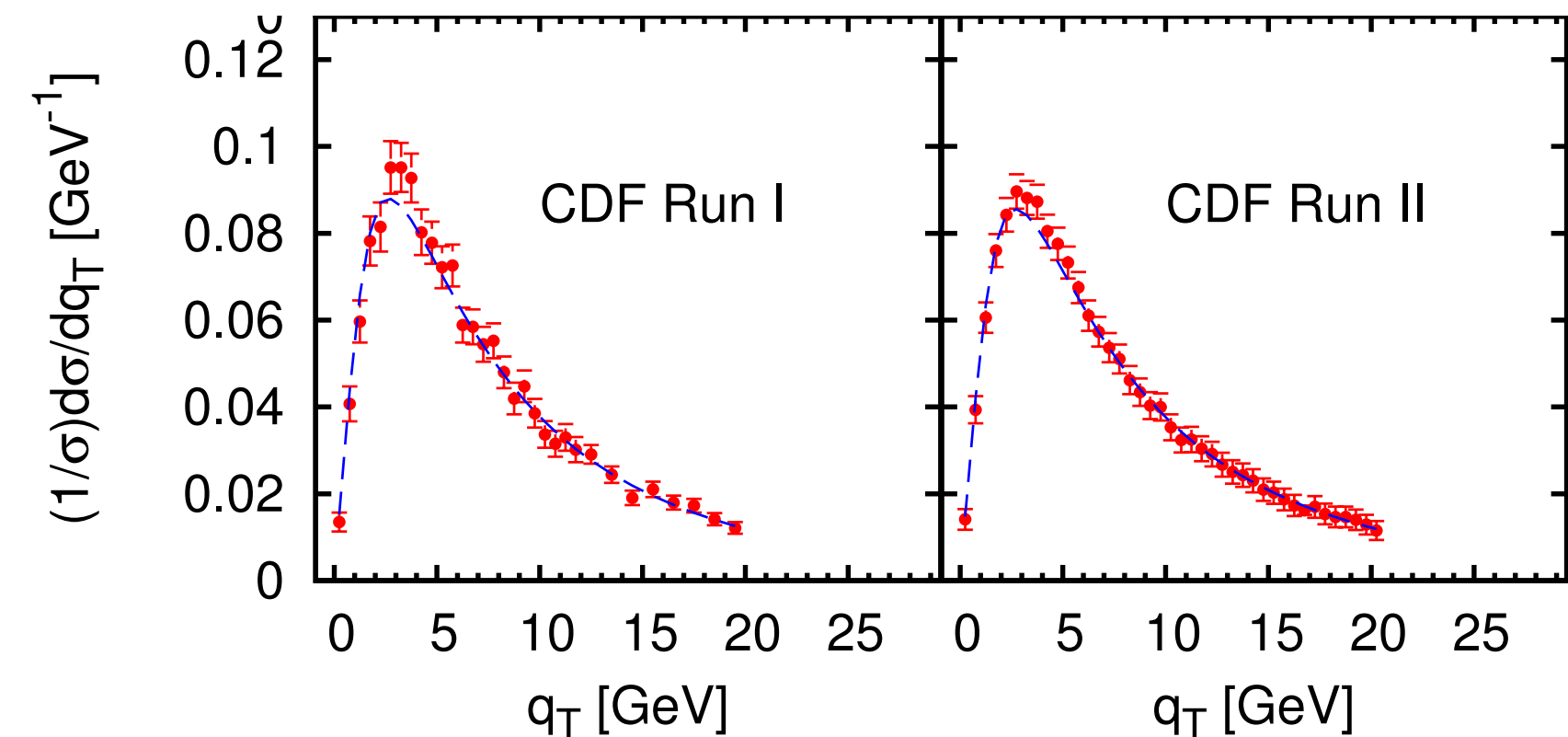
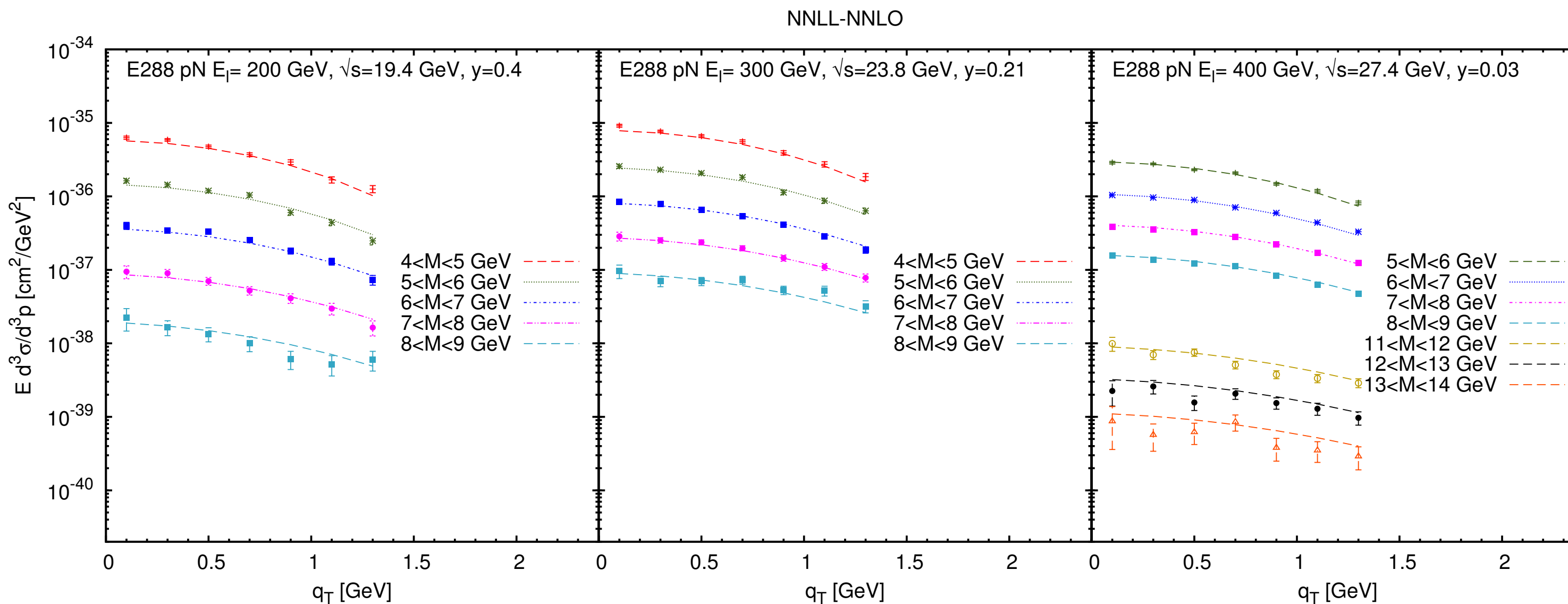
- We demonstrated for the first time that it is possible to fit simultaneously SIDIS, DY, and Z boson data
- We extracted unpolarized TMDs using several thousand data points
- The TMD framework seems to hold pretty well
- Most of the discrepancies come from the normalisation

Conclusions

- We demonstrated for the first time that it is possible to fit simultaneously SIDIS, DY, and Z boson data
- We extracted unpolarized TMDs using several thousand data points
- The TMD framework seems to hold pretty well
- Most of the discrepancies come from the normalisation
- Y terms still to be implemented

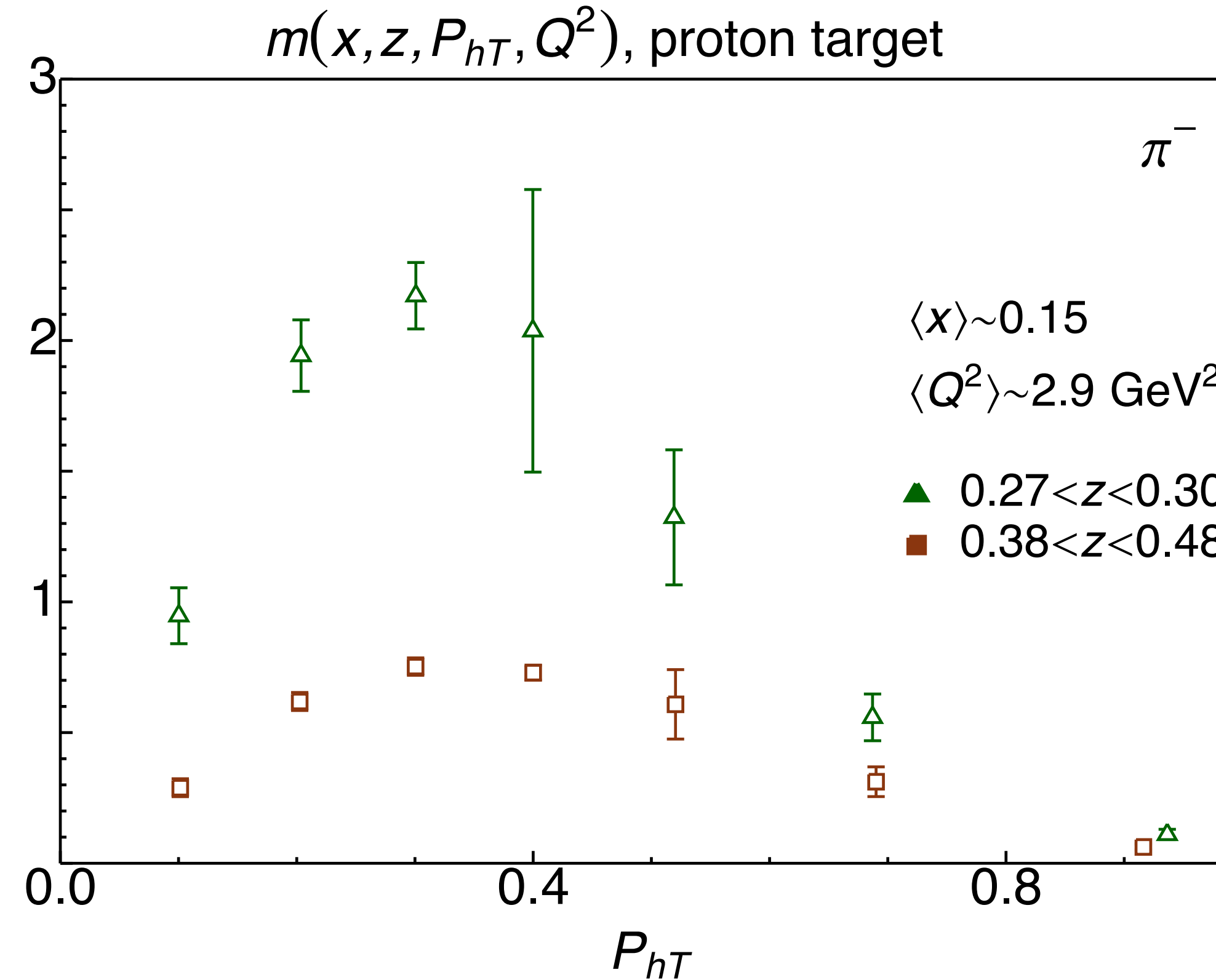
Drell-Yan + Z production data (DEMS 2014)

D'Alesio, Echevarria, Melis, Scimemi, JHEP 1411 (14)



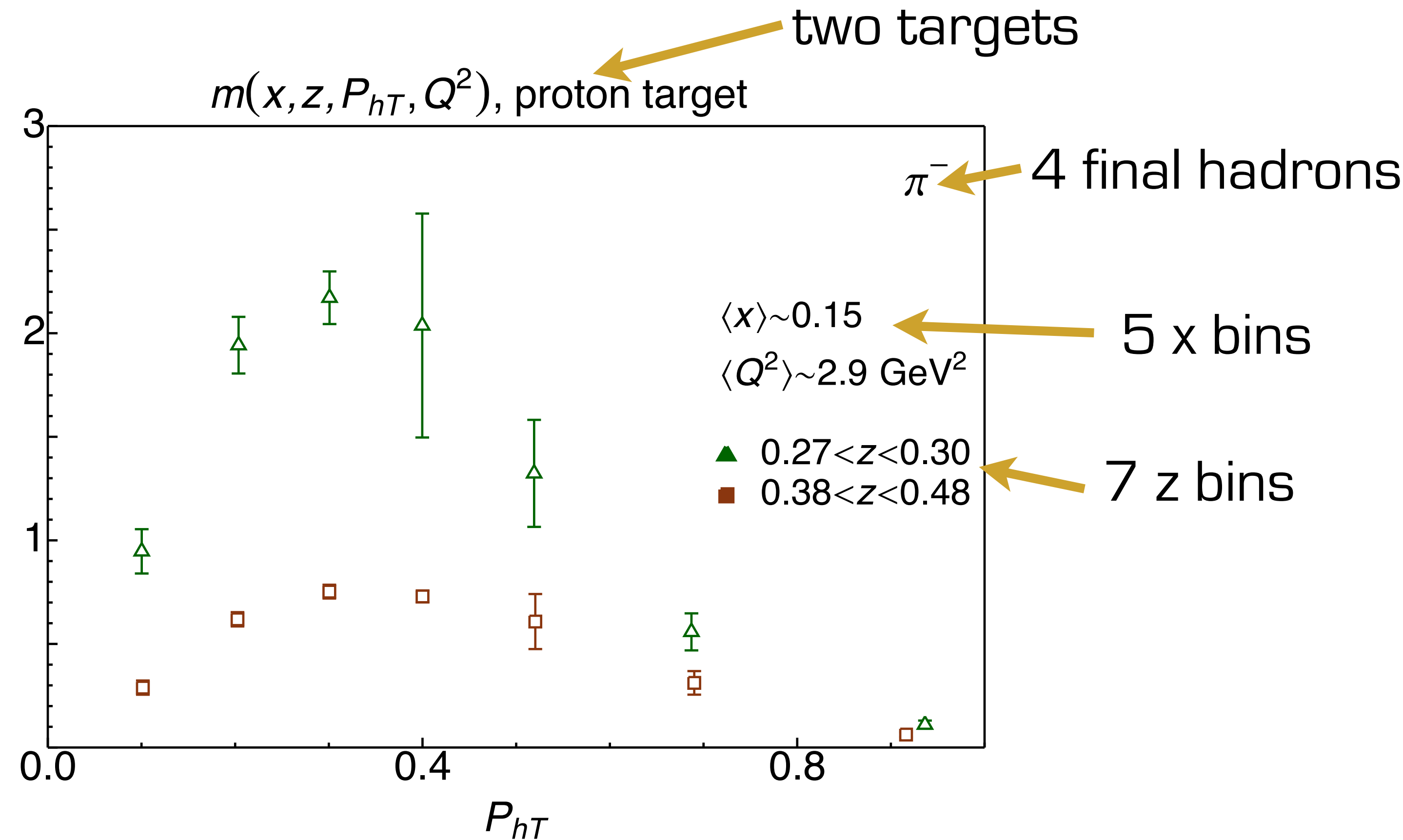
The fit implements TMD evolution at Next-to-Next-to-Leading log (state of the art)
Several choices are peculiar to this fit and not “standard”
The agreement with data is excellent ($\chi^2/\text{dof} = 1.10$)

The replica method



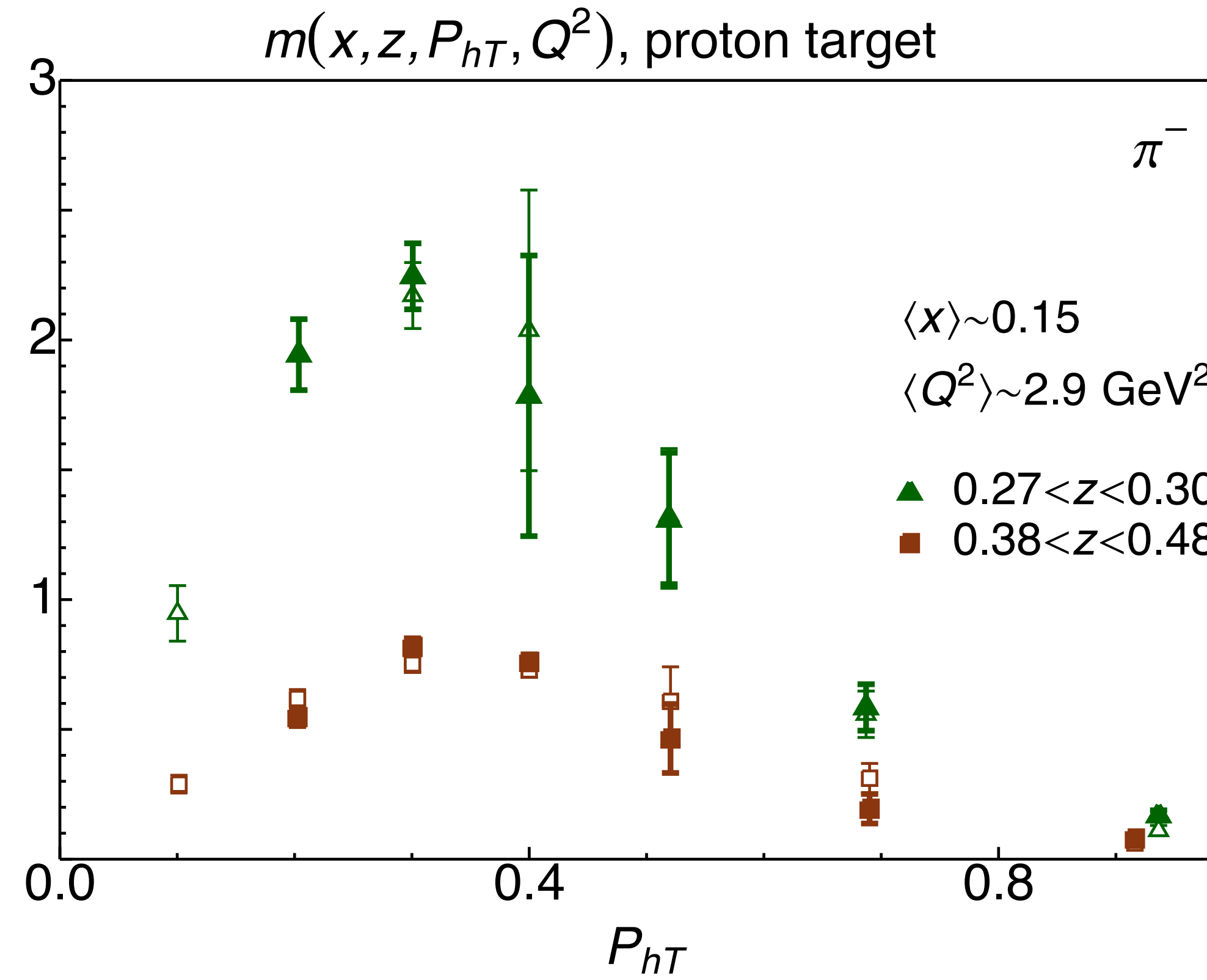
Example of original data

The replica method



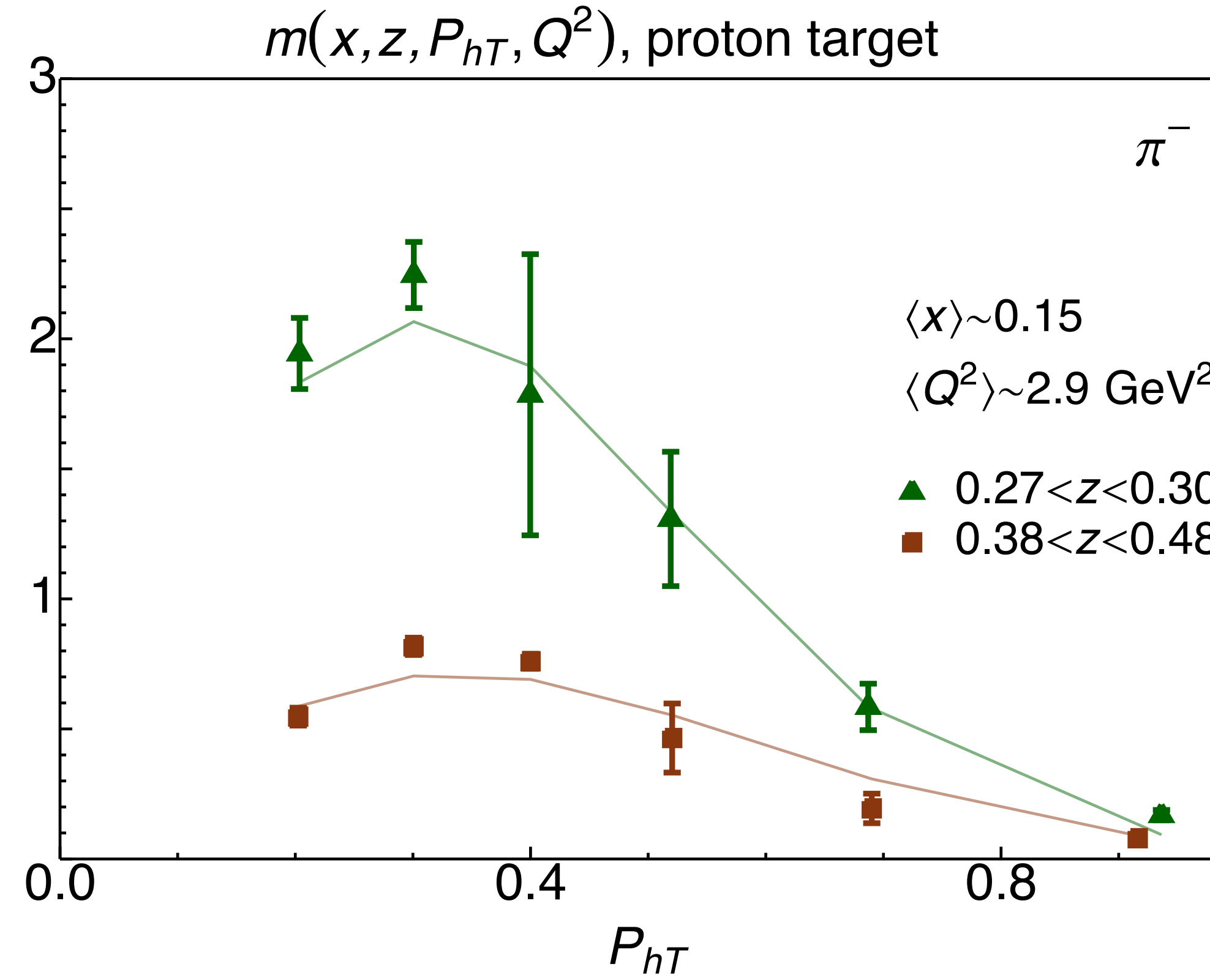
Example of original data

The replica method



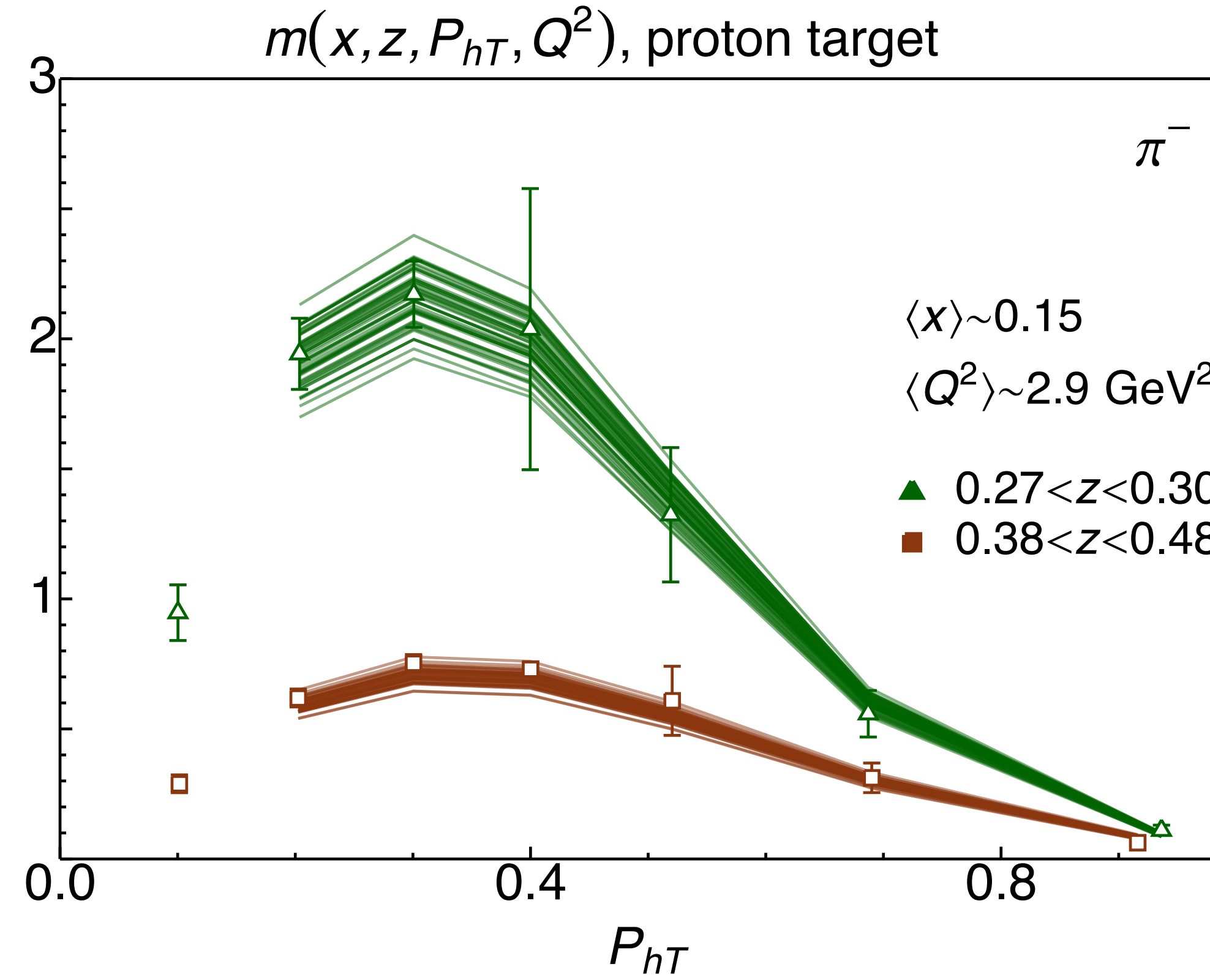
Data are replicated (with Gaussian distribution)

The replica method



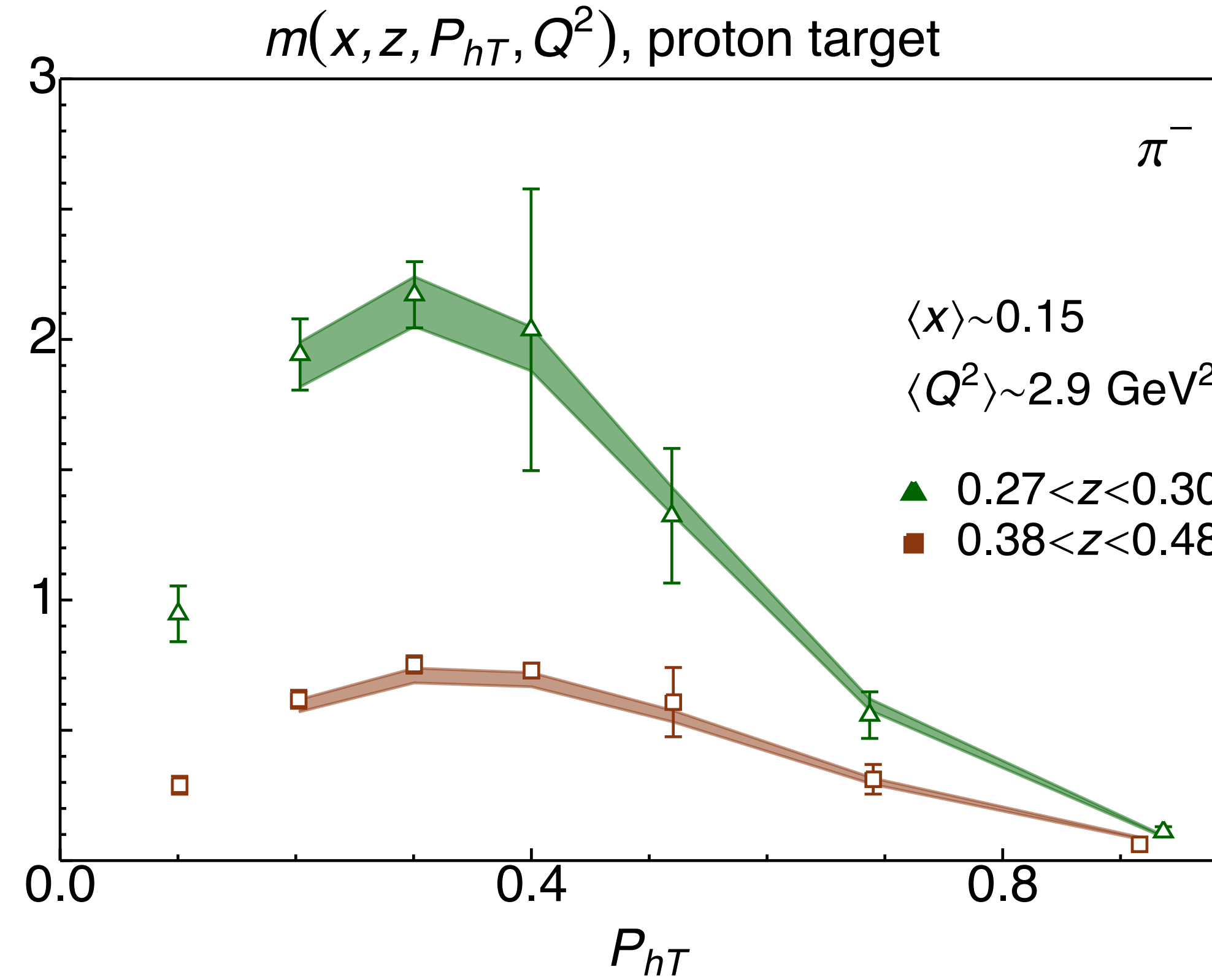
The fit is performed on the replicated data

The replica method



The procedure is repeated 200 times

The replica method



For each point, a central 68% confidence interval is identified